

D.J. Staziker

Water Wave Scattering by Undulating Bed Topography.

February 1995

Abstract

The purpose of this thesis is to investigate the scattering of a train of small amplitude harmonic surface waves on water by undulating one-dimensional bed topography.

The computational efficiency of an integral equation procedure that has been used to solve the mild-slope equation, an approximation to wave scattering, is improved by using a new choice of trial function. The coefficients of the scattered waves given by the mild-slope equation satisfy a set of relations. These coefficients are also shown to satisfy the set of relations when they are given by any approximation to the solution of the mild-slope equation.

A new approximation to wave scattering is derived that includes both progressive and decaying wave mode terms and its accuracy is tested. In particular, this approximation is compared with older approximations that only contain progressive wave mode terms such as the mild-slope approximation. The results given by the new approximation are shown to agree much more closely with known test results over steep topography, where decaying wave modes are significant. During this analysis, a new set of boundary conditions is found for the mild-slope equation and the subsequent results give much better agreement with established testtopoc - (ld-slope equT5-S9Td\$significa

Contents

1	Introduction	1
2	Background Fluid Dynamics	13
2.1	The linearised boundary-value problem	13
2.2	Time-independent solutions	16
2.3	Separation solutions	17
2.4	Approximations to time independent velocity potential ϕ	18
2.5	The 1-dimensional mild-slope equation	21
2.6	Integral equations and variational principles	25
3	Further development of Chamberlain's theory	31
3.1	Introduction to approximation methods	31
3.2	A one-dimensional trial space approximation	35
3.2.1	Outline of method	2

Chapter 1

Introduction

A long-standing but persistent problem in the area of water wave theory is the determination of the effect of bed topography and obstacles on a given wave field. An example of a practical problem faced by coastal engineers is to predict the amplitude of waves in harbours, where both man-made breakwaters and the shape of the sea bed affect the wave behaviour. Such problems involve the scattering, diffraction and refraction of waves and are mathematically formidable for linearised theory, even with relatively simple bed and/or obstacle geometries.

The work presented in this thesis is solely concerned with the effect of bed topography on an incident wave train. We do not address problems where an obstacle, such as a barrier, affects an incident wave train, except for mentioning them in this introduction and noting the solution methods used. The effect of variations in the still-water depth on an incident wave train is examined using linearised theory. We prescribe the incident wave train and the deviation in the still-water depth, and seek the additional waves, the scattered waves, caused by this deviation. A typical problem requires the determination of a velocity potential satisfying Laplace's equation within the fluid, a mixed boundary condition on the free surface, and a given normal velocity on rigid boundaries. If the fluid domain extends to infinity,

deviation from a flat sea bed. Problems where analytic solutions exist are usually for a limited selection of straightforward geometries which include horizon

mission or total reflection is possible. This approximation method proved less accurate when the ratio of barrier separation to barrier length became small. Newman [43] addressed this case, by a different approach which involved matching solutions both near the two obstacles and in the

s of wavelengths for which total transmission of the incident wave is possible, and the insertion of an additional barrier resulted in an infinity of wavelengths corresponding to zero reflection.

These problems with barriers that contain gaps become more difficult when the water is not assumed to be deep, as the motion is then also affected by the bed. Macaskill [34] considered the reflection of water waves by a thin vertical barrier of arbitrary permeability in water of finite depth. An integral equation for the horizontal fluid velocity was derived by an application of Green's theorem and was solved by collocation methods. A serious problem for the solution process to overcome involved the numerical difficulty of evaluating a Green's function given by an infinite series. We are faced with the same problem in Chapter 5.

In Porter [50], there is a general discussion about the refraction/diffraction problem for vertical-sided breakwaters of finite depth, in relation to Green's theory and integral equation methods. Examination of several special cases for the class of problems where the breakwaters are straight, parallel walls containing gaps showed that the resulting integral equations are conducive to straightforward numerical solution techniques. Indeed, a very efficient computational method which solves the problem of diffraction of a plane wave train through a gap in an infinite straight breakwater, and the complementary problem of diffraction by a finite strip, was given by Chu and Porter [11]. The solution procedure involved the conversion of known first-kind equations for these problems into second-kind equations which are much more amenable to numerical techniques. This was an early example of the use of the technique of invariant imbedding in water wave theory.

For all the problems discussed so far, the geometries have involved vertical boundaries in water of infinite or constant depth. Allowing the water depth to vary increases the difficulty of the problem, and consequently exact solutions are exceedingly rare for such problems. The exceptions to this are limiting cases such as shallow water, where the wavelength is assumed to be much larger than the water depth.

Lamb [28] derived an exact expression for the reflection coefficient for the problem of waves incident on a vertical step in shallow water. Bartholomeusz [1]

quation in the shallow water limit. Through this work, Eckart also discovered a useful approximation to the root of the well known ‘dispersion relation’, a transcendental equation which connects the deep-water wave number to the wave number in finite water depth. Eckart did not pursue his approximation to the full linear problem further possibly, according to Miles [40], because he had obtained a rather unsatisfactory approximation to the group velocity in his 1951 lecture notes.

A more recent and very popular approximation of the full linear problem was given by Berkhoff [2] & [3], whose ‘combined refraction-diffraction’ equation has now become known as the mild-slope equation. There have been many subsequent derivations of the mild-slope equation, which typically approximate the vertical structure of the motion and restrict the bed slope to be ‘small’ or ‘mild’ in a sense to be described later. The derivation given by Berkhoff [3] is a clarification of the original derivation given in Berkhoff [2]. However, the mathematical approach used in Berkhoff [3], which is a perturbation procedure in terms of two small parameters, is still not rigorous. Smith and Sprinks [54] gave a more mathematically sound derivation of the mild-slope equation, by expanding the vertical dependence of the velocity potential in terms of an orthogonal set of functions and remo

steepness was v

varying (mild-slope) component onto which a rapidly varying component of small amplitude is superimposed. Kirby then used a vertical integration procedure to derive what is now called the extended mild-slope equation. He verified that it gave much better agreement with the experimental data at the Bragg peaks for ripple bed problems than the mild-slope approximation. However, this improvement to the mild-slope approximation is only valid for ripple bed problems.

A further improvement to the mild-slope equation, which is valid over arbitrary depth profiles, was given by Chamberlain [6]. He followed the same procedure which Lozano and Meyer [32] used to derive the mild-slope equation. In other words, Chamberlain approximated the vertical structure of the velocity potential and removed the dependence on the vertical co-ordinate by integration over the depth. Chamberlain does not make the further assumption that the bed slope is mild, and consequently finds a new approximation to the velocity potential. Chamberlain and Porter [9] formalised the derivation of this new approximation, giving derivations using a variational approach and a Galerkin approach. They named the resulting equation the modified mild-slope equation, and showed that it reduced to the mild-slope equation when the bed slope is assumed to be mild. Chamberlain and Porter [9] also show that for ripple bed problems the modified mild-slope equation subsumes the extended mild-slope equation too. They found that the results given by the modified mild-slope equation are in better agree-

pensive. In Rey [52], the series of steps which approximates the depth profile is subdivided into smaller subsystems called patches. In each patch, the decaying modes generated at one step are not assumed negligible at neighbouring steps in the patch. However, the decaying modes generated in one patch are assumed negligible at neighbouring patches. This seems to be a superior approximation to that used by O'Hare and Davies [45]. Rey [52] goes on to test his approximation on Booij's [5] talud problem, finding good agreement with the full linear results computed by Booij. He also found that his results were quite different to those given by the mild-slope approximation, even for taluds with gradient less than one third, for which Booij [5] had claimed were in good agreement with the full linear model. Rey [52] also tested his approximation on ripple beds, finding good agreement with wave tank data.

After re-establishing the well-known full linearised equations for the scattering of waves by varying topography in Chapter 2, we go on to state the mild-slope equation and briefly review the integral equation procedure that Chamberlain [7] used to solve it.

Noting that coastal engineers require only about three decimal place accuracy in solutions of water wave problems, we go on, in Chapter 3, to improve the computational efficiency of Chamberlain's integral equation solution method. This is done by using a new choice of trial function and seeking solution accuracy to three decimal places rather than the machine accuracy achieved by Chamberlain. We also reinvestigate Eckart's [15] approximation and the symmetry properties of the coefficients of the reflected and transmitted waves.

much better agreement with the results that have been obtained using full linear theory and those found by Rey [52] than the results obtained using the original boundary conditions.

In Chapter 5, we consider the full linear wave scattering problem over an arbitrary hump. The term hump is used to describe a local elevation in an otherwise flat uniform bed. Using Green's theory, the boundary-value problem for the velocity potential is converted into a second-kind integral equation. Initially, an approximation in this equation is tried, but it proves to be rather inaccurate. It is found, however, that the second-kind integral equation for the potential can be converted into a first-kind integral equation for the tangential fluid velocity. The kernel of the first-kind equation is much easier to evaluate numerically than that of the second-kind equation. A variational approach is then used to obtain approximations to the coefficients of the reflected and transmitted waves which are second-order accurate compared to the approximation of the solution of the integral equation. These results are then used to test the accuracy of the new 'decaying mode' approximation derived in Chapter 4 and also to test the accuracy of the modified mild-slope and mild-slope approximations.

A summary of the work presented, together with conclusions and suggestions for future research concludes this thesis.

Chapter 2

Background Fluid Dynamics

In this chapter we present the linearised equations satisfied by the velocity potential for the irrotational flow of an incompressible, homogeneous fluid over a bed of varying depth. It is assumed that the fluid occupies a region which extends to infinity in every horizontal direction. The fluid is also bounded below by a bed of given permanent

the fluid velocity at time t and a given point (x, y, z) in the fluid be denoted by $\underline{q}(x, y, z, t)$. Assuming the fluid motion starts from rest, with gravity the only external force acting, then \underline{q} is necessarily irrotational. It follows that there exists a velocity potential $\Phi(x, y, z, t)$ such that $\underline{q} = -\tilde{\nabla}\Phi$ where $\tilde{\nabla} = (\frac{\partial}{\partial x}, \frac{\partial}{\partial y}, \frac{\partial}{\partial z})$. The assumption of the fluid being homogeneous and incompressible reduces the continuity equation to

$$\tilde{\nabla} \cdot \underline{q} = 0$$

and hence Φ satisfies Laplace's equation,

$$\tilde{\nabla}^2 \Phi = 0, \quad (2.1)$$

in the fluid.

The bed is assumed to be fixed and impermeable and is defined by $z = -h(x, y)$, as depicted in Fig.2.1. As the fluid cannot flow through the bed, the normal derivative of the velocity potential on the bed must be zero, giving rise to the boundary condition

$$\frac{\partial \Phi}{\partial n} = 0 \quad \text{on } z = -h(x, y) \quad (2.2)$$

where $\frac{\partial}{\partial n}$ denotes the outward normal derivative on $z = -h(x, y)$.

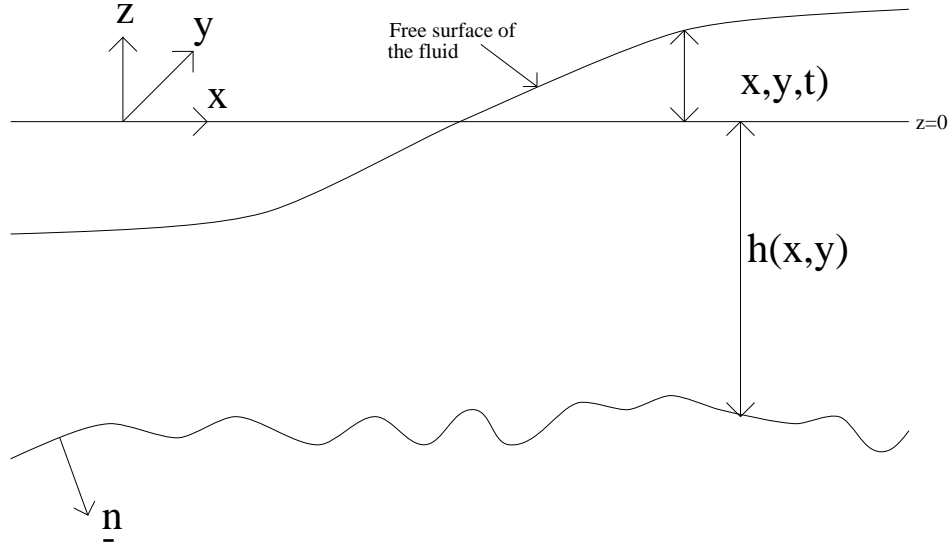


Figure 2.1: Vertical cross section of the fluid domain.

By considering the Stokes derivative $\frac{D}{Dt} = \frac{\partial}{\partial t} + \underline{q} \cdot \tilde{\nabla}$ which denotes differentiation following the motion of the fluid, this boundary condition may be rewritten

as a so-called ‘kinematic boundary condition’ as follows. On any fluid boundary given by $f(x, y, z, t) = 0$ we have

$$\frac{Df}{Dt} = 0 \tag{2.3}$$

as otherwise there would be a finite flow of fluid across the boundary (Lamb [28]). The bed is defined by $z = -hh$

and

$$\frac{\partial \Phi}{\partial t} = g\eta \quad \text{on } z = 0 . \quad (2.10)$$

On eliminating η from (2.9) and (2.10) we obtain the final boundary condition of the linear boundary-value problem, which is given by

$$\begin{aligned} \tilde{\nabla}^2 \Phi &= 0 & -h < z < 0 , \\ \frac{\partial \Phi}{\partial z} + \frac{1}{g} \frac{\partial^2 \Phi}{\partial t^2} &= 0 & \text{on } z = 0 , \\ \frac{\partial \Phi}{\partial z} + \nabla h \cdot \nabla \Phi &= 0 & \text{on } z = -h(x, y) , \end{aligned} \quad (2.11)$$

together with a radiation condition imposed as $x^2 + y^2 \rightarrow \infty$. If we write $\Phi = \Phi_i + \Phi_s$ where Φ_i represents the incident wave field, then the radiation condition causes Φ_s to represent only outgoing waves as $x^2 + y^2$

together with a radiation condition.

The free surface elev

Denoting the wavelength by λ , then using the fact that $\lambda = 2\pi/k$

is arrived at in the form

$$\nabla \cdot u \nabla \phi_0 + k^2 u \phi_0 = 0 , \quad (2.24)$$

where $Re(\phi_0 e^{-i\sigma t})$ is an approximation to the free surface shape,

$$u(h) = \frac{1 - e^{-2\nu h}}{2\nu} , \quad (2.25)$$

$$k^2 = \nu^2 \coth(\nu h) , \quad (2.26)$$

and $\nu = \frac{\sigma^2}{g}$ is the deep water wave number.

Eckart's equation (2.24) also reduces to the linearised shallow water equation under the same assumption as in the mild-slope case. Eckart notes that (2.26) actually approximates the root of the dispersion relation (2.18) to within 4% for all values of kh . However, he seemed to be discouraged from further development of his approximation due to the unsatisfactory approximation to the group velocity he obtained. Recently, Miles [40] has shed new light on Eckart's approximation, deriving (2.24) as well as (2.21) and (2.23), via an elegant variational procedure. Miles notes that the direct calculation of the group velocity from Eckart's dispersion relation (2.26), gives an approximation to the ratio of group velocity to phase velocity within 1% of the exact value for all values of kh . Miles also notes that while the mild-slope approximation conserves wave energy, Eckart's approximation does not (except in uniform depth). Also, on a gently sloping beach, Eckart's approx

solutions of which are approximated by variational techniques. For a specified incident wave, this procedure can calculate highly accurate approximations

cess outlined by Chamberlain [7], which may be summarised as follows. Let

$$\hat{x} = \frac{x}{l} ,$$

$$U(\hat{x}) = \frac{1}{h_0} u(l\hat{x}) ,$$

$$H(\hat{x}) = \frac{1}{h_0} h(l\hat{x}) ,$$

$$\hat{\phi}_0(\hat{x}) = \frac{1}{\sigma l^2} \phi_0(l\hat{x}) .$$

The following account discards the accents from these definitions in the pursuit of a simple notation. In the above circumstances, the mild-slope equation (2.21) may be written as

$$\frac{d}{dx} \left(U \frac{d\phi_{00}}{dx} \right)$$

and where the notation $\kappa_0 = \kappa(0)$ (and $\kappa_1 = \kappa(1)$) is used.

The coefficients appearing in the differential equation (2.30) are uniquely defined once H , α_0 and τ are assigned. The only remaining information necessary is the choice of incident waves. On the flat bed for $x \leq 0$, the non-dimensional mild-slope equation (2.27) reduces to $\phi_0'' + \kappa_0^2 \phi_0 = 0$. Similarly, on the flat bed for $x \geq 1$, (2.27) reduces to $\phi_0'' + \kappa_1^2 \phi_0 = 0$. Therefore, we suppose in general, that there are two incident waves with known coefficients A^\pm propagating from $x = \pm\infty$ respectively. This will result in two outgoing waves, with unknown coefficients B^\pm , propagating towards $x = \pm\infty$ respectively

where the terms involving U' are the consequences of allowing slope discontinuities in H at $x = 0, 1$. Greater detail of the derivation of these boundary conditions and the merit of writing them in the form of (2.32) can be found in Chamberlain [6].

Linearity allows superposition of solutions corresponding to waves incident from the left with solutions corresponding to waves incident from the right. This removes the need to solve the problem with two incident waves. By removing one incident wave, the amplitude of the remaining incident wave may be set equal to unity, without loss of generality. Accordingly the two reflection and transmission coefficients, denoted by R and T , for this problem are defined as follows.

$$\begin{aligned} \text{If } A^+ = 0 \text{ then } R_1 &= \frac{B^-}{A^-} \quad \text{and} \quad T_1 = \frac{B^+}{A^-} . \\ \text{If } A^- = 0 \text{ then } R_2 &= \frac{B^+}{A^+} \quad \text{and} \quad T_2 = \frac{B^-}{A^+} . \end{aligned}$$

The subscripts distinguish between waves incident from the left(1) or the right(2). Now we define ζ_1 to be the solution of (2.30) and (2.32) for an incident wave from the left (requiring $A^+ = 0$ in (2.32)). ζ_2 is defined to be the solution for an incident wave from the right (requiring $A^- = 0$ in (2.32)). Using the equations (2.31), the reflection and transmission coefficients can now be defined in terms of ζ_j ($j = 1, 2$) in the following way.

If $A^+ = 0$:

$$\begin{aligned} R_1 &= \frac{\zeta_1(0)}{A^-} - 1 , \\ T_1 &= \frac{\zeta_1(1)e^{-i\kappa_1}}{A^-} \sqrt{\frac{U(0)}{U(1)}} . \end{aligned} \tag{2.34}$$

If $A^- = 0$:

$$\begin{aligned} R_2 &= \frac{\zeta_2(1)e^{-i\kappa_1}}{A^+} \sqrt{\frac{U(0)}{U(1)}} - e^{-2i\kappa_1} , \\ T_2 &= \frac{\zeta_2(0)}{A^+} . \end{aligned} \tag{2.35}$$

The outgoing wave coefficient B^+ comprises of two parts – that part of A^- transmitted beyond the talud and that part of A^+ reflected back from the talud. We can make a similar statement about B^- , and these resulting relationships can be summarised as

$$\begin{pmatrix} B^+ \\ B^- \end{pmatrix} = \begin{pmatrix} T_1 & R_2 \\ R_1 & T_2 \end{pmatrix} \begin{pmatrix} A^- \\ A^+ \end{pmatrix} .$$

on defining two self-adjoint operators L and P by

$$(L\zeta)(x) = \frac{1}{2\kappa_0} \int_0^1 \sin(\kappa_0|x-t|) \zeta(t) dt$$

and

$$(P\zeta)(x) = \rho(x)\zeta(x) .$$

Then $\zeta \in L_2(0$

thus the coefficients in (2.40) have been found. Also, on finding $\zeta(0)$ and $\zeta(1)$, then the reflection and transmission coefficients are known through (2.34) and (2.35).

On substituting the above equation (2.40) for ζ into the right hand side of equations (2.38) and (2.39) and rearranging them, it can be shown that $\zeta(0)$ and $\zeta(1)$ are determined by solving the rank 2 system of equations

$$\begin{aligned} & \left(\left(\begin{array}{cc} b_2 & b_3 \\ b_5 & b_6 \end{array} \right) - i \left(\begin{array}{cc} B_1 & B_2 \\ \overline{B}_2 & B_1 \end{array} \right) \left(\begin{array}{cc} c_5 - b_2 & c_6 - b_3 \\ c_2 - b_5 & c_3 - b_6 \end{array} \right) \right) \begin{pmatrix} \zeta(0) \\ \zeta(1) \end{pmatrix} \\ & = - \begin{pmatrix} b_1 \\ b_4 \end{pmatrix} + i \left(\begin{array}{cc} B_1 & B_2 \\ \overline{B}_2 & B_1 \end{array} \right) \begin{pmatrix} c_4 - b_1 \\ c_1 - b_4 \end{pmatrix} \end{aligned} \quad (2.42)$$

in which

$$B_1 = \frac{1}{2}(A_{11} + A_{22}) \quad \text{and} \quad B_2 = \frac{1}{2}(A_{11} + 2iA_{12} - A_{22})$$

and

$$A_{jk} = \frac{1}{2\kappa_0} \int_0^1 \chi_j(t)\rho(t)f_k(t) dt = \frac{1}{2\kappa_0}(\chi_j, Pf_k) \quad (j, k = 1, 2).$$

Stationary principles are used to generate approximations to the inner products A_{jk} ($j, k = 1, 2$) with upper and lower bounds by firstly ensuring that the function ρ is entirely one-signed. This allows the non-self-adjoint operator A in the integral equations (2.41) to be replaced by a self-adjoint one. In general, ρ does not possess this property, but can be made to do so by adding to it or subtracting from it a known quantity. This process requires a slight change in the boundary conditions (2.32) which causes the definitions of the c_j ($j = 1, \dots, 6$) in (2.33) to be amended. Full details of this device are in Chamberlain [6]. With ρ one-signed, a new self-adjoint operator S can be defined by

$$(S\chi)(x) = s(x)\chi(x),$$

where

$$s(x) = \sqrt{\lambda\rho(x)}$$

and

$$\lambda = \text{sgn}(\rho) \quad (\text{that is } \lambda = \pm 1).$$

Then the integral equations for χ_j ($j = 1, 2$) given by (2.41) can be rewritten as

$$\hat{A}\hat{\chi}_j = Sf_j \quad (j = 1, 2), \quad (2.43)$$

where

$$\hat{\chi}_j = S\chi_j \quad (j = 1, 2)$$

and

$$\hat{A} = I - \lambda SLS.$$

Clearly \hat{A} is self-adjoint and as S is bounded, SLS is a compact operator.

It is easy to show that the functionals

$$J_k : L_2(0, 1) \rightarrow \mathbb{R} \quad (k = 1, 2),$$

$$J_3 : L_2(0, 1) \times L_2(0, 1) \rightarrow \mathbb{R}$$

given by

$$J_k(pA$$

\tilde{p}_k ($k = 1, 2$) determined by the second functional (2.45) as μ_k ($k = 1, 2$) respectively.

The further assumption that there exists $b > 0$ such that $\forall p \in L_2(0, 1)$,

$$b \|p\|^2 \leq (\hat{A}p, p) \leq a \|p\|^2, \quad (2.47)$$

where the existence of an $a > 0$ is guaranteed since \hat{A} is a bounded operator, establishes the following upper and lower bounds on the inner products of interest:

$$J_k(\xi_k) + \frac{1}{a} \|\hat{A}\xi_k - Sf_k\|^2 \leq (\hat{\chi}_k, Sf_k) \leq J_k(\xi_k) + \frac{1}{b} \|\hat{A}\xi_k - Sf_k\|^2 \quad (k = 1, 2) \quad (2.48)$$

and

$$G(\mu_1, \mu_2) - R(\mu_1, \mu_2) \leq (\hat{\chi}_1, Sf_2) \leq G(\mu_1, \mu_2) + R(\mu_1, \mu_2), \quad (2.49)$$

where the functionals G and R are given by

$$G(\mu_1, \mu_2) = J_3(\mu_1, \mu_2) + \frac{1}{2} \left(\frac{1}{b} + \frac{1}{a} \right) (\hat{A}\mu_1 - Sf_1, \hat{A}\mu_2 - Sf_2)$$

and

$$R(\mu_1, \mu_2) = \frac{1}{2} \left(\frac{1}{b} - \frac{1}{a} \right) \|\hat{A}\mu_1 - Sf_1\| \|\hat{A}\mu_2 - Sf_2\|.$$

An excellent derivation of these upper and lower bounds may be found in Porter and Stirling ([51], pp.254-257, 261-263). Approximations to a and b can be found in Chamberlain [6]. Disappointingly, the approximation to b can be negative in certain cases, resulting in just a stationary approximation to the inner products with no upper and lower bounds.

The implementation of the solution process follows by firstly assigning H , α_0 , τ and the direction of the incident wave. Then, after ensuring ρ is one-signed (by adjusting it to make it so if necessary) and choosing the dimension of the trial space, the trial functions given by (2.46) are generated and the approximations $J_1(\xi_1)$, $J_2(\xi_2)$ are

Chamberlain [7] has shown that 2- or 3- dimensional trial spaces can result in the determination of approximations to the reflection and transmission coefficients to machine accuracy.

This integral approach can also be used with the linearised shallow water equation and Eckart's equation with certain modifications. Chamberlain [6] has done this for the linearised shallow water equation, and the necessary modifications required to use this integral approach to solve Eckart's equation are given in Chapter 3.

Chapter 3

Further development of Chamberlain's theory

In this chapter some extensions to the work appearing in Chamberlain [7] & [8] are presented. A new computationally cheap integral equation solution method is developed for the three model equations mentioned in Chapter 2, namely the mild-slope equation, Eckart's equation and the linearised shallow water equation, over a range of parameter values. This method uses the approximation methods discussed in section 2.6 but with a new choice of trial functions. Eckart's equation is further investigated and improvements to it are suggested. Finally, the symmetry properties of the solutions of the three model equations are studied, and an unexpected property is discovered that any approximations of the solutions still possess the symmetry properties.

3.1 Introduction to approximation methods

This section begins by illustrating the interest in solving the model equations over a continuous range of their parameters for a specified bed shape. Booij [5] provided some experimental evidence concerning the accuracy of the mild-slope approximation to the velocity potential ϕ satisfying (2.13). As a part of that paper, a talud problem was considered and a graph (see Fig.3.1) was presented of reflected amplitude ($|R|$) given by the mild-slope equation against W_s , a parameter which denotes the length of Booij's talud. In terms of the notation used

in Chapter 2, the dimensionless parameters of the mild-slope equation are given in terms of W_s by $\alpha_0 = W_s/\sqrt{0.6}$ and $\tau = 0.6/W_s$ (See Chamberlain [6] p.114 for details). Booij computed $|R|$ using full linearised theory and superimposed it onto his graph, observing that the two sets of results coincide for talud slopes with gradien

three model equations over a range of their parameters. F

upper and lower bounds exist, extremely accurate approximations to R_k and T_k ($k = 1, 2$) are such that $\max_{k=1,2} \{ \|(I - LP)\xi_k - f_k\|, \|(I - LP)\mu_k - f_k\| \}$ is $O(10^{-4})$ for all values of α_0 and τ .

In future, whenever we specify the accuracy in the approximations to the reflection and transmission coefficients of any of the model equations, we shall just give the maximum error in $|R_k|$ and $|T_k|$ ($k = 1, 2$). In the case where the upper and lower bounds do not exist, this will imply that $\max_{k=1,2} \{ \|(I - LP)\xi_k - f_k\|^2, \|(I - LP)\mu_k - f_k\|^2 \}$ is $O(10^{-4})$.

(3.9) stationary within the N-dimensional trial spaces. We shall denote the functions \tilde{p}_k ($k = 1, 2$) determined by (3.8) as ξ_k ($k = 1, 2$) respectively, and the functions \tilde{p}_k ($k = 1, 2$) determined by (3.9) as μ_k ($k = 1, 2$) respectively.

As already noted, the Chamberlain solutions, ξ_k and μ_k ($k = 1, 2$), are very accurate approximations to the solutions χ_1 and χ_2 of the integral equations (3.4), but they also require considerable computer time to determine. The integral equation solution method we have used to solve the mild-slope equation at each value of α_0 and τ employs this expensive process of generating the Chamberlain solutions. Instead of this, we shall use the Chamberlain solutions at a chosen α_0 and τ to approximate χ_1 and χ_2 in the neighbourhood of α_0 and τ . In the present circumstances, we only need to consider problems where τ is either fixed or is a function of α_0 , as in the problem considered by Booij [5] given in section 3.1, where $\tau = \sqrt{0.6}/\alpha_0$. In the following we shall only refer to the value of α_0 at which we are solving the problem, and we shall not mention τ as we automatically know its value once α_0 is assigned.

A superscript is now introduced into our established notation to denote the value of α_0 at which each operator, function and functional is evaluated.

We introduce the 1-dimensional trial functions

$$p_k = r_k \xi_k^{\alpha_0} \quad (k = 1, 2) \quad (3.11)$$

as approximations to $\chi_1^{\alpha_0}$ and $\chi_2^{\alpha_0}$, for some $r_k \in \mathbb{R}$ ($k = 1, 2$) determined so as to make the functional (3.8) stationary. Therefore, substituting (3.11) into (3.8), we see that

$$J_k^{\alpha_0}(p_k) = J_k^{\alpha_0}(r_k) = 2r_k \left(\xi_k^{\alpha_0}, S^{\alpha_0} f_k^{\alpha_0} \right) - r_k^2 \left(\hat{A}^{\alpha_0} \xi_k^{\alpha_0}, \xi_k^{\alpha_0} \right) \quad (k = 1, 2)$$

regarded as a function of r_k , is stationary where

$$\frac{dJ_k^{\alpha_0}}{dr_k} = 0 \quad (k = 1, 2) .$$

Hence the constants r_k ($k = 1, 2$) are given by

$$r_k = \frac{\left(\xi_k^{\alpha_0}, S^{\alpha_0} f_k^{\alpha_0} \right)}{\left(\hat{A}^{\alpha_0} \xi_k^{\alpha_0}, \xi_k^{\alpha_0} \right)} \quad (k = 1, 2)$$

and the approximations to the inner products $(\chi_k^{\hat{\alpha}_0}, P^{\hat{\alpha}_0} f_k^{\hat{\alpha}_0})$ ($k = 1, 2$) are

$$J_k^{\hat{\alpha}_0}(p_k) = \frac{(\xi_k^{\alpha_0}, S^{\hat{\alpha}_0} f_k^{\hat{\alpha}_0})^2}{(\hat{A}^{\hat{\alpha}_0} \xi_k^{\alpha_0}, \xi_k^{\alpha_0})} \quad (k = 1, 2)$$

respectively.

To find an approximation to the inner product $(\chi_1^{\hat{\alpha}_0}, P^{\hat{\alpha}_0} f_2^{\hat{\alpha}_0})$, we use the 1-dimensional trial functions

$$q_k = \gamma_k \mu_k^{\alpha_0} \quad (k = 1, 2) \quad (3.12)$$

as approximations to $\chi_1^{\hat{\alpha}_0}$ and $\chi_2^{\hat{\alpha}_0}$, for some $\gamma_k \in \mathbb{R}$ ($k = 1, 2$) determined so as to make the functional (3.9) stationary. Therefore, substituting (3.12) into (3.9), we see that

$$\begin{aligned} J_3^{\hat{\alpha}_0}(q_1, q_2) &= J_3^{\hat{\alpha}_0}(\gamma_1, \gamma_2) \begin{matrix} 1 \\ 0 \end{matrix} \\ &= \gamma_2 (S^{\hat{\alpha}_0} f_1^{\hat{\alpha}_0}, \mu^{\alpha_0}) \end{aligned}$$

process, of solving the mild-slope equation over a range of values of α_0 , can be
contin

as we increase the tolerance in the error (and so increase the accuracy) of the ‘cheap’ solutions. Also, for a fixed tolerance in the error, we find that the value of α_{\max} varies from one depth profile to another.

Consider, for example, the solution of the mild-slope equation (MSE) for the test problem of Booij [5], mentioned in section 3.1, for an incident wave of unit amplitude from the left. Here the depth profile is given by

$$H(x) = 1 - \frac{2}{3}x \quad (0 \leq x \leq 1) .$$

In section 3.1, Chamberlain’s method was used in generating extremely accurate solutions of the MSE for this problem with α_0 taking values between 0.05 and 8.5 at intervals of 0.05 (with τ given at each value of α_0 by $\tau = \sqrt{0.6}/\alpha_0$) to produce the results seen in Fig.3.1. This required the use of a 3-dimensional trial space for $\alpha_0 < 2$ and a 6-dimensional trial space for $\alpha_0 > 4$. The total CPU run-time required to generate all these results was 51m 55s. It should be noted that the same Sun 1 workstation was used to generate all the CPU run-times for all the methods used in this chapter.

The new method is now used to solve this problem for the mild-slope equation over the same α_0 range. We choose the tolerance in the error to be a minimum of 2.s.f. accuracy in $|R_k|$ and $|T_k|$ ($k = 1, 2$). The new method produces ‘cheap’ solutions at the 29 values of α_0 in the range [0.05, 1.45]. For all $\alpha_0 > \alpha_{\max} = 1.45$, our new method has to use Chamberlain’s method to generate the solutions. Fig.3.2 depicts the amplitude of the reflected wave, generated by both methods over the α_0 range from 0.05 to 1.45, against W_s (the parameter used by Booij [5] in his corresponding graph), where $W_s = \sqrt{0.6}\alpha_0$. As one would expect with these prescribed tolerances in the error, there is practically no difference in the two sets of results. The new method uses Chamberlain solutions at 5 values of α_0 , which are

$$\alpha_0 = 0.05, 0.95, 1.2, 1.4 \text{ and } 1.45 ,$$

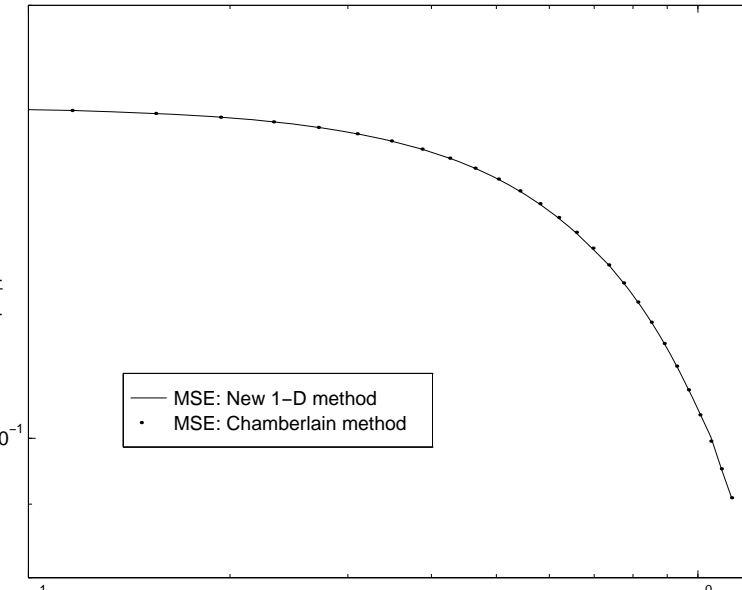


Figure 3.2: Reflected amplitude for the depth profile $H(x) = 1 - 2/3x$ ($0 \leq x \leq 1$).

CPU run-time to generate these results by Chamberlain's method is 7m 39s.

and hence $\|LP\|$ increase with α_0 , making more terms in the trial functions \tilde{p}_k ($k = 1, 2$) given by (3.10) (and consequently larger trial spaces) necessary

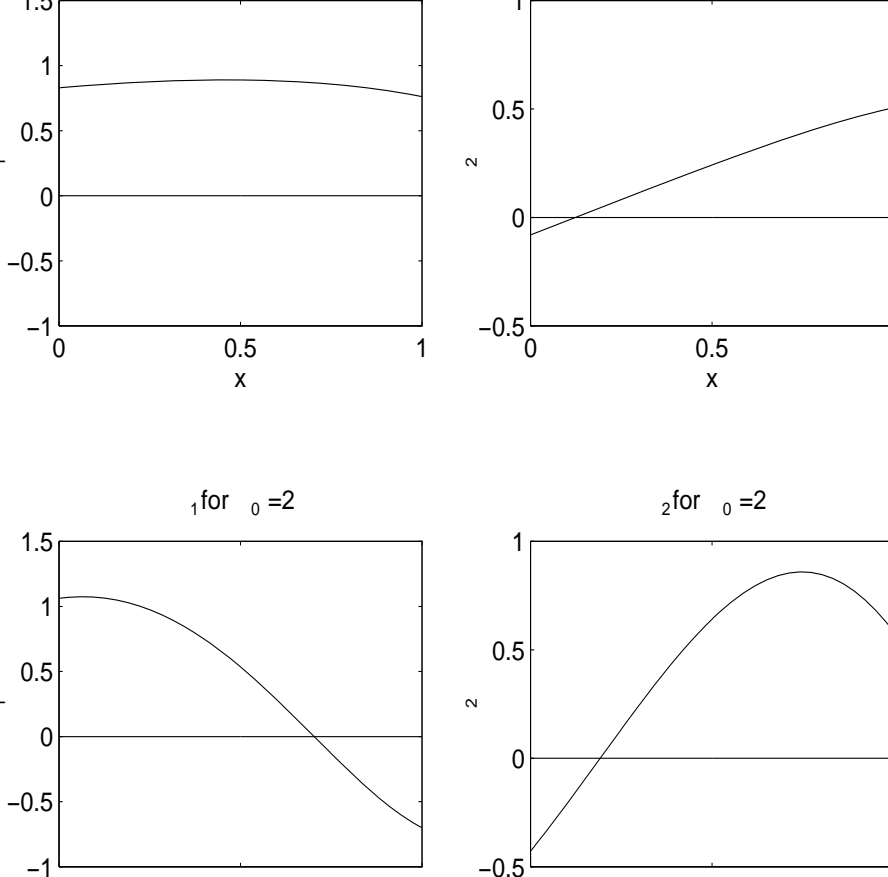


Figure 3.3: Comparison of Chamberlain solutions at two values of α_0

the functional (3.8), we see that

$$\begin{aligned}
J_k^{\alpha_0}(p_k) &= J_k^{\alpha_0}(r_k, s_k) \\
&= 2 \left[r_k \left(\xi_k^{\alpha_0}, S^{\alpha_0} f_k^{\alpha_0} \right) + s_k \left(\xi_k^{\tilde{\alpha}_0}, S^{\alpha_0} f_k^{\alpha_0} \right) \right] \quad (k = 1, 2) \\
&\quad - \left[r_k^2 \left(\hat{A}^{\alpha_0} \xi_k^{\alpha_0}, \xi_k^{\alpha_0} \right) + 2r_k s_k \left(\hat{A}^{\alpha_0} \xi_k^{\alpha_0}, \xi_k^{\tilde{\alpha}_0} \right) + s_k^2 \left(\hat{A}^{\alpha_0} \xi_k^{\tilde{\alpha}_0}, \xi_k^{\tilde{\alpha}_0} \right) \right],
\end{aligned}$$

regarded as a function of r_k and s_k ($k = 1, 2$), is stationary where

$$\frac{\partial J_k^{\alpha_0}}{\partial r_k} = 0 \quad \text{and} \quad \frac{\partial J_k^{\alpha_0}}{\partial s_k} = 0 \quad (k = 1, 2).$$

Hence the constants r_k and s_k ($k = 1, 2$) are given by the rank two system,

$$\begin{pmatrix} \left(\hat{A}^{\alpha_0} \xi_k^{\alpha_0}, \xi_k^{\alpha_0} \right) & \left(\hat{A}^{\alpha_0} \xi_k^{\alpha_0}, \xi_k^{\tilde{\alpha}_0} \right) \\ \left(\hat{A}^{\alpha_0} \xi_k^{\tilde{\alpha}_0}, \xi_k^{\alpha_0} \right) & \left(\hat{A}^{\alpha_0} \xi_k^{\tilde{\alpha}_0}, \xi_k^{\tilde{\alpha}_0} \right) \end{pmatrix} \begin{pmatrix} r_k \\ s_k \end{pmatrix} = \begin{pmatrix} \left(\xi_k^{\alpha_0}, S^{\alpha_0} f_k^{\alpha_0} \right) \\ \left(\xi_k^{\tilde{\alpha}_0}, S^{\alpha_0} f_k^{\alpha_0} \right) \end{pmatrix} \quad (k = 1, 2).$$

Clearly, the approximations to $\chi_1^{\hat{\alpha}_0}$ and $\chi_2^{\hat{\alpha}_0}$ given by (3.13) and (3.14) are very much quicker to calculate than the N -dimensional Chamberlain solutions, given by (3.10), when $N > 1$. We shall refer to the solutions generated by the trial functions (3.13) and (3.14) as the ‘cheap’ solutions. It is obvious that the approximations (3.13) and (3.14) to $\chi_1^{\hat{\alpha}_0}, \chi_2^{\hat{\alpha}_0}$

of the maximum error in all the ‘cheap’ solutions found in the previous interval $[\tilde{\alpha}_0, \alpha_0^*]$. We use the following ‘rule of thumb’ to choose α_0^{**} . If the maximum error in the ‘cheap’ solutions found in the interval $[\tilde{\alpha}_0, \alpha_0^*]$ is 2 (or more) orders of magnitude smaller than the specified tolerance, then α_0^{**} is chosen so that the length of the interval $[\alpha_0^*, \alpha_0^{**}]$ is greater than the length of the interval $[\tilde{\alpha}_0, \alpha_0^*]$. If the maximum error is the same order of magnitude as the specified tolerance, then α_0^{**} is chosen so that the length of the interval $[\alpha_0^*, \alpha_0^{**}]$ is less than the length of the interval $[\tilde{\alpha}_0, \alpha_0^*]$. Otherwise α_0^{**} is chosen so that the length of the interval $[\alpha_0^*, \alpha_0^{**}]$ is equal to the length of the interval $[\tilde{\alpha}_0, \alpha_0^*]$. The Chamberlain solutions are then found at α_0^{**} and the whole process starts again.

We clarify this situation in the following example. Fig.3.4 depicts a typical situation. In this case, the errors in all the ‘cheap’ solutions found in Interval

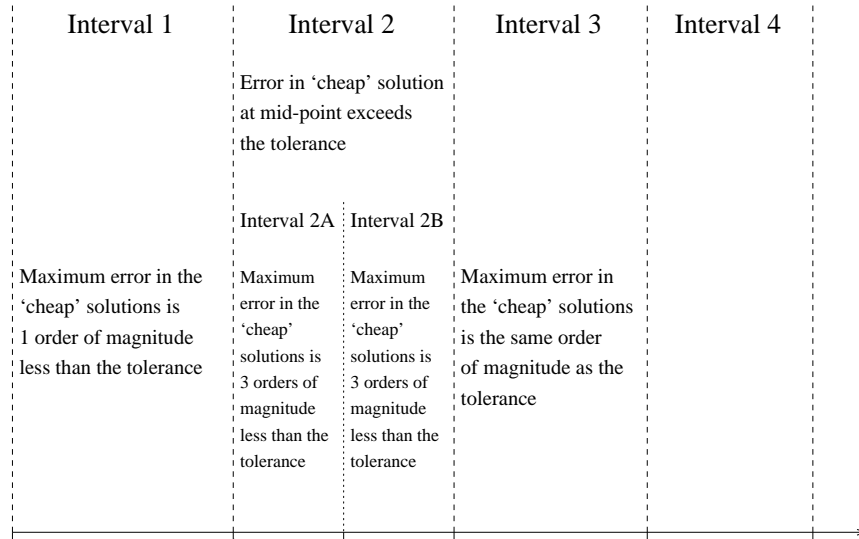


Figure 3.4: An example situation depicting the values of α_0 at which Chamberlain solutions are found.

1 are within the specified tolerance. No Chamberlain solutions are known at $\alpha_0 > \alpha_0^{(2)}$ and the maximum error of all these ‘cheap’ solutions is 1 order of magnitude less than the tolerance. Therefore, the next value of α_0 at which Chamberlain solutions are found is chosen so that the length of Interval 2 is equal to the length of Interval 1. This value of α_0 is denoted by $\alpha_0^{(4)}$ in Fig.3.4. The error in the ‘cheap’ solution at the mid-point of Interval 2 is not within the tolerance. Consequently, Chamberlain solutions at $\alpha_0 = \text{mid-point of Interval 2}$

are found. This value of α_0 is denoted by $\alpha_0^{(3)}$ in Fig.3.4. The errors in the ‘cheap’ solutions in Interval 2A are within the tolerance, and as the Chamberlain solutions are known at $\alpha_0 = \alpha_0^{(4)} > \alpha_0^{(3)}$, the next interval is 2B. Here the errors in the ‘cheap’ solutions are also within the tolerance. No Chamberlain solutions are known at $\alpha_0 > \alpha_0^{(4)}$ and the maximum error of all the ‘cheap’ solutions found in Interval 2B is 3 orders of magnitude less than the tolerance. Therefore, the next value of α_0 at which Chamberlain solutions are found, which is denoted by $\alpha_0^{(5)}$ in Fig.3.4, is chosen so that

$$\text{length of Interval 2B} < \text{length of Interval 3} < \text{length of Interval 2.}$$

Here, the upper bound arises because sufficiently accurate ‘cheap’ solutions could not be obtained at all values of α_0 in Interval 2, and therefore could not be obtained in Interval 3 if it had the same length as Interval 2. The errors in the ‘cheap’ solutions found in Interval 3 are within the tolerance, with the maximum error being the same order of magnitude as the tolerance. As no Chamberlain solutions are known at $\alpha_0 > \alpha_0^{(5)}$, the next Chamberlain solutions are found at $\alpha_0 = \alpha_0^{(6)}$, where $\alpha_0^{(6)}$ is chosen to make the length of Interval 4 less than the length of Interval 3. The process continues like this until solutions have been found for the required α_0 range.

We are now in a position to use this method. It is implemented by firstly assigning the depth profile H , the tolerance in the error, the initial α_0 range ($\tilde{\alpha}_0, \tilde{\tilde{\alpha}}_0$), the final value of α_0 , the relationship between α_0 and τ and the increment to be added to α_0 to give the next α_0 at which a solution is to be found. Chamberlain solutions are then found at $\alpha_0 = \tilde{\alpha}_0$ and

α_0

τ given at each value of α_0 by $\tau = \sqrt{0.6\alpha_0}$). Using Chamberlain's method to generate extremely accurate solutions of Eckart's equation, with three-dimensional

trialCham

CPU time compared with using Chamberlain solutions at each value of α_0 , which is slightly higher than that achieved in the mild-slope and Eckart examples due to the larger decrease in the number of Chamberlain solutions used. From Fig.3.6, we notice that there is no observable difference in the results, as expected with

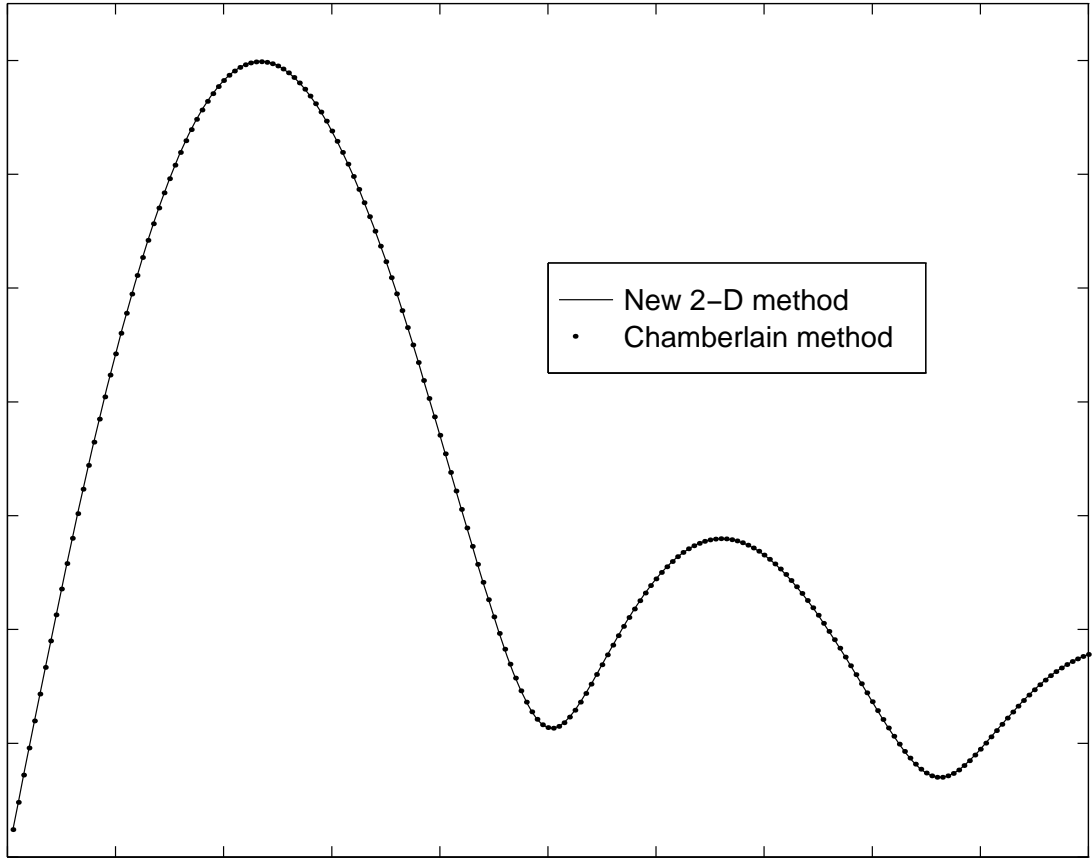


Figure 3.6: SWE reflected amplitude for depth profile $H(x) = 1+x(1-x^2)(0 \leq x \leq 1)$.

the choice in the tolerance of the errors. Similar percentage savings have been found for all three model equations on all bed profiles tested, with the tolerance in the error as specified above.

This section has shown that the two-dimensional trial space method significantly reduces CPU run-times by approximately one third for all three model equations on all depth profiles tested. Although this is an excellent improvement, we can do even better as shown in the next subsection.

3.3.3 Extra computational saving

A further source of computational saving can be effected without compromising the approximations already described. As already mentioned in this chapter, by substituting trial functions $\xi_k^{\alpha_0}$ ($k = 1, 2$) into the functionals $J_k^{\alpha_0}$ ($k = 1, 2$), given by

$$J_k^{\alpha_0}(\xi_k^{\alpha_0}) = 2(\xi_k^{\alpha_0}, S^{\alpha_0} f_k^{\alpha_0}) - (\hat{A}^{\alpha_0} \xi_k^{\alpha_0}, \xi_k^{\alpha_0}) \quad (k = 1, 2),$$

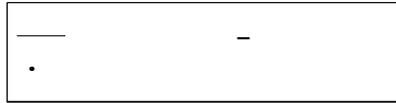
we generate approximations to the inner products

$$(\chi_k^{\alpha_0}, P^{\alpha_0} f_k^{\alpha_0}) \quad (k = 1, 2). \quad (3.15)$$

Similarly, by substituting trial functions $\mu_k^{\alpha_0}$ ($k = 1, 2$) into the functional $J_3^{\alpha_0}$, given by

$$J_3^{\alpha_0}(\mu_k^{\alpha_0})$$

It turns out that $J_3^{\alpha_0}(\xi_1^{\alpha_0}, \xi_2^{\alpha_0})$ and $J_3^{\alpha_0}(\mu_1^{\alpha_0}, \mu_2^{\alpha_0})$



had a run-time of 51m55s and Eckart's equation had one of 49m37s. Miles [40] also revived Eckart's equation, when he derived it from a new variational approach. Miles' notes that Eckart's equation conserves wave action but, unlike the mild-slope equation, does not conserve wave energy (except for uniform depth). Miles compares the two approximations through the calculation of reflection from a gently sloping beach of finite offshore depth and finds that Eckart's equation is inferior to the mild-slope equation in its prediction of the amplitude in the reflection problem if the offshore depth is neither shallow or deep. This agrees with the evidence appearing in Fig.3.5 where the reflected amplitudes of the mild-slope and Eckart approximations are compared over a talud with depth profile $H(x) = 1 - \frac{2}{3}x$ ($0 \leq x \leq 1$). The similarity of the mild-slope and Eckart solutions, depicted in Fig.3.5 for the depth profile $H(x) = 1 - \frac{2}{3}x$ ($0 \leq x \leq 1$) encouraged attempts to improve Eckart's approximation without compromising its advantageous explicit form.

The depth profiles of concern here are the ones which vary only linearly [rapatadv-w-TD-tageous

numbers could be resolved by simply using the correct wave number, given by the positive real root of the dispersion relation (3.3) in Eckart's equation instead of Eckart's approximation to it, which is given by (3.19). However, this device defeats the advantage offered by Eckart's equation – that each term in the equation was explicit. So the issue is whether a new, explicit approximation to the positive real root of (3.20) can be generated which is more accurate than (3.21). This is indeed possible.

A direct approach is used in which the solution x of (3.20) is approximated by adding a small correction term to (3.21). Thus x is approximated in the form

$$x = x_0 + x_1$$

where $x_0 = a\sqrt{\coth(a)}$ and x_1 is a small correction term. Substituting for x in (3.20) gives

$$a = (x_0 + x_1) \tanh(x_0 + x_1) ,$$

that is,

$$a = (x_0 + x_1) \left[\frac{\tanh(x_0) + \tanh(x_1)}{1 + \tanh(x_0) \tanh(x_1)} \right] . \quad (3.22)$$

Then, using the expansion $\tanh(x_1) = x_1 + O(x_1^3)$,

$$\begin{aligned} & a(1 + \tanh(x_0) \tanh(x_1)) \\ &= a + a \tanh(x_0) \tanh(x_1) \\ &= a + (x_0 + x_1) \left[\frac{\tanh(x_0) + \tanh(x_1)}{1 + \tanh(x_0) \tanh(x_1)} \right] \tanh(x_0) \tanh(x_1) \\ &= a + (x_0 + x_1) \left[\frac{\tanh(x_0) + x_1 + O(x_1^3)}{1 + [x_1 + O(x_1^3)] \tanh(x_0)} \right] \tanh(x_0) [x_1 + O(x_1^3)] \\ &= a + [x_0 \tanh^2(x_0)] x_1 + O(x_1^2) , \end{aligned}$$

and

$$(x_0 + x_1)[\tanh(x_0) + \tanh(x_1)] = x_0 \tanh(x_0) + x_1(x_0 + \tanh(x_0)) + O(x_1^2) .$$

Thus (3.22) becomes

$$a + [x_0 \tanh^2(x_0)] x_1 = x_0 \tanh(x_0) + x_1(x_0 + \tanh(x_0)) + O(x_1^2) ,$$

and neglecting second and higher order terms in x_1 (as x_1 is assumed to be small) gives

$$x_1 = \frac{a - x_0 \tanh(x_0)}{x_0 + \tanh(x_0) - x_0 \tanh^2(x_0)} .$$

Thus, the new two-term explicit approximation to (3.20) is given by

$$\begin{aligned} x &= x_0 + x_1 \\ &= x_0 + \frac{a - x_0 \tanh(x_0)}{x_0 + \tanh(x_0) - x_0 \tanh^2(x_0)} , \end{aligned}$$

which simplifies to

$$x = \frac{x_0^2 \operatorname{sech}^2(x_0) + a}{x_0 \operatorname{sech}^2(x_0) + \tanh(x_0)} . \quad (3.23)$$

Computations have shown that (3.23) gives the solution x of (3.20) to machine accuracy for $a > 3.1$, and for $0 < a < 3.1$, the maximum difference is 0.04%. Thus (3.23) is a new explicit approximation to (3.20) which is a significant improvement on (3.21).

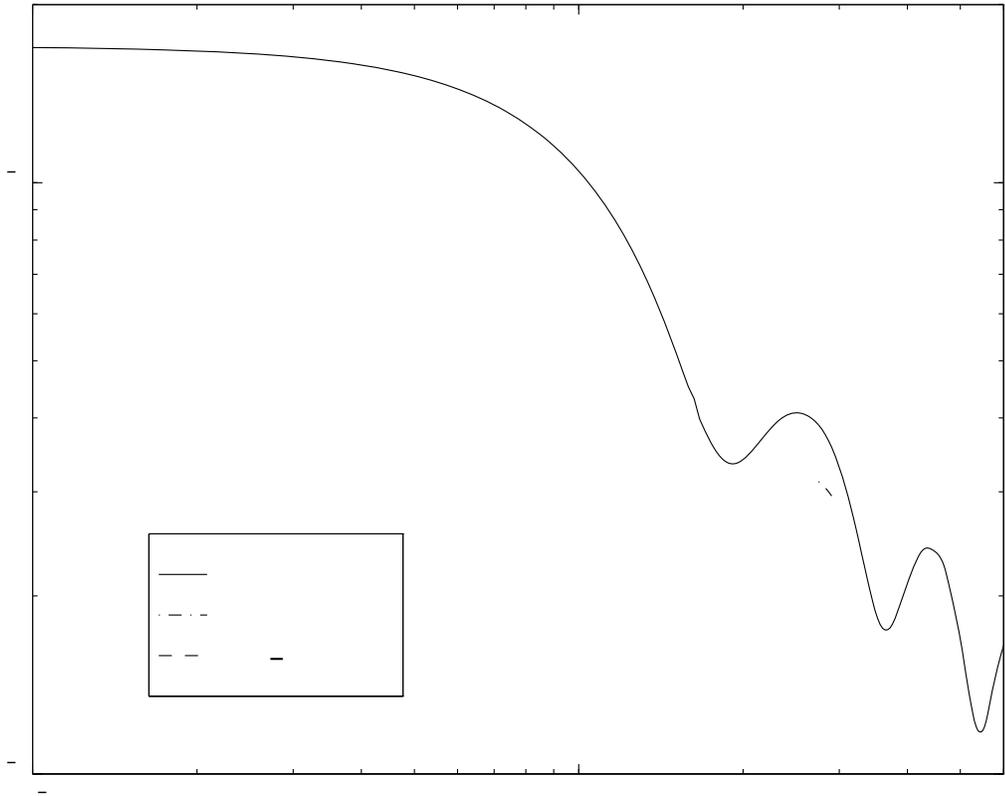
We shall now replace the function $\kappa = \kappa(x)$ defined by (3.19) by

$$\kappa(x) = \frac{1}{\tau H} \left(\frac{[v \operatorname{sech}(v)]^2 + \lambda \tau H}{v \operatorname{sech}^2(v) + \tanh(v)} \right) , \quad (3.24)$$

where $v = v(x) = \lambda \tau H \sqrt{\coth(\lambda \tau H)}$, in Eckart's equation, and call the resulting equation the new Eckart equation. We now find the solution of the new Eckart equation for an incident wave of unit amplitude from $x = -\infty$ over the depth profile given by

$$H(x) = 1 - \frac{2}{3}x \quad (0 \leq x \leq 1) .$$

We use the streamlined two-dimensional method to solve this problem with α_0 taking values between 0.05 and 8.5 at intervals of 0.05 (with τ given at each value of α_0 by $\tau = \sqrt{0.6\alpha_0}$). We choose again the tolerance in the error to be a minimum of 2.s.f. accuracy in $|R_k|$ and $|T_k|$ ($k = 1, 2$). The amplitude of the reflected wave given by the new Eckart equation is depicted in Fig.3.8, along with the corresponding results from the mild-slope and Eckart's equations. We see that the peaks and troughs of the reflected amplitudes predicted by the mild-slope and new Eckart equations are almost in line. The size of the reflected amplitude predicted by the new Eckart equation is also an increase on that given by Eckart's equation. However, the reflected amplitude given by the new Eckart equation is still not as large as that given by the mild-slope equation. The difference in results from both is now due to the difference of the mild-slope and Eckart U functions. As yet, no approximation has been found, such as the one used in conjunction with the wave number functions, that can rectify this difference. The new Eckart



on the bed shape and so it was hoped that this device would bring the reflected amplitude into line. The flat bed depths for the Eckart problem in $0 \leq x$ and $x \geq 1$ were chosen so that the Eckart and mild-slope wave numbers were identical at each α_0 and τ over these flat regions. This guaranteed that at each value of α_0 and τ , the mild-slope and Eckart problems had the same incident wave. A variety of c

approximation is effected by replacing the κ function (3.19) in Eckart's equation by (3.24). The new equation still gives a slightly inferior reflected amplitude than that given by the MSE. The very accurate, explicit approximation (3.23) to the root of the dispersion relation (3.20) has never been seen before, and is an excellent first term to use in an iteration method to give machine accurate solutions of (3.20). (See Newman [44] for details of such iterative methods.)

3.5 Symmetry Properties

Here, certain intrinsic properties of a particular type of second-order differential

where the constants e_i

scattered waves propagating towards $x = \pm\infty$ respectively. As already noted in Chapter 2, the reflection and transmission coefficients for an incident wave from the left ($A^+ = 0$) are defined by

$$R_1 = \frac{B^-}{A^-} \quad \text{and} \quad T_1 = \frac{B^+}{A^-} \quad (3.32)$$

and those for an incident wave from the right ($A^- = 0$) are defined by

$$R_2 = \frac{B^+}{A^+} \quad \text{and} \quad T_2 = \frac{B^-}{A^+} \quad (3.33)$$

Using the equations (3.31) and enforcing the continuity of ϕ_0 and ϕ'_0 at $x = 0$ and $x = 1$ gives the boundary conditions

$$\begin{aligned} \phi'_0(0) + i\kappa_0\phi_0(0) &= 2A^-i\kappa_0, \\ \phi'_0(1) - i\kappa_1\phi_0(1) &= -2A^+i\kappa_1e^{-i\kappa_1}. \end{aligned} \quad (3.34)$$

Choosing p , q , r and m of the differential equation (3.25) to be the corresponding terms in differential equation (3.30), that is, $p = U$, $q = \kappa^2U$, $r = 0$ and $m = 0$, reduces (3.29) to the identity

$$\begin{aligned} 0 &= U(1) \left\{ \phi(1)\psi(1) \left[\frac{a_1}{b_1} - \frac{e_1}{f_1} \right] + \frac{g_1}{f_1}\phi(1) - \frac{c_1}{b_1}\psi(1) \right. \\ &\quad \left. - U(0) \left\{ \phi(0)\psi(0) \left[\frac{a_0}{b_0} - \frac{e_0}{f_0} \right] + \frac{g_0}{f_0}\phi(0) - \frac{c_0}{b_0}\psi(0) \right\} \right. \end{aligned} \quad (3.35)$$

Now the symmetry relations of the reflection and transmission coefficients can be easily found. Firstly, choose ϕ to be the solution of (3.30) and (3.34) for an incident wave of unit amplitude from the left (so $A^- = 1$, $A^+ = 0$) and choose ψ to be the complex conjugate of ϕ . Hence ψ satisfies (3.30) and the constants in the boundary conditions (3.27) and (3.28) satisfied by ϕ and ψ respectively are given by

$$\begin{aligned} a_0 = i\kappa_0 = \bar{e}_0, \quad b_0 = 1 = f_0, \quad c_0 = 2i\kappa_0 = \bar{g}_0, \\ a_1 = -i\kappa_1 = \bar{e}_1, \quad b_1 = 1 = f_1, \quad c_1 = 0 = \bar{g}_1 \end{aligned} \quad (3.36)$$

and from (3.31) and (3.32) we see that the functions ϕ and ψ have end-point values

$$\phi(0) = 1 + R_1 = \overline{\psi(0)} \quad \text{and} \quad \phi(1) = T_1e^{i\kappa_1} = \overline{\psi(1)}. \quad (3.37)$$

Substituting (3.36) and (3.37) into the identit

Substituting into the identity (3.35) gives the final symmetry relation

$$|R_2$$

Substituting $x = 0$ and $x = 1$ into the integral equation satisfied by ψ_j ($j = 1, 2$) yields

$$\begin{aligned}\frac{i}{2\kappa_0} \int_0^1 f^+(t)\rho(t)\psi_j(t) dt &= \alpha_j + \beta_j - \psi_j(0) , \\ \frac{i}{2\kappa_0} \int_0^1 f^-(t)\rho(t)\psi_j(t) dt &= \alpha_j + \beta_j e^{-2i\kappa_0} - e^{-i\kappa_0}\psi_j(1) ,\end{aligned}$$

and hence it follows that

$$S(\psi_1, \psi_2) = \alpha_1\psi_2(0) - \alpha_2\psi_1(0) + (\beta_1\psi_2(1) - \beta_2\psi_1(1))e^{-i\kappa_0} = 0 . \quad (3.50)$$

This identity is equivalent to the identity (3.35) which was derived within the framework of differential equations. Before the symmetry relations are rederived, the definitions of the reflection and transmission coefficients, as given previously in Chapter 2, are restated here for convenience as follows:

$$\begin{aligned}R_1 &= \zeta_1(0) - 1 , \\ T_1 &= \zeta_1(1)e^{-i\kappa_1} \sqrt{\frac{U(0)}{U(1)}} .\end{aligned} \quad (3.51)$$

$$\begin{aligned}R_2 &= \zeta_2(1)e^{-i\kappa_1} \sqrt{\frac{U(0)}{U(1)}} - e^{-2i\kappa_1} , \\ T_2 &= \zeta_2(0) ,\end{aligned} \quad (3.52)$$

where the subscripts 1, 2 distinguish between waves incident from the left or the right respectively.

Substituting $\psi_1 = \zeta_1$ (and therefore $\alpha_1 = \hat{a}_1$, $\beta_1 = \hat{b}_1$) and $\psi_2 = \bar{\zeta}_1$ (and therefore $\alpha_2 = \tilde{a}_1$, $\beta_2 = \tilde{b}_1$) in S gives

$$S(\zeta_1, \bar{\zeta}_1) = \bar{\zeta}_1(0) + \zeta_1(0) - |\zeta_1(0)|^2 - \frac{\kappa_1}{\kappa_0} |\zeta_1(1)|^2 = 0 ,$$

and employing (3.51) reduces this to the symmetry relation (3.38), namely,

$$|R_1|^2 + \frac{\kappa_1 U(1)}{\kappa_0 U(0)} |T_1|^2 = 1 .$$

By the same procedure

$$\begin{aligned}S(\zeta_1, \zeta_2) = 0 &\quad \text{implies} \quad \kappa_1 U(1) T_1 = \kappa_0 U(0) T_2 , \\ S(\zeta_1, \bar{\zeta}_2) = 0 &\quad \text{implies} \quad \kappa_1 U(1) \bar{R}_2 T_1 = -\kappa_0 U(0) \bar{T}_2 R_1 , \\ S(\zeta_2, \bar{\zeta}_2) = 0 &\quad \text{implies} \quad |R_2|^2 + \frac{\kappa_0 U(0)}{\kappa_1 U(1)} |T_2|^2 = 1 .\end{aligned}$$

In the final part of this section, we need to recall the rank two system of equations defined in Chapter 2. This relates $\zeta_j(0)$ and $\zeta_j(1)$ ($j = 1, 2$), the end point values of the solutions ζ_j ($j = 1, 2$) of the integral equation (3.44) with the inner products (χ_j, Pf_k) ($j, k = 1, 2$). The χ_j ($j = 1, 2$) $\in L_2(0, 1)$ are the solutions of the real valued integral equations

$$(I - LP)\chi_j = f_j \quad (j = 1, 2),$$

where I is the identity operator and the operators L and P are defined by

$$(L\chi)(x) = \frac{1}{2\kappa_0} \int_0^1 \sin(\kappa_0|x-t|) \chi(t) dt \quad \text{and} \quad (P\chi)(x) = \rho(x)\chi(x),$$

and where the free terms are defined by $f_1(x) = \cos(\kappa_0 x)$ and $f_2(x) = \sin(\kappa_0 x)$. In Chapter 2 and the first part of Chapter 3, we have used variational techniques to approximate the values of these inner products. For convenience we give the rank two system of equations here, namely,

$$\begin{aligned} & \left(\left(\begin{array}{cc} b_2 & b_3 \\ b_5 & b_6 \end{array} \right) - i \left(\begin{array}{cc} B_1 & B_2 \\ \overline{B}_2 & B_1 \end{array} \right) \left(\begin{array}{cc} c_5 - b_2 & c_6 - b_3 \\ c_2 - b_5 & c_3 - b_6 \end{array} \right) \right) \begin{pmatrix} \zeta_j(0) \\ \zeta_j(1) \end{pmatrix} \\ & = - \begin{pmatrix} b_1 \\ b_4 \end{pmatrix} + i \left(\begin{array}{cc} B_1 & B_2 \\ \overline{B}_2 & B_1 \end{array} \right) \begin{pmatrix} c_4 - b_1 \\ c_1 - b_4 \end{pmatrix} \quad (j = 1, 2), \end{aligned} \quad (3.53)$$

where the values of known constants b_i and c_i ($i = 1, \dots, 6$) are chosen according to whether ζ_j corresponds to the solution of the integral equation (3.44) for an incident wave from the left or right, or the complex conjugate of the solution of (3.44) for an incident wave from the left or right (as seen earlier in this section), and

$$B_1 = \frac{1}{2}(A_{11} + A_{22}) \quad \text{and} \quad B_2 = \frac{1}{2}(A_{11} + 2iA_{12} - A_{22})$$

and

$$A_{jk} = \frac{1}{2\kappa_0} (\chi_j, Pf_k) \quad (j, k = 1, 2).$$

Now the reflection and transmission coefficients are defined by (3.51) and (3.52) in terms of $\zeta_j(0)$ and $\zeta_j(1)$ ($j = 1, 2$) and therefore, through the rank two system of equations (3.53), in terms of the inner products (χ_j, Pf_k) ($j, k = 1, 2$). When calculating the reflection and transmission coefficients, it was noticed that

where

$$\underline{x}_j = \begin{pmatrix} d_j \\ e_j \end{pmatrix}, \quad \underline{y}_j = \begin{pmatrix} \alpha_j - d_j \\ \beta_j - e_j \end{pmatrix} \quad \text{and} \quad W = \begin{pmatrix} B_1 & B_2 \\ \overline{B_2} & B_1 \end{pmatrix}.$$

Now as B_1 is real, $W^* = W$, where $*$ denotes the conjugate transpose.

It follows that

$$\underline{y}_2^* \underline{x}_1 = \underline{y}_2^* (iW \underline{y}_1) = (-i \underline{y}_1^* W^* \underline{y}_2)^* = (-i \underline{y}_1^* W \underline{y}_2)^* = (-\underline{y}_1^* \underline{x}_2)^* = -\underline{x}_2^* \underline{y}_1,$$

and so the identity

$$\underline{y}_2^* \underline{x}_1 + \underline{x}_2^* \underline{y}_1 = 0 \tag{3.58}$$

results. Recapping the above procedure, the two forms of (3.57) have been used to eliminate the W matrix to give the identity (3.58). The inner products $(\chi_j, P f_k)$ ($j, k = 1, 2$) only appear in the W matrix which only occurs in equation (3.57) of our breakdown of the rank two system. So now an identity (3.58), very similar to the previous identity (3.50) found in our integral equation framework, has been derived that relates $\zeta_j(0)$ and $\zeta_j(1)$ ($j = 1, 2$) and is independent of the inner products. Therefore this identity will always be satisfied no matter what ν is.

the symmetry relations. It follows that the symmetry relations are an intrinsic part of the problem rather than of its exact solution, in the sense that they are always satisfied whatever the accuracy of the solution.

In this chapter, several extensions to the work appearing in Chamberlain [7] & [8] have been presented. A new integral equation method has been developed which solves the mild-slope, Eckart and linearised shallow water equations over a range of their parameters in less than one half of the CPU time required by Chamberlain's [7] integral equation procedure. Eckart's approximation has been investigated and improved and, as a by-product, a new, explicit and very accurate approximation to the solution of the dispersion relation has also been found. Finally, after rederiving the symmetry relations of the reflection and transmission coefficients of these approximations, we have shown that these coefficients satisfy the symmetry relations even when they are inaccurately calculated, an unexpected property.

Chapter 4

new approximation to wave scattering

In this chapter, a new approximation to the full linear wave scattering problem is derived. A Galerkin approach is used to derive an approximation to the time-independent velocity potential ϕ which takes account of decaying wave modes as well as progressive wave modes. The present approach uses an n -term approximation based on the propagating wave mode and the first $(n - 1)$ decaying wave modes over a flat bed. If none of the decaying wave mode terms are used and if we discard terms that are second-order on the basis of the mild-slope assumption $|\nabla h| \ll kh$, where h is the undisturbed fluid depth and k is the corresponding wave number, then this approach reduces to the mild-slope approximation. The extended approximation is then tested on a selection of beds of varying steepness and the results are compared with the corresponding results given by the mild-slope approximation.

4.1 A Galerkin approximation method

Recall from Chapter 2, that the time-independent velocity potential ϕ satisfies

$$\tilde{\nabla}^2 \phi = 0 \quad -h < z < 0, \quad (4.1)$$

$$\frac{\partial \phi}{\partial z} - \nu \phi = 0 \quad \text{on } z = 0, \quad (4.2)$$

$$\frac{\partial \phi}{\partial z} + \nabla h \cdot \nabla \phi = 0 \quad \text{on } z = -h(x, y), \quad (4.3)$$

where $\tilde{\nabla} = (\frac{\partial}{\partial x}, \frac{\partial}{\partial y}, \frac{\partial}{\partial z})$ and $\nabla = (\frac{\partial}{\partial x}, \frac{\partial}{\partial y})$. We also require additional conditions on lateral boundaries or a radiation condition if the fluid extends to infinity to completely specify ϕ . For the moment, we do not concern ourselves with these additional conditions as our initial aim is to reduce the dimension of the boundary-value problem for ϕ by approximating its dependence on the z co-ordinate. This is achieved via a direct application of the classical Galerkin method.

We seek a weak solution $\xi \approx \phi$ of (4.1) – (4.3) in the sense that the residual $\tilde{\nabla}^2 \xi$ is required to be orthogonal to a given function ψ . In other words, we require

$$\iint_D \left(\int_{-h}^0 \psi \tilde{\nabla}^2 \xi dz \right) dx dy = 0 ,$$

where D can be any domain in the plane $z = 0$. Integrating by parts gives

$$\iint_D \left(\int_{-h}^0 (\psi \nabla^2 \xi + \xi \psi_{zz}) dz + [\psi \xi_z - \xi \psi_z]_{z=-h}^{z=0} \right) dx dy = 0 ,$$

which becomes

$$\iint_D \left(\int_{-h}^0 (\psi \nabla^2 \xi + \xi \psi_{zz}) dz - [\xi (\psi_z - \nu \psi)]_{z=0} + [\xi \psi_z + \psi \nabla h \cdot \nabla \xi]_{z=-h} \right) dx dy = 0, \quad (4.4)$$

when boundary conditions (4.2) and (4.3) are imposed on ξ . Equation (4.4) is a weak form of the boundary-value problem (4.1) – (4.3) and can be used to generate approximations to the solution of that problem.

We shall use a Galerkin approximation $\xi \approx \phi$ of the form

$$\xi(x, y, z) = \sum_{j=0}^{n-1} \phi_j(x, y) w_j(x, y, z) , \quad (4.5)$$

where w_j ($j = 0, 1, \dots, n-1$) are given functions and ϕ_j ($j = 0, 1, \dots, n-1$) are to be determined from (4.4). We choose our given function ψ as

$$\psi(x, y, z) = w_k(x, y, z) ,$$

for some $k \in (0, 1, \dots, n-1)$. After some simple manipulation, which includes use of the identity

$$\nabla^2 (\phi_j w_j) = w_j \nabla^2 \phi_j + 2 \nabla \phi_j \cdot \nabla w_j + \phi_j \nabla^2 w_j ,$$

it is found that the functions ϕ_k ($k = 0, \dots, n-1$) must satisfy the coupled system of differential equations

$$\sum_{j=0}^{n-1} \left\{ \nabla^2 \phi_j \int_{-h}^0 w_j w_k dz + \right.$$

for $k = 0, 1, \dots, n - 1$, where

$$\tilde{\mathbf{f}}_{jk} = \tilde{\mathbf{f}}_{jk}(w_j, w_k) = \nabla h(w_j w_k)_{z=-h} + 2 \int_{-h}^0 w_k \nabla w_j dz$$

and

$$\begin{aligned} \tilde{g}_{jk} = \tilde{g}_{jk}(w_j, w_k) = & \left[w_j \left(\nu w_k - \frac{\partial w_k}{\partial z} \right) \right]_{z=0} + \left[w_j \frac{\partial w_k}{\partial z} + w_k \nabla h \cdot \nabla w_j \right]_{z=-h} \\ & + \int_{-h}^0 w_k \nabla^2 w_j dz . \end{aligned}$$

Chamberlain and Porter [9] have used this Galerkin approach with a 1-term approximation (that is, $n = 1$ in (4.5)) to derive a new approximation to ϕ that contains the mild-slope approximation as a special case. They also show that this new approximation to ϕ can be derived via a variational approach, which is similar to the recent work of Miles [40]. Indeed, Chamberlain and Porter [9] use the same trial function in both the Galerkin and variational approaches. The variational principle used in [9] is $\delta L = 0$ where L is the functional given by

$$L(\xi) = \iint_D \left(\frac{1}{2} \nu (\xi^2)_{z=0} - \frac{1}{2} \int_{-h}^0 (\tilde{\nabla} \xi)^2 dz \right) dx dy .$$

By considering variations which vanish on the lateral boundary $C \times [-h, 0]$, where C is the boundary of D , it follows that L is stationary at $\xi = \phi$ if and only if ϕ satisfies (estoT//Tf2/imation t//TDf2//TD2ifandand//Tf2//TprincipSo/TD2vonalhvTj2//TD2/

of the relation

$$-\nu = B_j \tan(B_j h) , \quad (4.8)$$

arranged in ascending order of magnitude. Equation (4.8) has an imaginary root $B_0 = -ik$, and so we can write \tilde{w}_0 in the form

$$\tilde{w}_0 = \frac{\cosh(k(z+h))}{\cosh(kh)} , \quad (4.9)$$

where $k = k(h)$ is the real positive root of the local dispersion relation

$$\nu = k \tanh(kh) . \quad (4.10)$$

For each fixed value of ν , the equations (4.8) and (4.10) implicitly define $B_j = B_j(h)$ ($j = 1, \dots, n-1$) and $k = k(h)$ respectively. Notice that these w_j ($j = 0, \dots, n-1$) are an orthogonal set for $z \in [-h, 0]$ and they satisfy the same surface condition as ϕ , namely

$$\nu w_j - \frac{\partial w_j}{\partial z} = 0 \quad \text{on } z = 0 \quad (j = 0, 1, \dots, n-1) .$$

It follows that the function $\phi_0 w_0$ is an approximation to the progressive wave mode part of ϕ and the functions $\phi_1 w_1, \phi_2 w_2, \dots, \phi_{n-1} w_{n-1}$ are approximations to the 1st, 2nd, \dots , $(n-1)$ th decaying wave mode parts of ϕ respectively.

With this choice for the functions w_j ($j = 0, 1, \dots, n-1$), it follows from equations (4.8) and (4.10) that, at each x ,

$$\int_{-h}^0 \tilde{w}_j \tilde{w}_k dz = \begin{cases} 0 & j \neq k , \\ u_j(h) & j = k . \end{cases}$$

where

$$u_j(h) = \frac{1}{2B_j} \tan(B_j h) \left(1 + \frac{2B_j h}{\sin(2B_j h)} \right) \quad (j = 0, 1, \dots, n-1) ,$$

with $B_0 = -ik$. The approximate solution $\xi(x, z) = \sum_{j=0}^{n-1} \phi_j w_j \approx \phi$ satisfies the same free surface condition as ϕ , namely

$$\frac{\partial \xi}{\partial z} - \nu \xi = 0 \quad \text{on } z = 0 .$$

We recall from Chapter 2 that over a flat bed, the general solution of (4.1) – (4.3) is given by $\phi = \sum_{j=0}^{\infty} \phi_j w_j$. Hence, over a flat bed, $\phi = \sum_{j=0}^{n-1} \phi_j w_j$ is the only solution

of (4.1) – (4.3) corresponding to the progressive wave mode and the first $(n - 1)$ decaying wave modes. Also, since the free surface elevation η is defined by

$$\eta(x, t) = Re \left\{ \frac{-i\sigma}{g} \phi(x, 0) e^{-i\sigma t} \right\} ,$$

then the approximate solution is such that $\eta \approx Re \left\{ e^{-i\sigma t} \sum_j^{n-1} \right\}$

This is a relatively new approximation to the progressive wave mode part of ϕ and equation (4.15) is known as the modified mild-slope equation (MMSE). This equation was first derived by Chamberlain [6] and more recently by Chamberlain and Porter [9] via the Galerkin and variational procedures given earlier in this section. Investigations of the modified mild-slope equation over a variety of bed profiles are carried out in Chamberlain and Porter [9] and in a subsequent paper by Chamberlain and Porter [10]. Similarly, with the 1-term trial approximation,

Other approximations for wave scattering by a bed of varying topography that include decaying wave mode terms have been given by O'Hare and Davies [45] and Rey [52]. The approximation used by both sets of authors is very similar and involves replacing the bed profile by a series of horizontal shelves joining at vertical steps. Over each flat shelf, the velocity potential has an infinite series represen

and

$$\tilde{w}_j'' = \frac{\partial^2 \tilde{w}_j}{\partial h^2} (h')^2 + \frac{\partial \tilde{w}_j}{\partial h} h'' \quad (j = 0, \dots, n-1).$$

Therefore, the functions f_{jk} and g_{jk} ($j, k = 0, \dots, n-1$) defined by (4.12) and (4.13) respectively can be written as

$$f_{jk}(x) = \left([\tilde{w}_j \tilde{w}_k]_{z=-h} + 2 \int_{-h}^0 \tilde{w}_k \frac{\partial \tilde{w}_j}{\partial h} dz \right) h' \quad (4.21)$$

and

$$g_{jk}(x) = \left(\int_{-h}^0 \tilde{w}_k \frac{\partial \tilde{w}_j}{\partial h} dz \right) h'' + \left(\left[\tilde{w}_k \frac{\partial \tilde{w}_j}{\partial h} \right]_{z=-h} + \int_{-h}^0 \tilde{w}_k \frac{\partial^2 \tilde{w}_j}{\partial h^2} dz \right) (h')^2. \quad (4.22)$$

A little algebra incorporating the use of relations (4.8) and (4.10) shows that the integrals appearing in (4.21) and (4.22) are given by

$$\int_{-h}^0 \tilde{w}_k \frac{\partial \tilde{w}_j}{\partial h} dz = \begin{cases} \sec(B_k h) \sec(B_j h) \left(\frac{B_j^2}{B_k^2 - B_j^2} \right) & (k \neq j), \\ \frac{\sec^2(B_k h)}{4(D_k + \sin(D_k))} \left[\sin(D_k) - D_k \cos(D_k) \right] & (k = j) \end{cases}$$

and

$$\int_{-h}^0 \tilde{w}_k \frac{\partial^2 \tilde{w}_j}{\partial h^2} dz = \frac{-4B_j^3 \sec(B_k h) \sec(B_j h)}{D_k + \sin(D_k)} \left(\frac{2B_k^2 + (B_j^2 - B_k^2) \sin^2(B_j h)}{((B_k + B_j)(B_k - B_j))^2} \right) \quad (k \neq j)$$

and

$$\int_{-h}^0 \tilde{w}_k \frac{\partial^2 \tilde{w}_k}{\partial h^2} dz = \frac{-B_k \sec^2(B_k h)}{12(D_k + \sin(D_k))^3} \left[(D_k)^4 + 4(D_k)^3 \sin(D_k) + 3D_k(D_k + 2\sin(D_k))(\sin^2(D_k) - 2\cos(D_k)) + 6\sin^2(D_k) \left(1 + 2\cos^2\left(\frac{1}{2}D_k\right) \right) \right],$$

where $D_k = 2B_k h$, and $B_0 = -ik$. It is simple to see that the remaining terms in (4.21) and (4.22) are given by

$$\left[\tilde{w}_k \tilde{w}_j \right]_{z=-h} = \sec(B_k h) \sec(B_j h) \quad (j, k = 0, \dots, n-1)$$

and

$$\left[\tilde{w}_k \frac{\partial \tilde{w}_j}{\partial h} \right]_{z=-h}$$

4.2 Sc ling

We choose the same class of depth profiles as in Chapter 2, which are varying only in some finite interval of x . We assume that

$$h(x) = \begin{cases} h_0 & \forall x \leq 0, \\ h_1 & \forall x \geq l, \end{cases}$$

where h_0 , h_1 and l are given constants, and where $h(x)$ is continuous on $(-\infty, \infty)$. We allow h to have a slope discontinuity at the ends of the varying bed, that is, at $x = 0$ and $x = l$. At the moment we shall consider the scattering of plane harmonic waves normally incident on a given depth profile. The generalisation to obliquely incident waves will be dealt with later.

The scaling process now employed is the same as that used in Chapter 2.

Remembering that $B_0 = -ik$, we also define the real dimensionless parameter κ by $\kappa = i\beta_0$. As in Chapter 2, we shall discard the accents from the scaled independent variable and from the ϕ_k ($k = 0, \dots, n-1$) in the pursuit of a simple notation.

In terms of these dimensionless quantities the coupled system of equations (4.11) is

$$U_k \left(\phi_k'' - \beta_k^2 \phi_k \right) + \sum_{j=0}^{n-1} \left\{ F_{jk} \phi_j' + G_{jk} \phi_j \right\} = 0 \quad (k = 0, 1, \dots, n-1), \quad (4.23)$$

where the prime denotes differentiation with respect to x . The functions U_k are given by

$$U_k = \frac{1}{2\beta_k \tau} \tan(\beta_k \tau H) \left(1 + \frac{2\beta_k \tau H}{\sin(2\beta_k \tau H)} \right) \quad (k = 0, \dots, n-1) \quad (4.24)$$

and the functions β_k are the positive real roots of

$$-\alpha_0^2 \tau = \beta_k \tan(\beta_k \tau H) \quad \left(\frac{1}{\kappa} \frac{D\phi_j}{dx} + \beta_j \phi_j \right) = \sigma_j \phi_j \quad (j = 0, \dots, n-1)$$

and

$$G_{kk} = \sec^2(\beta_k \tau H$$

to a hump arising from putting $h_0 = h_1$ and therefore $\kappa_0 = \kappa_1$ and $\beta_k^0 = \beta_k^1$ ($k = 1, \dots, n - 1$).

The fluid domain under consideration extends to infinity. Therefore, we prescribe radiation conditions for ϕ_k ($k = 0, \dots, n - 1$) that are based on the radiation condition for ϕ described in Chapter 2. Hence, we assume that two plane waves propagating from $x = \pm\infty$ with known coefficients A^\pm respectively are incident on the talud. The 1-dimensional analogue of the radiation condition for ϕ implies that the outgoing wave solutions must be bounded at $x = \pm\infty$. Hence, there will result 2 outgoing plane waves with unknown coefficients B_0^\pm heading towards $x = \pm\infty$ respectively. There will also result $2(n - 1)$ outgoing decaying wave modes with $(n - 1)$ of these heading towards $x = \infty$ with unknown coefficients B_k^+ ($k = 1, \dots, n - 1$) and with $(n - 1)$ heading towards $x = -\infty$ with unknown coefficients B_k^- ($k = 1, \dots, n - 1$). Therefore, we assume

$$\phi_0(x) = \begin{cases} A^- e^{i\kappa_0 x} + B_0^- e^{-i\kappa_0 x} & x \leq 0, \\ A^+ e^{-i\kappa_1 x} + B_0^+ e^{i\kappa_1 x} & x \geq 1, \end{cases} \quad (4. \quad B_1) =$$

Here, we have used the notation $W_j^0 = W_j(0, z)$, $W_j^1 = W_j(1, z)$ ($j = 0, \dots, n-1$), where $W_j = \frac{i}{\alpha_0^2 \tau} \tilde{W}_j$, and the functions \tilde{W}_j ($j = 0, \dots, n-1$) are given by

$$\tilde{W}_0(x, z) = \frac{\cosh(\kappa\tau(z+H))}{\cosh(\kappa\tau H)} \quad \text{and} \quad \tilde{W}_j(x, z) = \frac{\cos(\beta_j\tau(z+H))}{\cos(\beta_j\tau H)}.$$

The set of functions $\{\tilde{W}_j : j+1 \in \mathbb{N}\}$ is orthogonal for $z \in [-H, 0]$ and in particular

$$\int_{-H}^0 \tilde{W}_j \tilde{W}_k dz = \begin{cases} 0 & k \neq j, \\ U_j & k = j, \end{cases}$$

where $U_j = U_j(x)$ is defined by (4.24).

We wish our approximation ξ to possess as many properties of ϕ as possible, and so we certainly need to require that ξ and $\frac{\partial \xi}{\partial x}$ are continuous at the ends of the talud, that is, at $x = 0$ and $x = 1$, throughout the fluid depth. In other words, we require

$$\begin{aligned} \xi_1 &= \xi_2, & \frac{\partial \xi_1}{\partial x} &= \frac{\partial \xi_2}{\partial x} & (x = 0; -H(0) \leq z \leq 0), \\ \xi_2 &= \xi_3, & \frac{\partial \xi_2}{\partial x} &= \frac{\partial \xi_3}{\partial x} & (x = 1; -H(1) \leq z \leq 0). \end{aligned}$$

Boundary conditions on ϕ_j ($j = 0, \dots, n-1$) are now derived from the above matching equations by employing the same Galerkin procedure used in section 4.1 to derive the differential equation system satisfied by ϕ_j ($j = 0, \dots, n-1$).

Invoking the continuity of ξ at $x = 0$ gives

$$\sum_{j=0}^{n-1} C_j^- \tilde{W}_j^0 = \sum_{j=0}^{n-1} \phi_j(0) \tilde{W}_j^0 \quad (-H(0) \leq z \leq 0), \quad (4.33)$$

where

$$C_j^- = \begin{cases} A^- + B_0^- & (j = 0), \\ B_j^- & (j = 1, \dots, n-1). \end{cases}$$

Multiplying (4.33) by \tilde{W}_k^0 (for some $k \in [0, 1, \dots, n-1]$) and integrating with respect to z from $-H(0)$ to 0 gives

where

$$C_k^+ = \begin{cases} A^+ e^{-i\kappa_1} + B_0^+ e^{i\kappa_1} & (k = 0) , \\ B_k^+ e^{-\beta_k^1} & (k = 1, \dots, n-1) . \end{cases}$$

As we allow the depth function $H(x)$ to have a slope discontinuity at $x = 0$ and $x = 1$, then it follows that for $j = 0, \dots, n-1$

$$\left. \frac{\partial \tilde{W}_j}{\partial x} \right|_{x=0+} \neq 0 , \quad \left. \frac{\partial \tilde{W}_j}{\partial x} \right|_{x=0-} = 0 , \quad \left. \frac{\partial \tilde{W}_j}{\partial x} \right|_{x=1-} \neq 0 \quad \text{and} \quad \left. \frac{\partial \tilde{W}_j}{\partial x} \right|_{x=1+} = 0 ,$$

since the depth function $H(x)$ is constant for $x \leq 0$ and $x \geq 1$. Therefore, invoking continuity of $\frac{\partial \xi}{\partial x}$ at $x = 0$ gives

$$\sum_{j=0}^{n-1} D_j^- \tilde{W}_j^0 = \sum_{j=0}^{n-1} \left\{ \phi_j' \tilde{W}_j + \phi_j \frac{\partial \tilde{W}_j}{\partial x} \right\}_{x=0+} , \quad (4.36)$$

where

$$D_j^- = \begin{cases} i\kappa_0 (A^- - B_0^-) & (j = 0) , \\ \beta_j^0 B_j^- & (j = 1, \dots, n-1) . \end{cases}$$

Multiplying (4.36) by \tilde{W}_k^0 (for some $k \in [0, 1, \dots, n-1]$) and integrating with respect to z from $-H(0)$ to 0 gives

$$D_k^- = \phi_k'(0+) + \phi_k(0)[$$

and $d_{jk}^1 = d_{jk}(1-)$. Substituting (4.34) into the expression for D_k^- and (4.35) into the expression for D_k^+ gives the coupled boundary conditions

$$\phi_0'(0) + \phi_0(0)[i\kappa - \tau(\kappa H)'\tanh(\kappa\tau H)]|_{x=0} - \sum_{j=0}^{n-1} d_{j0}^0 \phi_j(0) = 2i\kappa_0 A^-, \quad (4.37)$$

$$\phi_0'(1) - \phi_0(1)[i\kappa + \tau(\kappa H)'\tanh(\kappa\tau H)]|_{x=1} - \sum_{j=0}^{n-1} d_{j0}^1 \phi_j(0) = -2i\kappa_1 e^{-i\kappa_1} A^+, \quad (4.38)$$

$$\phi_k'(0) - \phi_k(0)[\beta_k - \tau(\beta_k H)'\tan(\beta_k\tau H)]|_{x=0} - \sum_{j=0}^{n-1} d_{jk}^0 \phi_j(0) = 0, \quad (4.39)$$

$$\phi_k'(1) + \phi_k(1)[\beta_k + \tau(\beta_k H)'\tan(\beta_k\tau H)]|_{x=1} - \sum_{j=0}^{n-1} d_{jk}^1 \phi_j(1) = 0, \quad (4.40)$$

where $k = 0, \dots, n-1$ and where the derivatives are evaluated inside the interval $(0, 1)$.

The approximation to the free surface elevation is given by

$$\eta(x, t) \approx \text{Re} \left\{ e^{-i\sigma t} \xi(x, 0) \right\} \quad (-\infty < x < \infty).$$

These boundary conditions also make the approximation to the free surface continuous at $x = 0$ and $x = 1$. However, the approximation to the slope of the free surface is continuous at $x = 0$ and $x = 1$ only when the slope of the bed is also continuous at $x = 0$ and $x = 1$.

Massel [36] uses the same approach to derive the boundary conditions for his version of the z independent system (4.23). However, in his approach, Massel omits the $\frac{\partial \tilde{W}_j}{\partial x} \Big|_{x=0+}$ terms when he imposes his version of the matching condition

$$\frac{\partial \xi_1}{\partial x} = \frac{\partial \xi_2}{\partial x} \text{ at } x = 0 \quad (-H(0) \leq z \leq 0) \text{ and omits the } \frac{\partial \tilde{W}_j}{\partial x} \Big|_{x=0+} \text{ terms.}$$

the talud joins the flat beds. Therefore, the results given by Massel [36] for the 1-term approximation for Booij's test problem are wrong because he uses inappropriate boundary conditions.

In the case of a 1-term approximation, the differential equation system (4.23) reduces to the modified mild-slope equation

$$(U_0\phi_0')' + (\kappa^2 U_0 + G_{00})\phi_0 = 0 .$$

This is the differential equation that Massel [36] solved with his incorrect boundary conditions. Chamberlain and Porter [10], [9] have also used this equation in a variety of test problems. The above equation reduces to the well-known mild-slope equation if the G_{00} term is omitted. Some of the authors that have used this equation include Berkhoff [2], [3], Smith and Sprinks [54], Booij [5], Kirby [26], O'Hare and Davies [45], Chamberlain [7], [8], Rey [52], Chamberlain and Porter [10] and [9]. For both the modified mild-slope and mild-slope equations, all the above authors have used the boundary conditions which arise from enforcing the continuity of ϕ_0 and ϕ_0' at the junctions where the varying depth region meets the flat beds. For the scaling used in this chapter, these boundary conditions are given by

$$\phi_0'(0) +$$

are

$$\begin{aligned} \phi'_0(0+) + \phi_0(0) \left[i\kappa - \left(\frac{1}{2\kappa} - \frac{2\tau H \cosh^2(\kappa\tau H)}{\sinh(2\kappa\tau H) + 2\kappa\tau H} \right) \kappa' \right] \Big|_{0+} &= 2i\kappa_0 A^-, \\ \phi'_0(1-) - \phi_0(1) \left[i\kappa + \left(\frac{1}{2\kappa} - \frac{2\tau H \cosh^2(\kappa\tau H)}{\sinh(2\kappa\tau H) + 2\kappa\tau H} \right) \kappa' \right] \Big|_{1-} &= -2i\kappa_1 e^{-i\kappa_1} A^+. \end{aligned} \quad (4.42)$$

As far as is known, these boundary conditions are completely new and reduce to (4.41) only when the varying bed has a continuous slope at the junctions with the flat beds.

We shall refer to the sets (4.41) and (4.42) of boundary conditions for the mild-slope and modified mild-slope equations as the old set and new set of boundary conditions respectively.

In Section 4.8, we refer to the sets (4.41) and (4.42) of boundary conditions for the mild-slope and modified mild-slope equations as the old set and new set of boundary conditions respectively.

From equations (4.31) and (4.32) we see that $\phi_0(0) = A^- + B_0^-$, $\phi_0(1) = A^+ e^{-i\kappa_1} + B_0^+ e^{i\kappa_1}$, $\phi_k(0) = B_k^-$ ($k = 1, \dots, n-1$) and $\phi_k(1) = B_k^+ e^{-\beta}$

We only need to consider the problem of approximating the reflection, transmission and decay coefficients, and then the B_k^\pm ($k = 0, \dots, n - 1$) can be determined through (4.47) for any A^\pm .

4.4 A system of Fredholm integral equations

We wish to solve the coupled differential equation system (4.23) together with boundary conditions (4.37) – (4.40). We know from Chamberlain [7] that when the system (4.23) is a scalar equation (that is, when (4.23) is generated using a 1-term approximation) then an integral equation procedure can be used to solve the boundary-value problem to a high degree of accuracy. When the system (4.23) is a vector equation (that is, when (4.23) is generated using an n ($n > 1$) term approximation) an integral equation solution method is much more difficult to implement. A method of converting the system (4.23) and boundary conditions (4.37) – (4.40) into a system of Fredholm integral equations is now given. The resulting system of integral equations presents serious problems for numerical solution methods and no attempt is made to solve this integral equation system here.

Chamberlain [6] expends much effort in finding a straightforward method to convert the mild-slope equation and its boundary conditions into an integral equation. He uses a variation of parameters method to obtain the integral equation. We can also use this method for our system (4.23) and boundary conditions (4.37) – (4.40). As the idea here is only to indicate the form of the system of integral equations that results, we just give the major steps that occur in the conversion process to the vector integral equation.

We introduce the variable changes

$$\phi_k(x) = \zeta_k(x) \sqrt{\frac{U_k^0}{U_k(x)}} \quad (k = 0, \dots, n - 1), \quad (4.48)$$

where $U_k^0 = U_k(0)$ ($k = 0, \dots, n - 1$). Substituting (4.48) into (4.23) and rearranging, we find that the functions ζ_k ($k = 0, \dots, n - 1$) satisfy the coupled

differential equation system

$$\zeta_k'' - (\beta_k^0)^2 \zeta_k = \rho_k \zeta_k - \sum_{\substack{j=0 \\ j \neq k}}^{n-1} \left\{ \left[M_{jk} - \frac{U_j'}{2U_j} N_{jk} \right] \zeta_j + N_{jk} \zeta_j' \right. \quad (4.49)$$

Here, we have used the notation

$$\rho_k = \beta_k^2 - (\beta_k^0)^2 + \frac{U_k''}{2U_k} - \left(\frac{U_k'}{2U_k} \right)^2 - \frac{G_{kk}}{U_k} \quad (k = 0, \dots, n-1),$$

$$M_{jk} = \sqrt{\frac{U_j^0}{U_k^0}} U_j^{-\frac{1}{2}} U_k^{-\frac{1}{2}} G_{jk} \quad (k = 0, \dots, n-1),$$

$$N_{jk} = \sqrt{\frac{U_j^0}{U_k^0}} U_j^{-\frac{1}{2}} U_k^{-\frac{1}{2}} F_{jk} \quad (k = 0, \dots, n-1),$$

where G_{jk} and F_{jk} ($j, k = 0, \dots, n-1$) are given by equations (4.27) – (4.30) and the functions β_k ($k = 0, \dots, n-1$) are given by equations (4.25) and (4.26). As usual, we have used the notation $\beta_k^0 = \beta_k(0)$, $\beta_k^1 = \beta_k(1)$ and $U_k^0 = U_k(0)$ ($k = 0, \dots, n-1$).

The boundary conditions satisfied by the functions ζ_k ($k = 0, \dots, n-1$) can be found in exactly the same method as that used to find the boundary conditions for ϕ_k ($k = 0, \dots, n-1$) in section 4.3. Omitting the details of this process, it turns out that we can write these boundary conditions in the form

$$\zeta_k'(0+) - \beta_k^0 \zeta_k(0) = -2\beta_k^0 r_k \quad (k = 0, \dots, n-1), \quad (4.50)$$

$$\zeta_k'(1-) + \beta_k^0 \zeta_k(1) = 2\beta_k^0 e^{\beta_k^0} s_k \quad (k = 0, \dots, n-1), \quad (4.51)$$

where

$$r_0 = \frac{1}{2i\kappa_0} \left\{ 2i\kappa_0 A^- + \zeta_0(0) \left[\frac{U_0'}{2U_0} - \tau(\kappa H)' \tanh(\kappa\tau H) \right] \Big|_{0+} + \sum_{j=0}^{n-1} d_{j0}^0 \zeta_j(0) \right\},$$

$$s_0 = \frac{e^{i\kappa_0}}{2i\kappa_0} \left\{ 2i\kappa_1 A^+ \theta^- \quad n \right. \\ \left. < \xi \phi \right.$$

$$s_k = \frac{-e^{-\beta_k^0}}{2\beta_k^0} \left\{ \zeta_k(1) \left(\beta_k^1 - \beta_k^0 - \left[\frac{U_k'}{2U_k} - \tau(\beta_k H)' \tan(\beta_k \tau H) \right] \right) \right. \\ \left. + \sqrt{\frac{U_k^1}{U_k^0}} \sum_{j=0}^{n-1} \sqrt{\frac{U_j^0}{U_j^1}} d_{jk}^1 \zeta_j(1) \right\} ,$$

for $(k = 1, \dots, n - 1)$, and where $U_k^1 = U_k(1)$ ($k = 0, \dots, n - 1$).

The merit of writing the boundary conditions for ζ_k ($k = 0, \dots, n - 1$) in the form given by (4.50) and (4.51) is that it is now simple to use a variation of parameters procedure to convert the boundary-v

Therefore, it follows that we can rewrite F_{jk} (for $j \neq k$) as

$$F_{jk}(x) = \left(\int_{-H}^0 \left\{ \tilde{W}_k \frac{\partial \tilde{W}_j}{\partial H} - \tilde{W}_j \frac{\partial \tilde{W}_k}{\partial H} \right\} dz \right) H'(x).$$

Hence, for $j \neq k$, we find that F'_{jk} and G_{jk} are related by

where

$$\underline{\zeta}(x) = \left(\zeta_0(x), \zeta_1(x), \dots, \zeta_{n-1}(x) \right)^T,$$

$$\underline{f}(x) = \left(\tilde{r}_0 e^{i\kappa_0 x} + \tilde{s}_0 e^{-i\kappa_0 x}, \tilde{r}_1 e^{-\beta_1^0 x} + \tilde{s}_1 e^{\beta_1^0 x}, \dots, \tilde{r}_{n-1} e^{-\beta_{n-1}^0 x} + \tilde{s}_{n-1} e^{\beta_{n-1}^0 x} \right)^T,$$

and the operator L is defined by

$$\left(L \underline{\zeta} \right)$$

convert the second-order system (4.23) into a first-order system by introducing the functions

$$\psi_k = \phi'_k \quad (k = 0, \dots, n-1) .$$

Therefore, the system (4.23) can be rewritten as

$$\underline{p}' = \underline{q}(x, \underline{p}) , \quad (4.55)$$

where the $2n$ vectors \underline{p} and \underline{q} are given by

$$\underline{p} = (\phi_0, \phi_1, \dots, \phi_{n-1}, \psi_0, \psi_1, \dots, \psi_{n-1})^T ,$$

$$\underline{q} = \begin{pmatrix} \psi_0 \\ \psi_1 \\ \vdots \\ \psi_{n-1} \\ \beta_0^2 \phi_0 - \frac{1}{U_0} \sum_{j=0}^{n-1} (F_{j \ 0} \psi_j + G_{j \ 0} \phi_j) \\ \beta_1^2 \phi_1 - \frac{1}{U_1} \sum_{j=0}^{n-1} (F_{j \ 1} \psi_j + G_{j \ 1} \phi_j) \\ \vdots \\ \beta_{n-1}^2 \phi_0 - \frac{1}{U_{n-1}} \sum_{j=0}^{n-1} (F_{j \ n-1} \psi_j + G_{j \ n-1} \phi_j) \end{pmatrix} .$$

Let $\underline{\chi} = (\phi_0, \dots, \phi_{n-1})^T$, denote the solution of the boundary-value problem (4.23), (4.37) – (4.40). If we knew the initial conditions that $\underline{\chi}$ and $\underline{\chi}'$ satisfy at $x = 0$, then we would only require a numerical method to solve one initial-value problem, given by (4.55) and these initial conditions, to find an approximation to $\underline{\chi}$ at $x = 1$. However, this isyowww

We can write the boundary conditions (4.37) – (4.40) in vector form as

$$\underline{\chi}'(0) + D_0 \underline{\chi}(0) = \underline{s}_0 \quad (4.56)$$

and

$$\underline{\chi}'(1) + D_1 \underline{\chi}(1) = \underline{s}_1 . \quad (4.57)$$

Here, the $n \times n$ matrices D_0 and D_1 are given by

$$D_0 = \begin{bmatrix} -\beta_0^0 - \tilde{d}_{0\ 0}^0 & -d_{1\ 0}^0 & \cdots & -d_{n-1\ 0}^0 \\ -d_{0\ 1}^0 & -\beta_1^0 - \tilde{d}_{1\ 1}^0 & \cdots & -d_{n-1\ 1}^0 \\ \vdots & \vdots & \ddots & \vdots \\ -d_{0\ n-1}^0 & -d_{1\ n-1}^0 & \cdots & -\beta_{n-1}^0 - \tilde{d}_{n-1\ n-1}^0 \end{bmatrix} ,$$

and

$$D_1 = \begin{bmatrix} \beta_0^1 - \tilde{d}_{0\ 0}^1 & -d_{1\ 0}^1 & \cdots & -d_{n-1\ 0}^1 \\ -d_{0\ 1}^1 & \beta_1^1 - \tilde{d}_{1\ 1}^1 & \cdots & -d_{n-1\ 1}^1 \\ \vdots & \vdots & \ddots & \vdots \\ -d_{0\ n-1}^1 & -d_{1\ n-1}^1 & \cdots & \beta_{n-1}^1 - \tilde{d}_{n-1\ n-1}^1 \end{bmatrix} ,$$

where

$$\tilde{d}_{kk}^0 = d_{kk}^0 - [\tau(\beta_k H)' \tan(\beta_k \tau H)]|_{x=0+} \quad (k = 0, \dots, n-1)$$

and

$$\tilde{d}_{kk}^1 = d_{kk}^1 - [\tau(\beta_k H)' \tan(\beta_k \tau H)]|_{x=1-} \quad (k = 0, \dots, n-1) .$$

The n vectors \underline{s}_0 and \underline{s}_1 are given by

$$\underline{s}_0 = \left(-2\beta_0^0 A^-, 0, \dots, 0 \right)^T$$

and

$$\underline{s}_1 = \left(2\beta_0^1 e^{\beta_0^1} A^+, 0, \dots, 0 \right)^T .$$

Here, we have employed the usual notation $\beta_j^0 = \beta_j(0)$, $\beta_j^1 = \beta_j(1)$ ($j = 0, \dots, n-1$) and $\beta_0 = -i\kappa$ with κ and β_j ($j = 1, \dots, n-1$) the solutions of the relations (4.26) and (4.25) respectively.

Now let $\underline{\chi}_1, \underline{\chi}_2, \dots, \underline{\chi}_{2n}$ denote linearly independent solutions of (4.55), and therefore also linearly independent solutions of the coupled system (4.23). Then,

as we have already noted, the solution $\underline{\chi}$ of the boundary-value problem is given by

$$\underline{\chi} = c_1 \underline{\chi}_1 + c_2 \underline{\chi}_2 + \dots + c_{2n} \underline{\chi}_{2n} \quad (4.58)$$

for some constants $c_j \in \mathbb{C}$ ($j = 1, \dots, 2n$). These constants are chosen so that $\underline{\chi}$ given by (4.58) satisfies the boundary conditions (4.56) and (4.57). Therefore, substituting (4.58) into (4.56) and (4.57) leaves a matrix equation for the constants c_j ($j = 1, \dots, 2n$), which is given by

$$M \underline{c} = \underline{s}, \quad (4.59)$$

where M is a $2n \times 2n$ matrix given by $M = [\underline{m}_1, \underline{m}_2, \dots, \underline{m}_{2n}]$ with the $2n$ vectors \underline{m}_j ($j = 1, \dots, 2n$) and \underline{s} given by

$$\underline{m}_j = \begin{pmatrix} \underline{\chi}'_j(0) + D_0 \underline{\chi}_j(0) \\ \underline{\chi}'_j(1) + D_1 \underline{\chi}_j(1) \end{pmatrix} \quad (j = 1, \dots, 2n)$$

and

$$\underline{s} = \begin{pmatrix} \underline{s}_0 \\ \underline{s}_1 \end{pmatrix}.$$

Once (4.59) has been solved, then we can find the value of $\underline{\chi}$, the solution of the boundary-value problem, at $x = 1$ and hence calculate the reflection, transmission and decay coefficients.

All that remains to be done is to find the $2n$ independent solutions of (4.55). We shall use a Runge-Kutta method of the form

$$\underline{p}_{n-1} - \underline{p}_n = h \sum_{j=0}^R d_j \underline{q}_j^n,$$

in which h is the step size, $x_0 = 0$, $x_n = x_0 + nh$, $\underline{p}_n \approx \underline{p}(x_n)$ and $\underline{q}_j^n = \underline{q}(x_n + \gamma_j h, \underline{p}_n + h \sum_{s=1}^{j-1} \eta_{js} \underline{q}_s^n)$, to approximate $\underline{p}(1)$. These Runge-Kutta numerical schemes are defined on choosing h , γ_j and η_{js} ($j = 1, \dots, R$ and $s = 1, \dots, j$) and their use is well-documented (see Lambert [29], for example). The results we produce in this chapter will be found using the 6th-stage method ($R = 6$) given by Fehlberg [19] which is of order 5, that is, accurate to $O(h^5)$. This fifth-order Runge-Kutta procedure uses a corresponding fourth-order Runge-Kutta procedure for step size control. Fehlberg uses the fact that

the difference between his 5th-order Runge-Kutta method and the corresponding 4th-order method provides an approximation of the leading term of the truncation error in the 4th-order method. He assumes that if the truncation error is represented, with sufficient accuracy, by its leading term, then a step size control can easily be implemented into the 5th-order Runge-Kutta procedure. A test is made to see whether the truncation error, as obtained from the difference between the 4th and 5th-order methods, exceeds a certain pre-set tolerable error. If it does, the step size is halved, the step is recomputed and tested again. On

and parameter values $\alpha_0 = 3$ and $\tau = 0.1$, the functions κ and β_k ($k = 3$ and $k = 3$) are plotted in Figure 3.

Example 4.1

Suppose that a wave of unit amplitude is incident from $x = -\infty$ on a talud whose scaled depth profile is given by

$$H(x) = 1 - \frac{1}{2}x^2 \quad (0 \leq x \leq 1) .$$

This depth profile represents a concave talud. We choose parameter values

$$\alpha_0 = 2 ,$$

$$\tau = 0.5 .$$

(This could represent the physical situation where $h_0 = 1m$, $l = 2m$, $\sigma = \sqrt{g}s^{-1}$).

We shall seek approximations to the reflection coefficient of the progressive wave and the coefficients of the reflected decaying wav

mode at $x = 0$ $|R_1^1|$ calculated using the above tolerances in the Runge-Kutta method. We can see that both amplitudes of reflection have converged to 6.d.p.

Tolerance	$ R_1^0 $ (6d.p.)	$ R_1^1 $ (6d.p.)
10^{-3}	0.064150	0.006390
10^{-6}	0.064150	0.006390
10^{-9}	0.064150	0.006390

Table 4.2: Approximations to $|R_1^0|$ and $|R_1^1|$ for the 2-term approximation

when the tolerance in the Runge-Kutta method is 10^{-3} .

Now, remember that we wish to compare our results with those given by the mild-slope equation (MSE) and the modified mild-slope equation (MMSE). We can either use Chamberlain's integral equation procedure to do this or use the Runge-Kutta method given in this chapter. In keeping with the spirit of this chapter, we use the Runge-Kutta method with a tolerance of 10^{-6} to find the following approximations to the coefficient of the reflected plane wave.

$$\text{MSE: } R_1^0 = -0.038531 - 0.041166i \quad (|R_1^0| = 0.056385)$$

$$\text{MMSE: } R_1^0 = -0.047743 - 0.044376i \quad (|R_1^0| = 0.065181)$$

These results are accurate to 6.d.p., in the sense that they agree to 6.d.p. with results given by the Runge-Kutta method with an increased tolerance of 10^{-9} . Now with a 2-term trial approximation, the coefficient of the reflected plane wave (using a tolerance of 10^{-6} in the Runge-Kutta method) is given by

$$\text{2-term: } R_1^0 = -0.052240 - 0.037232i .$$

We shall now investigate the solutions of the initial-value problem (4.55), (4.60) and (4.61) as we increase the number of terms in the trial approximation. For the MMSE (that is, the 1-term approximation), the Runge-Kutta method gives approximations to $\underline{\chi}_1(1)$ and $\underline{\chi}_2(1)$ as

$$\underline{\chi}_1(1) = -0.898 \quad \text{and} \quad \underline{\chi}_2(1) = 0.209 .$$

Comparing these solutions of the initial-value problem (4.55),(4.60) and (4.61) with those given in Table 4.1 for the 2-term approximation illustrates that in the

2-term appro

with the corresponding reflection coefficient given by the 2-term approximation in the first 2 decimal places.

If we now use the 4-term approximation, then with a tolerance of 10^{-6} in the Runge-Kutta method, we find that

$$\underline{\chi}_1(1) \sim O(10^5), \quad \underline{\chi}_2(1) \sim O(10^7), \quad \underline{\chi}_3(1) \sim O(10^8), \quad \underline{\chi}_4(1) \sim O(10^9),$$

$$\underline{\chi}_5(1) \sim O(10^5), \quad \underline{\chi}_6(1) \sim O(10^6), \quad \underline{\chi}_7(1) \sim O(10^7), \quad \underline{\chi}_8(1) \sim O(10^8),$$

again illustrating the large growth in the solutions of the initial-value problem from $x = 0$ to $x = 1$. The condition number of the matrix M in equation (4.59) is now

$$\text{cond}(M) = 2.5 \times 10^{11}.$$

MATLAB can still solve (4.59), but the constants c_j ($j = 1, \dots, 6$) are only given correct to 7.d.p. The coefficient of the reflected progressive wave is given by

$$\text{4-term: } R_1^0 = -0.053629 - 0.034675i \quad (|R_1^0| = 0.063862).$$

The above estimate for R_1^0 agrees to 3.d.p. with that given when the tolerance in the method is increased to 10^{-9} . With a tolerance of 10^{-9} in the Runge-Kutta method, the estimate for R_1^0 is given by

$$\text{4-term: } R_1^0 = -0.053699 - 0.034580i \quad (|R_1^0| = 0.063869).$$

This estimate for R_1^0 agrees to 7.d.p. with that given when the tolerance in the method is increased to 10^{-10} . So, as the size of the solutions of the initial-value problem grow, we need to increase the tolerance in the Runge-Kutta method in order to maintain the solution accuracy.

Finally, if we use the 5-term approximation, then with a tolerance of 10^{-9} in the Runge-Kutta method, we find that

$$\underline{\chi}_1(1) \sim O(10^8), \quad \underline{\chi}_2(1) \sim O(10^9), \quad \underline{\chi}_3(1) \sim O(10^{10}),$$

$$\underline{\chi}_4(1) \sim O(10^{11}), \quad \underline{\chi}_5(1) \sim O(10^{12}), \quad \underline{\chi}_6(1) \sim O(10^8),$$

$$\underline{\chi}_7(1) \sim O(10^9), \quad \underline{\chi}_8(1) \sim O(10^9), \quad \underline{\chi}_9(1) \sim O(10^{10}), \quad \underline{\chi}_{10}(1) \sim O(10^{11}),$$

illustrating huge growth in the solutions of the initial-value problem from $x = 0$ to $x = 1$. The condition number of the matrix M in equation (4.59) is now

$$\text{cond}(M) = 6.0 \times 10^{14} .$$

MATLAB can still solve (4.59), but the constants c_j ($j = 1, \dots, 6$) are only given correct to 4.d.p. The coefficient of the reflected progressive wave is given by

$$\text{5-term: } R_1^0 = -0.0539 - 0.0341i \quad (|R_1^0| = 0.0638).$$

The above estimate for R_1^0 agrees to 4.d.p. with that given when the tolerance in the method is increased to 10^{-10} .

With 6 or more terms in the approximation, we find that the solutions of the initial-value problems at $x = 1$ are so large that MATLAB can no longer solve (4.59) and so solutions of the BVP cannot be found. It follows from the relation (4.25) that once α_0 and τ have been prescribed, the maximum value of the functions β_k ($k = 1, \dots, n - 1$) occurs at the minimum value of $theu <$

for some constants S_k and T_k ($k = 1, \dots, n - 1$). Initial conditions of the form

$$\phi_k(0) = 1 \quad \phi'_k(0) = -\beta_k^0 \quad (k = 1, \dots, n - 1) ,$$

clearly remove the growing exponential term in these flat bed solutions. We have found that if we use these $n - 1$ initial conditions with the first-order system (4.55), the solutions of the revised IVP at $x = 1$ are smaller by up to 3 orders in magnitude than the solutions obtained with the original initial conditions,

$$\left. \begin{array}{l} \underline{\chi}_j(0) = \underline{\epsilon}_j \\ \underline{\chi}'_j(0) = \underline{\mathbf{0}} \end{array} \right\} \quad j = 2, \dots, n .$$

We have not yet found an improved choice for the remaining $n + 1$ initial conditions and so we retain the present ones. Therefore, the initial conditions we are now going to employ with the first-order system (4.55) are

$$\left. \begin{array}{l} \underline{\chi}_j(0) = \underline{\epsilon}_j \\ \underline{\chi}'_j(0) = \underline{d}_j \end{array} \right\} \quad j = 1, \dots, n \quad (4.62)$$

and

$$\left. \begin{array}{l} \underline{\chi}'_j(0) = \underline{\epsilon}_{j-n} \\ \underline{\chi}_j(0) = \underline{\mathbf{0}} \end{array} \right\} \quad j = n + 1, \dots, 2n , \quad (4.63)$$

where $\underline{d}_j = -\beta_j^0 \underline{\epsilon}_j$ ($j = 2, \dots, n$) and \underline{d}_1 is the zero vector. With this choice of initial conditions, the functions $\underline{\chi}_j$ ($j = 1, \dots, 2n$) are clearly linearly independent.

We now return to the example at hand. For the 2-term approximation, using a tolerance of 10^{-6} in the numerical method, we find that the solution $\underline{\chi}_2$ of (4.59) together with initial condition (4.62) is

$$\underline{\chi}_2(1) = \begin{pmatrix} -0.710 \\ -5.409 \end{pmatrix} ,$$

which is a reduction of 2 orders in magnitude on the previous solution. Now $\text{cond}(M) = 1.8 \times 10^3$ which is a reduction of 1 order of magnitude on the previous value.

For the 3-term trial approximation, using a tolerance of 10^{-6} in the numerical method, the solutions $\underline{\chi}_2(1)$ and $\underline{\chi}_3(1)$ of (4.59) with initial conditions given by

(4.62) are

$$\underline{\chi}_2(1) = \begin{pmatrix} -0.276 \\ 1.494 \\ 4.809 \end{pmatrix} \times 10^3 \quad \underline{\chi}_3(1) = \begin{pmatrix} 0.213 \\ \\ \end{pmatrix}$$

However, the solutions of the initial-value problem (4.55), (4.62) and (4.63) for a 6 or higher term approximation are still too large and so MATLAB cannot solve the system (4.59).

Let us now compare these n-term approximation estimates for R_1^0 where $n = 1, \dots, 5$. From above we recall that

$$\begin{aligned}
 \text{MMSE: } R_1^0 &= -0.047743 - 0.044376i & (|R_1^0| &= 0.065181) , \\
 \text{2-term: } R_1^0 &= -0.052240 - 0.037232i & (|R_1^0| &= 0.064150) , \\
 \text{3-term: } R_1^0 &= -0.053247 - 0.035397i & (|R_1^0| &= 0.063939) , \\
 \text{4-term: } R_1^0 &= -0.053699 - 0.034580i & (|R_1^0| &= 0.063869) , \\
 \text{5-term: } R_1^0 &= -0.05395 - 0.03411i & (|R_1^0| &= 0.06384) .
 \end{aligned}$$

From these results, we can see that as we increase the number of terms in the approximation, the estimate of R_1^0 converges. We also notice that $|R_1^0|$ given by the 4-term and 5-term approximations agree to 4.d.p.

The coefficient of the first decaying wave mode evaluated at $x = 0$ given by the 2-term, 3-term, 4-term and 5-term approximations calculated using a tolerance of 10^{-6} , 10^{-6} , 10^{-9} and 10^{-9} respectively are

$$\begin{aligned}
 \text{2-term: } R_1^1 &= -0.005600 + 0.003077i & (|R_1^1| &= 0.006390) , \\
 \text{3-term: } R_1^1 &= -0.005755 + 0.003181i & (|R_1^1| &= 0.006576) , \\
 \text{4-term: } R_1^1 &= -0.005813 + 0.003225i & (|R_1^1| &= 0.006647) , \\
 \text{5-term: } R_1^1 &= -0.00584 + 0.00324i & (|R_1^1| &= 0.00668) .
 \end{aligned}$$

Again, we see convergence in the estimate of R_1^1 as the number of terms in the trial function is increased, with $|R_1^1|$ given by the 4-term and 5-term approximations the same to 4.d.p.

The coefficient of the second decaying wave mode evaluated at $x = 0$ given by the 3-term, 4-term and 5-term approximations calculated using a tolerance of 10^{-6} , 10^{-9} and 10^{-9} respectively are

$$\begin{aligned}
 \text{3-term: } R_2^1 &= -0.000000 + 0.000000i & (|R_2^1| &= 0.000000) , \\
 \text{4-term: } R_2^1 &= -0.000000 + 0.000000i & (|R_2^1| &= 0.000000) , \\
 \text{5-term: } R_2^1 &= -0.000000 + 0.000000i & (|R_2^1| &= 0.000000) .
 \end{aligned}$$

The coefficient of the second decaying wave mode evaluated at $x = 0$ given by the 4-term and 5-term approximations calculated using a tolerance of 10^{-9} are

$$\begin{aligned} \text{4-term: } R_1^3 &= -0.000059 + 0.000118i & (|R_1^3| &= 0.000197) , \\ \text{5-term: } R_1^3 &= -0.00006 + 0.00019i & (|R_1^3| &= 0.00020) , \end{aligned}$$

which agree to the first 4 decimal places. The coefficient of the fourth decaying wave mode evaluated at $x = 0$ given by the 5-term approximation calculated using a tolerance of 10^{-9} is

$$\text{5-term: } R_1^4 = 0.00001 - 0.00008i \quad (|R_1^4| = 0.00008) .$$

The coefficient of the first decaying wave mode evaluated at $x = 0$ is one order of magnitude larger than the corresponding coefficient of the second decaying wave mode. As $\beta_k < \beta_{k+1}$ ($k \in \mathbb{N}$), the $(k + 1)^{\text{th}}$ decaying wave mode decays away more rapidly than the k^{th} as $x \rightarrow \pm\infty$. This clearly illustrates that the first decaying wave mode is much more significant than the second decaying wave mode, which will be more significant than the third, etc.

W

$$\underline{\chi}_3(1) = \begin{pmatrix} 4.891 \\ 90.87 \end{pmatrix}, \quad \underline{\chi}_4(1) = \begin{pmatrix} 0.053 \\ 1.017 \end{pmatrix} \times 10^6,$$

Now, $\text{cond}(M) = 3.9 \times 10^7$, where M is the matrix in equation (4.59), and MATLAB can determine the constants c_j ($j = 1, \dots, 4$) accurate to 9.d.p.

For a 3-term approximation

$$\begin{aligned} \underline{\chi}_1 &\sim O(10^{12}), & \underline{\chi}_2 &\sim O(10^{12}), & \underline{\chi}_3 &\sim O(10^{12}), \\ \underline{\chi}_4 &\sim O(10^{11}), & \underline{\chi}_5 &\sim O(10^{12}), & \underline{\chi}_6 &\sim O(10^{14}). \end{aligned}$$

Now, $\text{cond}(M) = 4 \times 10^{16}$, where M is the matrix in equation (4.59), and we cannot now determine the constants c_j ($j = 1, \dots, 6$).

the MMSE before the bed profile becomes too mild for results to be found. These results are presented graphically in section 4.7.

4.7 Graphic results

In this section, we consider three examples where the results are best presented graphically. In the first example we plot the approximation to the free surface at two different time intervals for normal incidence. In the other two examples, we show how the amplitude of the reflected progressive wave varies with the steepness of the bed profile. We consider two shapes of bed profile – a talud and a hump, and compare results given by the MSE, MMSE, 2-term, 3-term and 4-term approximations. We also compare results given by the MSE and MMSE with the two sets of boundary conditions discussed in section 4.3.

Example 4.2

Here the depth profile is given by

$$H(x) = \frac{3}{4} + \frac{1}{4} \cos(2\pi x^2) \quad (0 \leq x \leq 1),$$

which represents an asymmetric hump whose height is half the still water depth. The parameters α_0 and τ are chosen to be

$$\begin{aligned} \alpha_0 &= 2.5, \\ \tau &= 0.4. \end{aligned}$$

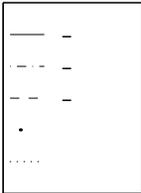
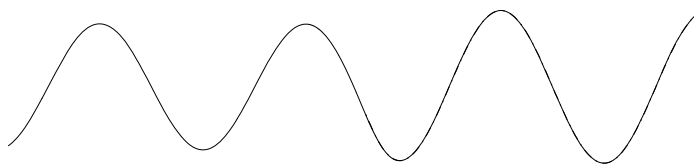
The n-term approximation to the free surface elevation is given by

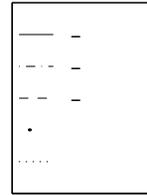
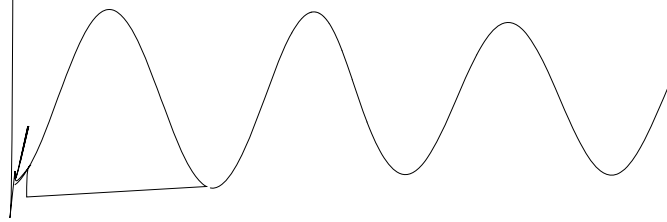
$$\eta \approx \operatorname{Re} \left\{ e^{-i\sigma t} \sum_{j=0}^{n-1} \phi_j \right\}.$$

For an incident wave of unit amplitude from $x = -\infty$, the approximation to the free surface at time $t = 2j\frac{\pi}{\sigma}$ ($j + 1 \in \mathbb{N}$) is given by

$$\eta(x, t) \approx \operatorname{Re} \begin{cases} e^{i\kappa_0 x} + R_1^0 e^{-i\kappa_0 x} + \sum_{j=1}^{n-1} R_1^j e^{\beta_j^0 x} & (x \leq 0), \\ \sum_{j=0}^{n-1} \phi_j(x) & (0 \leq x \leq 1), \\ T_1^0 e^{i\kappa_1 x} + \sum_{j=1}^{n-1} T_1^j e^{-\beta_j^1 x} & (x \geq 1). \end{cases}$$

The results displayed in Fig.4.1 were obtained by running the computer program with a tolerance of 10^{-6} in the Runge-Kutta method for the MSE, MMSE, 2-term





Returning to the definitions of α_0 and τ , we recall that

$$\alpha_0 = \frac{\sigma l}{\sqrt{gh_0}}, \quad \tau = h_0/l.$$

So with α_0 and τ given in terms of W_s as above, we see that

$$\sqrt{0.6}\alpha_0 = \frac{\sigma^2}{g}l, \quad \frac{\tau}{0.6} = \frac{1}{\frac{\sigma^2}{g}l}.$$

It follows that varying W_s is equivalent to varying the length l of the talud, and therefore the steepness of the talud at each fixed value of $\frac{\sigma^2}{g}$, the deep water wave number. Following Booij [5], we seek results for our new approximation for values of W_s from 0.1 to 6 at intervals of 0.05. As W_s varies from 0.1 to 6, $\alpha_0\tau = \sqrt{0.6}$ and τ decreases monotonically. Therefore, the functions β_k ($k = 1, \dots, n-1$), the roots of the relations

$$-(\alpha_0\tau)^2 H = (\beta_k\tau H) \tan(\beta_k\tau H) \quad (k \in \mathbb{N}),$$

monotonically increase as W_s increases. Note that the minimum depth in this example occurs at $x = 1$, and so the maximum value of β_k ($k = 1, \dots, n-1$) in the interval $[0, 1]$ is at $x = 1$. When $W_s = 0.1$, we find that

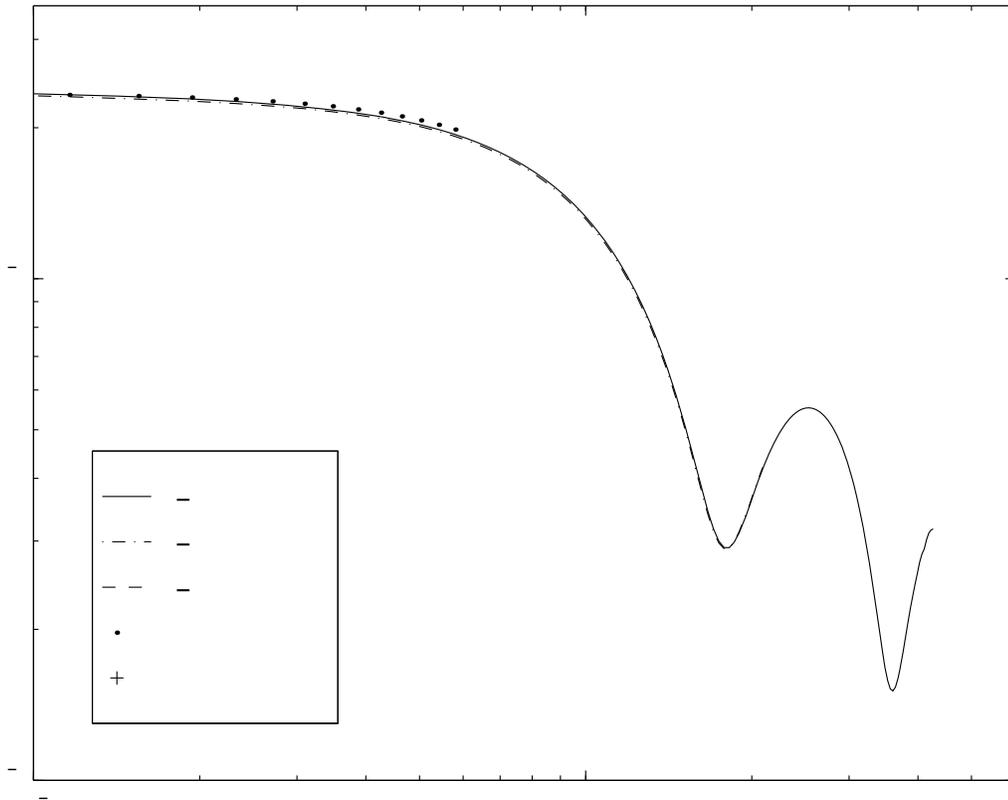
$$\beta_1(1) = 1.54$$

$\text{cond}(M) = 3.9 \times 10^{15}$ and equation (4.59) cannot be solved to the minimum accuracy we have specified. When



given by the MSE and MMSE with the new boundary conditions (4.42) is much larger than that given with the old boundary conditions (4.41). Booij [5] claimed that the results given by the full linear theory and the MSE with the old boundary conditions (4.41) were in ‘good agreement’ for $W_s > 1.2$. He does not publish any values of $|R_1^0|$ for full linearised theory for $W_s > 1.2$ to confirm this claim, but from the evidence in Fig.4.3 it is reasonable to suppose that these results would be much closer to those given with the new boundary conditions (4.42) rather than those given by the old ones as claimed.

In Fig.4.4 we present the results obtained from the boundary-value problem



when $W_s > 1.6$, which corresponds to taluds with gradient less than $\frac{1}{4}$. In other words, taluds with gradients of up to $\frac{1}{4}$ are mild enough to make the contribution from the first (and largest) decaying mode negligible. Therefore, it is not of great importance that we cannot find results for the 2-term approximation for $W_s > 4$.

With these definitions for α_0 and τ , varying ω corresponds to varying the length l of the hump or, equivalently, to varying the steepness of the depth profile, as in Example 4.3. As ω increases, $\alpha_0\tau = 1$ and τ decreases, so (as in Example 4.3) the functions β_k ($k = 1, \dots, n - 1$) monotonically increase. The minimum depth in this example occurs at $x = \frac{1}{2}$, and so the maximum value of β_k ($k = 1, \dots, n - 1$) in the interval $[0, 1]$ is at $x = \frac{1}{2}$. When $\omega = 0.05$, we find that

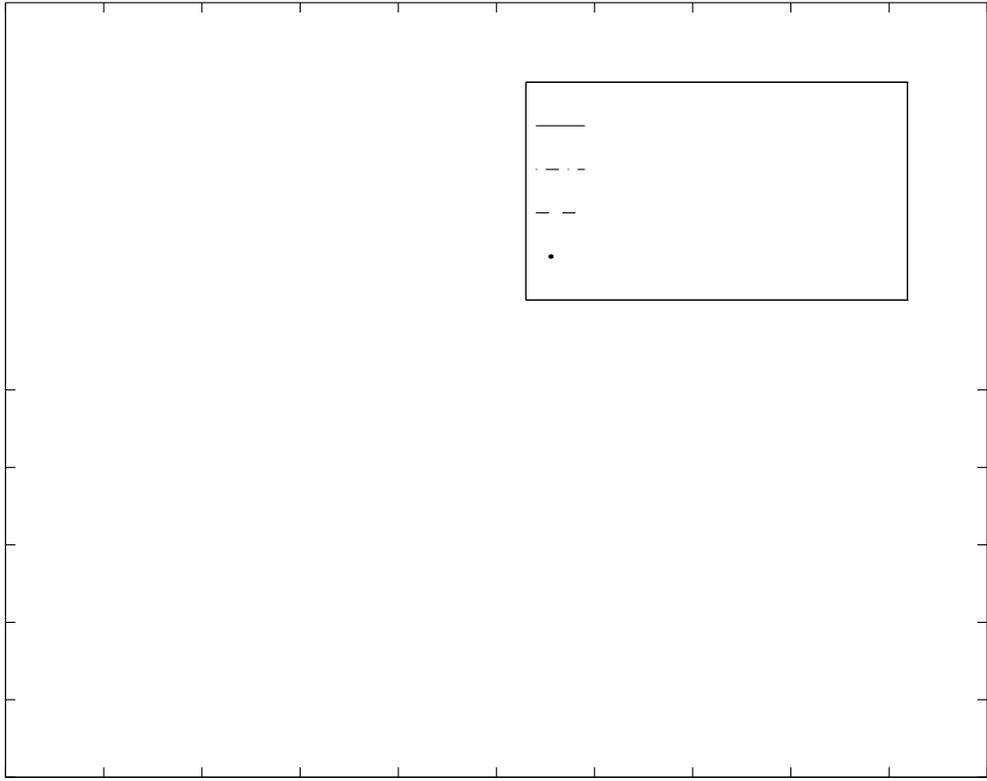
$$\beta_1\left(\frac{1}{2}\right) = 0.30, \quad \beta_2\left(\frac{1}{2}\right) = 0.62, \quad \beta_3\left(\frac{1}{2}\right) = 0.94, \quad \beta_4\left(\frac{1}{2}\right) = 1.25.$$

and when $\omega = 10$, we find that

$$\beta_1\left(\frac{1}{2}\right) = 59.50, \quad \beta_2\left(\frac{1}{2}\right) = 124.06, \quad \beta_3\left(\frac{1}{2}\right) = 187.43, \quad \beta_4\left(\frac{1}{2}\right) = 250.53.$$

As in Example 4.3, as ω increases, there is a value of ω at which the function β_1 is large enough to make the solutions of the initial-value problem for the 2-term approximation too large for the system (4.59) to be solved to the minimum accuracy (3.d.p.). Similarly, at smaller values of ω , solutions for the 3-term and 4-term approximations will not be available. It turns out that for the 2-term approximation, when $\omega = 7.75$, $\beta_2(\frac{1}{2}) = 46.11$, $\text{cond}(M) = 2.4 \times 10^{15}$ and equation (4.59) cannot be solved to the minimum accuracy we have specified. When $\omega = 3.75$, $\beta_2(\frac{1}{2}) = 46.52$ and the results given by the 3-term approximation(tio(-

prrhaco



$\omega = 2.4$. Therefore, the contribution from the fourth decaying mode becomes essentially negligible for $\omega > 2.4$. From the similarity between the 3-term and 4-term approximation results, we conclude that the n -term approximation has essentially converged when $n=4$ and so we do not compute solutions for the 5-term or higher term approximations. In this example we have not seen the same convergence in the results given by the n -term ($n > 1$) approximations as we did in the previous example. This is because the steepness of a hump of the same maximum height as a talud and the same length is effectively twice that of the talud. So unfortunately, the slope of the hump does not become mild enough for us to see the same convergence in the results given by the n -term ($n > 1$) approximations as seen in Example 4.3 before the results given by these n -term ($n > 1$) approximations become inaccurate.

For small values of ω , the hump we are considering is similar to a thin rectangular block, whose height is half the fluid depth. Mei and Black [4] considered this type of problem using full linear theory, for blocks of various width and the limiting case of a thin barrier. For small wave numbers, their results show that there is a large difference in the amplitude of the reflected wave given by a thin barrier and the blocks they considered. The results given in Fig.4.6 by the 2, 3 and 4-term approximations when $\omega = 0.05$, that is, when the flat bed depth is 20 times the length of the hump are consistent with those of Mei and Black, in the sense that they lie between the corresponding estimates Mei and Black give for the thin barrier and the narrowest block they consider, where the flat bed depth is half the length of the step.

In Chapter 5, we find that our decay mode approximation results for this hump problem are in good agreement with the results we compute using full linearised theory.

We round off this chapter by developing the theory given so far to encompass obliquely incident waves.

4.8 Obliquely incident waves

In this chapter, the theory employed so far is only for 1-dimensional problems. In other words, it applies to waves that are normally incident on depth profiles which are independent of y . We shall now generalise this to allow waves incident other than normally on such profiles. Consider a plane wave train arriving from $x = -\infty$ whose direction of propagation makes an angle θ_0 to the normal to the y axis. Let the angle which the transmitted wave makes to the normal be denoted by θ_1 , where $\theta_1 \neq \theta_0$ in general.

If the fluid depth in $x < 0$ is less than that in $x > 1$ then $\theta_1 > \theta_0$ (Mei [37], for example). We note that there exists a critical angle θ_{crit} which for any incident wave with angle of incidence in the interval $[\theta_{\text{crit}}, \frac{\pi}{2}]$ total reflection occurs – a well-known result in optics. We do not consider these total reflection problems here as this would require us to derive alternative boundary conditions, with which we are not concerned. We shall consider wave scattering problems in which part of the incident wave is reflected and part of it is transmitted. If the fluid depth in $x < 0$ is greater than that in $x > 1$, that is, if $h_0 > h_1$, then $\theta_1 < \theta_0$ – this is the case depicted in Fig. 4.7 In this case the incident wave

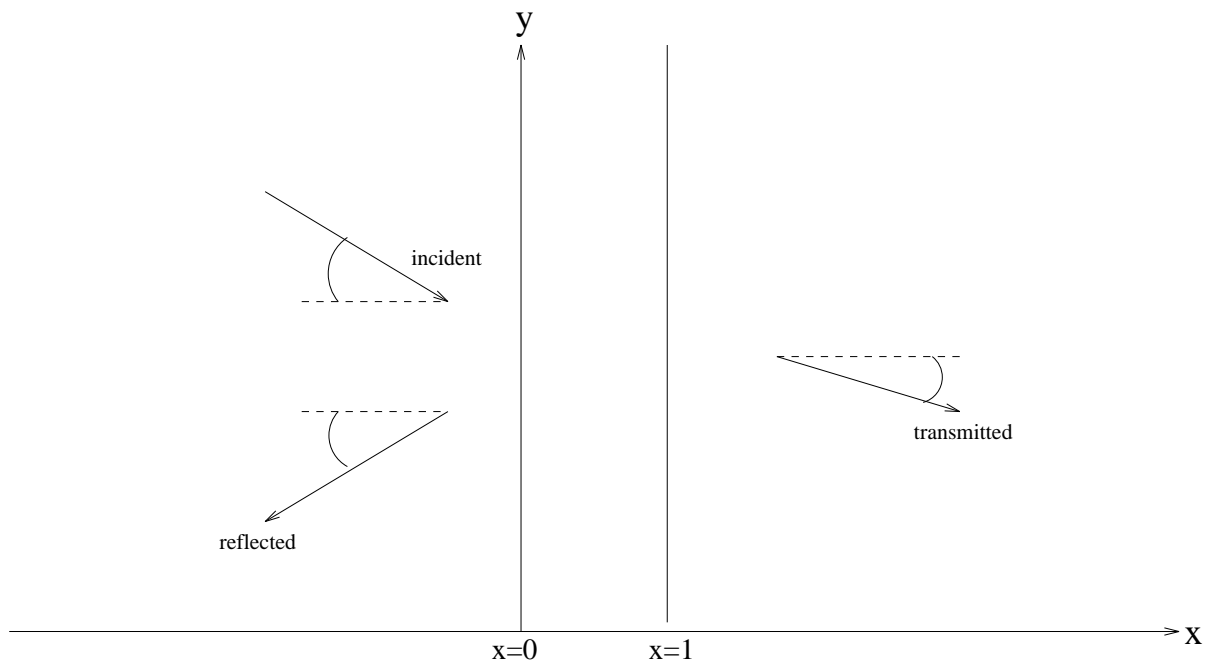


Figure 4.7: Top view of an obliquely incident wave approach

is always transmitted whatever the angle of incidence. For an oblique incidence problem as depicted in Fig. 4.7, we can follow the same procedure used in section 4.1 to see that the approximation to the free surface elevation η is given by

$$\eta \approx \operatorname{Re} \left\{ e^{-i\sigma t} \sum_{k=0}^{n-1} \tilde{\phi}_k \right\} .$$

Here the functions $\tilde{\phi}_k = \tilde{\phi}_k(x, y)$ ($k = 0, \dots, n-1$), after scaling, satisfy

$$U_k \left(\nabla^2 \tilde{\phi}_k - \beta_k^2 \tilde{\phi}_k \right) + \sum_{j=0}^{n-1} \left\{ F_{jk} \frac{\partial \tilde{\phi}_j}{\partial x} + G_{jk} \tilde{\phi}_j \right\} = 0 \quad (k = 0, \dots, n-1), \quad (4.64)$$

with $U_k = U_k(x)$, $\beta_k = \beta_k(x)$, $F_{jk} = F_{jk}(x)$ and $G_{jk} = G_{jk}(x)$ ($j, k = 0, \dots, n-1$), defined by (4.24) and (4.30) respectively, since $H = H(x)$.

The wave numbers κ_0 and κ_1 of the incident and the scattered progressive wav

$$\phi_k(x) = \begin{cases} R_k e^{\beta_k^0 x \cos \theta_0} & x \leq 0 \quad (k = 1, \dots, n-1), \\ T_k e^{-\beta_k^T x} & x \geq 1 \quad (k = 1, \dots, n-1). \end{cases} \quad (4.68)$$

Here, κ_T is the x -component of the wave number of the transmitted progressive wave, and β_k^T ($k = 1, \dots, n-1$) are the x -components of the corresponding terms of the transmitted decaying wave modes. The procedure outlined in section 4.3 can be used to derive the boundary conditions for ϕ_k ($k = 0, \dots, n-1$) from equations (4.67) and (4.68). The transmitted progressive wave has wave number κ_1 and we know in advance that its y -component is $\kappa_0 \sin \theta_0$. Therefore

$$\kappa_T = \sqrt{\kappa_1^2 - \kappa_0^2 \sin^2 \theta_0}.$$

Similarly, the y -component of the functions $\beta_1^1, \dots, \beta_{n-1}^1$ and the β_T

approximations are very similar, so we just present the results for the 2-term approximation here. The 2-term approximation to the free surface elevation at time $t = 2j\frac{\pi}{\sigma}$ ($j + 1 \in \mathbb{N}$) is given by

$$\eta \approx \operatorname{Re} \left\{ e^{i\kappa_0 y \sin \theta_0} \left\{ \begin{array}{ll} e^{i\kappa_0 x \cos \theta_0} + R_0 e^{-i\kappa_0 x \cos \theta_0} + R_1 e^{\beta_1^0 x \cos \theta_0} & (x \leq 0) , \\ \phi_0(x) + \phi_1(x) & (0 \leq x \leq 1) , \\ T_0 e^{i\kappa_T x} + T_1 e^{-\beta_1^T x} & (x \geq 1) . \end{array} \right. \right\}$$

Fig. 4.8 displays the approximation to the free surface elevation given by the 2-term approximation. To give the figure more meaning we have included the depth profile used, and the amplitude of the waves has been exaggerated to improve clarity. Notice the presence of constructive interference in $x \leq 0$.



It is clear that the numerical method that we have used to solve the boundary-value problem (4.23), (4.37) – (4.40) is restricted by the size of the functions β_k ($k = 1, \dots, n - 1$). A major objective of any future work will be to develop a solution routine that overcomes this problem. The size of the functions β_k ($k = 1, \dots, n - 1$) will cause problems in most numerical solution procedures of the boundary-value problem. These problems might be avoided by developing an approximate solution method to solve the integral equation equivalent to this boundary-value problem which we presented in section 4.4.

In this chapter, we have shown that by incorporating decaying wave mode terms into the formulation of the original mild-slope approximation to the velocity potential for the full linearised wave scattering problem, we can find good approximations to the velocity potential. This new approximation has been compared with two older approximations that only contain progressive wave mode terms, namely the mild-slope and modified mild-slope approximations. We have shown that for steep depth profiles, where the decaying wave modes are significant, the results given by the new approximation agreed much more closely with results Booij [5] obtained using full linear theory. From the results given in sections 4.6 and 4.7, the new ‘decaying mode’ approximation of the coefficients of the scattered waves is seen to essentially converge when the number of decaying wave modes included has reached three, even for the steepest bed profiles. The milder the depth profile, the fewer the number of decaying modes needed for convergence, until eventually the gradient of the depth profile becomes mild enough to make all the decaying modes negligible. In the course of developing this approximation, it has been found that the boundary conditions that have been used in the past by all authors with the mild-slope approximation are incorrect. By this, we mean that an alternative set of boundary conditions can be found which make the mild-slope approximation results agree far more closely with computed results of the full linear problem than the original ones.

of another Green's function evaluated on the hump. It follows that the kernel in the first-kind equation is much easier to compute numerically than the kernel of the second-kind equation. It is shown that the first-kind integral equation can be derived directly from the corresponding boundary-value problem for the associated stream function. A variational principle is used to deliver approximations to the coefficients of the scattered waves which are second-order accurate compared to the approximation of the solution of the first-kind equation. The subsequent results are used to further test the accuracy of the decay mode approximation derived in Chapter 4 and also to test the accuracy of the modified mild-slope and mild-slope approximations.

5.1

From Chapter 2, we recall that in this situation ϕ satisfies

$$\hat{\nabla}^2 \phi = 0 \quad -h < z < 0 ,$$

$\partial\phi$

where the domain D and boundary C will be defined as required and where $\frac{\partial}{\partial n}$ is the outward normal derivative, which is defined as

$$\frac{\partial}{\partial n} = -\frac{\frac{\partial}{\partial z} + h'(x)\frac{\partial}{\partial x}}{\left(1 + (h'(x))^2\right)^{\frac{1}{2}}},$$

where the prime denotes differentiation with respect to x . The Green's function G is chosen to satisfy

$$\begin{aligned} \hat{\nabla}^2 G &= -\delta(x - x_0)\delta(z - z_0) && -h_0 < z < 0, \\ \frac{\partial G}{\partial z} - \nu G &= 0 && \text{on } z = 0, \\ \frac{\partial G}{\partial n} &= 0 && \text{on } z = -h_0, \end{aligned} \tag{5.5}$$

together with a radiation condition ensuring that G behaves like an outgoing wave as $|x| \rightarrow \infty$. In other words,

$$G \sim e^{\pm ik_0 x} \quad \text{as } x \rightarrow \pm\infty. \tag{5.6}$$

This Green's function is well-known and one can find derivations of its integral or series forms in Wehausen and Laitone [59] and Thorne [56]. The infinite series representation of G is given by

$G ($

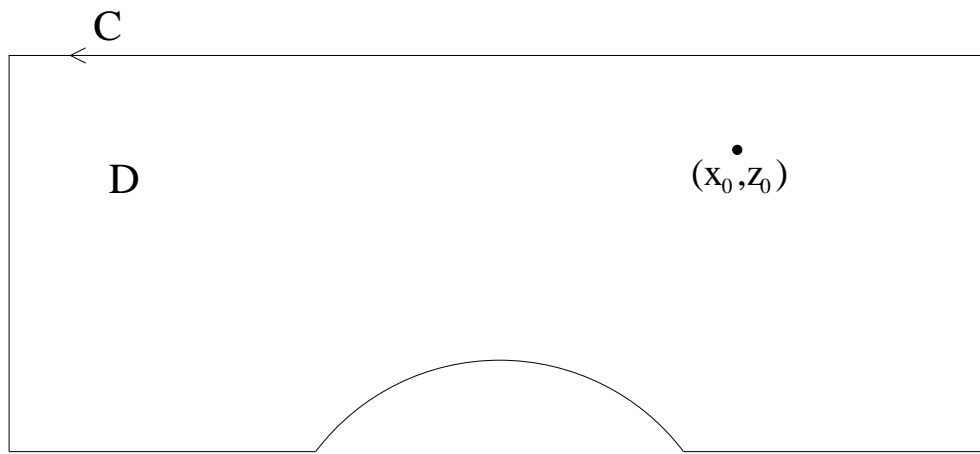


Figure 5.2: First domain used in Green's iDwr

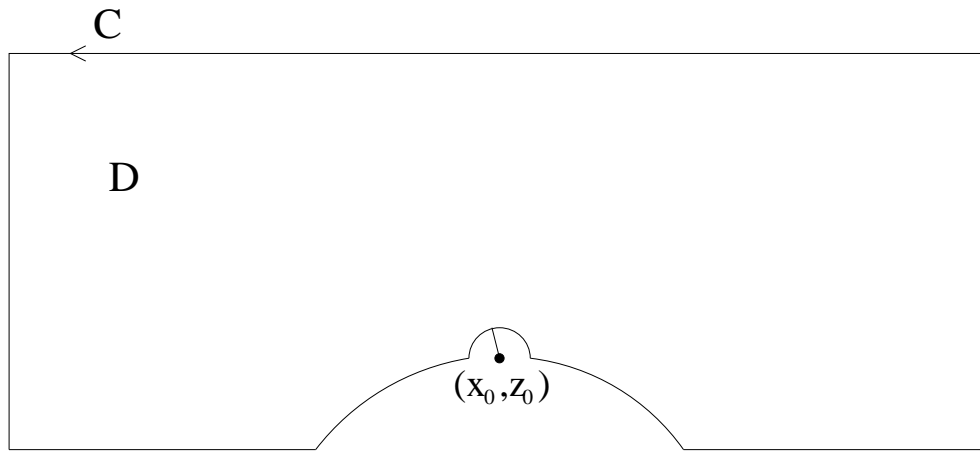


Figure 5.3: Second domain used in Green's identity.

ϕ on the hump. On the hump, $z_0 = -h(x_0)$ and so we can rewrite this equation as

$$\begin{aligned} \frac{1}{2}\phi(x_0, -h(x_0)) = & \frac{\cosh(k_0(h_0 - h(x_0)))}{\cosh(k_0 h_0)} [A^- e^{ik_0 x_0} + A^+ e^{-ik_0 x_0}] \\ & + \int_0^l \left(\left[h'(x) \frac{\partial G}{\partial x} + \frac{\partial G}{\partial z} \right]_{\substack{z=-h(x) \\ z_0=-h(x_0)}} \phi(x, -h(x)) \right) dx . \end{aligned} \quad (5.9)$$

Therefore, in order to find the velocity potential in the fluid domain, the integral equation (5.9) must be solved and its solution then substituted into equation (5.8). The kernel of the above integral equation is not easy to compute numerically because the series which defines it has poor convergence properties. Hence, we wish to avoid solving this second-kind integral equation. Initially, we try making an approximation in (5.9) which simplifies the second-kind integral equation, and this process is outlined in the next section.

We finish this section by finding expressions for the coefficients of the reflected and transmitted waves in terms of the velocity potential evaluated on the hump. Suppose we have an incident wave from $x = -\infty$ (so that $A^+ = 0$), then if, in equation (5.8), we take the limit $x_0 \rightarrow -\infty$ and compare the result with the appropriate radiation condition (5.2) for ϕ , we find that the reflection coefficient is given by

$$R_1 = \frac{B^-}{A^-} = \frac{c_0^2 \cosh(k_0 h_0)}{2A^-} \int_0^l \left[-h'(x) \cosh(k_0(h_0 - h(x))) + i \sinh(k_0(h_0 - h(x))) \right] e^{ik_0 x} \phi(x, -h(x)) dx. \quad (5.10)$$

The approximation to the velocity potential in the fluid is given by

$$\begin{aligned} \tilde{\phi}(x_0, z_0) = & \frac{\cosh(k_0(z_0 + h_0))}{\cosh(k_0 h_0)} \left[A^- e^{ik_0 x_0} + A^+ e^{-ik_0 x_0} \right] \\ & + \frac{c_0^2}{2} \cosh(k_0(z_0 + h_0)) \int_0^l \left[\operatorname{sgn}(x_0 - x) h'(x) \cosh(k_0(h_0 - h(x))) \right. \\ & \left. + i \sinh(k_0(h_0 - h(x))) \right] e^{ik_0|x-x_0|} \phi_0(x) dx. \end{aligned} \quad (5.15)$$

We shall refer to this new approximation to the velocity potential as the integral approximation.

Therefore, in order to find the approximation $\tilde{\phi}(x_0, z_0)$ to the velocity potential in the fluid, we must solve the second-kind integral equation (5.14) and substitute its solution into equation (5.15). The kernel of the second-kind integral equation (5.14) is discontinuous at $x = x_0$, which will cause problems in numerical integration routines if we attempt to solve this integral equation as it stands. These problems are avoided by using a variable change and some straightforward manipulation to give a new second-kind integral equation whose kernel is continuous.

We define a new function $\zeta = \zeta(x)$ by

$$\zeta(x) = \frac{1}{2} \phi_0(x) \operatorname{sech}(k_0(h_0 - h(x))) \cosh(k_0 h_0). \quad (5.16)$$

Then equation (5.14) can be rewritten as

$$\begin{aligned} \zeta(x_0) = & \left[A^- e^{ik_0 x_0} + A^+ e^{-ik_0 x_0} \right] \\ & + c_0^2 \int_0^l \left[\operatorname{sgn}(x_0 - x) h'(x) \cosh^2(k_0(h_0 - h(x))) \right. \\ & \left. + \frac{i}{2} \sinh(2k_0(h_0 - h(x))) \right] e^{ik_0|x-x_0|} \zeta(x) dx. \end{aligned} \quad (5.17)$$

We now differentiate the above integral equation twice with respect to x_0 to find the boundary-value problem satisfied by ζ . Differentiating (5.17) once gives

$$\begin{aligned} \zeta'(x_0) = & ik_0 \left[A^- e^{ik_0 x_0} - A^+ e^{-ik_0 x_0} \right] + 2c_0^2 h'(x_0) \cosh^2(k_0(h_0 - h(x_0))) \zeta(x_0) \\ & + ik_0 c_0^2 \int_0^{x_0} \left[h'(x) \cosh^2(k_0(h_0 - h(x))) + \frac{i}{2} \sinh(2k_0(h_0 - h(x))) \right] e^{ik_0(x_0 - x)} \zeta(x) dx \\ & + ik_0 c_0^2 \int_{x_0}^l \left[h'(x) \cosh^2(k_0(h_0 - h(x))) - \frac{i}{2} \sinh(2k_0(h_0 - h(x))) \right] e^{ik_0(x - x_0)} \zeta(x) dx, \end{aligned}$$

where the prime denotes differentiation with respect to x_0 . Differentiating this equation for ζ' gives

$$\zeta''(x_0) - 2u(x_0)\zeta'(x_0) = [2(u'(x_0) - k_0v(x_0)) - k_0^2]\zeta(x_0) \quad (0)$$

and $\kappa_0 = k_0 l$ is the positive real root of

$$\alpha_0^2 \tau = \kappa_0 \tanh(\kappa_0 \tau) ,$$

and where α_0 and τ are two dimensionless parameters given by

$$\alpha_0 = \frac{\sigma l}{\sqrt{gh_0}} , \quad \tau = h_0/l .$$

We need to convert (5.19) into self-adjoint form, which is done by introducing an integrating factor J given by

$$\begin{aligned} J(x_0) &= \exp\left(-2 \int_0^{x_0} U(x) dx\right) \\ &= \exp\left(\frac{C_0^2}{2\kappa_0} \left[2\kappa_0 \tau (1 - H(x_0)) + \sinh(2\kappa_0 \tau (1 - H(x_0)))\right]\right) . \end{aligned} \quad (5.20)$$

The self-adjoint form of equation (5.19) is then given by

$$\left(J(x_0)\zeta'(x_0)\right)' = J(x_0) \left[2(U'(x_0) - \kappa_0 V(x_0)) - \kappa_0^2\right] \zeta(x_0) . \quad (5.21)$$

This equation is of the same form as the mild-slope equation which was given in Chapters 2 & 4. Therefore, we can solve this equation using the integral equation procedure Chamberlain [7] used to solve the mild-slope equation. Following this procedure, which is outlined in Chapter 2, we introduce a new variable ξ defined by

$$\xi(x_0) = \zeta(x_0) \sqrt{J(x_0)} \quad (0 \leq x_0 \leq 1)$$

and find that ξ satisfies the second-kind integral equation

$$\begin{aligned} \xi(x_0) &= \left(c_1 + c_2 \xi(0) + c_3 \xi(1)\right) e^{i\kappa_0 x_0} \\ &+ \left(c_4 + c_5 \xi(0) + c_6 \xi(1)\right) e^{-i\kappa_0 x_0} \quad (0 < x_0 < 1) , \quad (5.22) \\ &- \frac{i}{2\kappa_0} \int_0^1 e^{i\kappa_0 |x_0 - t|} \rho(t) \xi(t) dt \end{aligned}$$

where

$$\rho(t) = \frac{J''(t)}{2J(t)} - \left(\frac{J'(t)}{2J(t)}\right)^2 + 2(U'(t) - \kappa_0 V(t))$$

and where the constants c_j ($j = 1, \dots, 6$) are given by

$$\begin{aligned} c_1 &= A^-, & c_2 &= -\frac{i\tau}{2\kappa_0} C_0^2 H'(0+), & c_3 &= 0 , \\ c_4 &= A^+, & c_5 &= 0, & c_6 &= \frac{i e^{i\kappa_0}}{2\kappa_0} \tau C_0^2 H'(1-) . \end{aligned}$$

From the definition of the in

This corresponds to a hump whose height is one quarter of the still-water depth and whose slope is discontinuous at $x = 0$ and at $x = 1$, where it meets the flat beds. We choose parameter values

$$\begin{aligned}\alpha_0 &= 2 , \\ \tau &= 0.2 .\end{aligned}$$

Using a 3-dimensional trial space we find that for the integral approximation

$$\begin{aligned}\text{maximum error in } |R_1| &= 7.9 \times 10^{-9} , \\ R_1 &= 0.1681 + 0.1641i , \\ |R_1| &= 0.2350 .\end{aligned}$$

Similarly, using a 3-dimensional trial space we find that for the mild-slope approximation gives

$$\begin{aligned}\text{maximum error in } |R_1| &= 4.6 \times 10^{-14} , \\ R_1 &= 0.0883 + 0.0727i , \\ |R_1| &= 0.1143 .\end{aligned}$$

Finally, using a 3-dimensional trial space we find that for the modified mild-slope approximation gives

$$\begin{aligned}\text{maximum error in } |R_1| &= 5.2 \times 10^{-14} , \\ R_1 &= 0.0920 + 0.0735i , \\ |R_1| &= 0.1177 .\end{aligned}$$

It is clear that the integral approximation predicts a much larger reflected amplitude than either the mild-slope or modified mild-slope approximations.

We now consider an example where we find solutions given by the modified mild-slope, mild-slope and integral approximations as we vary the steepness of the hump depth profile.

Example 5.2

We consider a depth profile given by

$$H(x) = 2x^2 - 2x + 1 \quad (\leq x \leq 1) .$$

This corresponds to a hump whose height is half the still-water depth which has slope discontinuities at x

seek solutions given by the modified mild-slope, mild-slope and integral approximations at values of a parameter ω starting at 0.05, finishing at 10, with intervals of 0.05. The parameters α_0 and τ are defined in terms of ω by

$$\alpha_0 = \omega, \quad \tau = \frac{1}{\omega}.$$

We have already considered this problem for the new ‘decaying mode’ approximation in Chapter 4 and recall that with these definitions for α_0 and τ , varying ω corresponds to varying the length l of the hump, which translates to varying the steepness of the depth profile.

We use the ‘cheap’ solution method given in Chapter 3 to find results for each approximation imposing the usual two significant figure tolerance in the error. The results are depicted in Fig. 5.4. The reflected amplitude given by

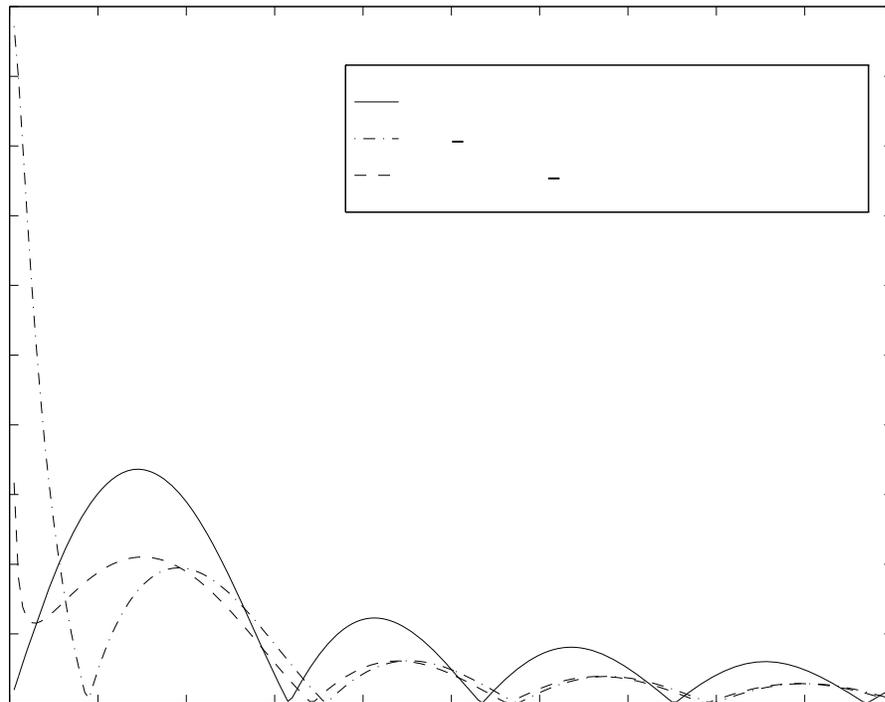


Figure 5.4: Reflected amplitude over the depth profile $H(x) = 2x^2 - 2x + 1$ ($0 \leq x \leq 1$).

the integral approximation has muc

and for large values of ω ($\omega > 7$), that is, as the slope of the hump becomes milder, the reflected amplitude given by the new integral approximation is closer to that given by the other two approximations.

The evidence given by these two examples clearly suggests that the integral approximation $\tilde{\phi}$ to ϕ which was derived by omitting all the decaying wave mode terms in the kernel of the second-kind integral equation (5.9), is not equivalent to either the modified mild-slope or the mild-slope approximations. From the evidence given in Chapter 4 for Booij's [5] talud problem, we saw that both the modified mild-slope and the mild-slope approximations gave good approximations to the full linear results. When decaying modes were added to the approximation, the results became even closer to the full linear ones that Booij had computed. Similarly, we expect that the results given in Chapter 4 by the new 'decaying mode' approximation for this current hump problem are tending to those given by full linear theory as the number of decaying modes is increased. From Fig.4.6 in Chapter 4, we see that the height of the peaks in the amplitude of the reflected wave for this scattering problem given by the new 'decaying mode' approximations and the modified mild-slope and mild-slope approximations are very similar. As the peaks in the amplitude of the reflected wave given by the integral approximation are nearly twice the height of the peaks given by both the modified mild-slope and mild-slope approximations, then we conclude that the integral approximation is a poor approximation to the full linear problem.

If we recall how we made the integral approximation, it is really quite surprising that the integral approximation produces recognisable results at all. We approximated the kernel of the integral equation (5.9), which is an infinite series, with just the first term of this series. From the results we have obtained, it is clear that this estimate of the infinite series is quite poor, a not surprising fact.

Instead of trying to improve the approximation in the full linear integral equation (5.9), we find that accurate estimates of the solutions of the full linear problem itself can be obtained. This is achieved by firstly converting the second-kind integral equation (5.9) for the velocity potential on the hump into a first-kind integral equation for the tangential fluid velocity on the hump.

5.3 A first-kind integrl equation

We now return to the full linearised problem which was stated in section 5.1. The Green's identity domain under consideration is as depicted in Fig.5.5. In this pic-

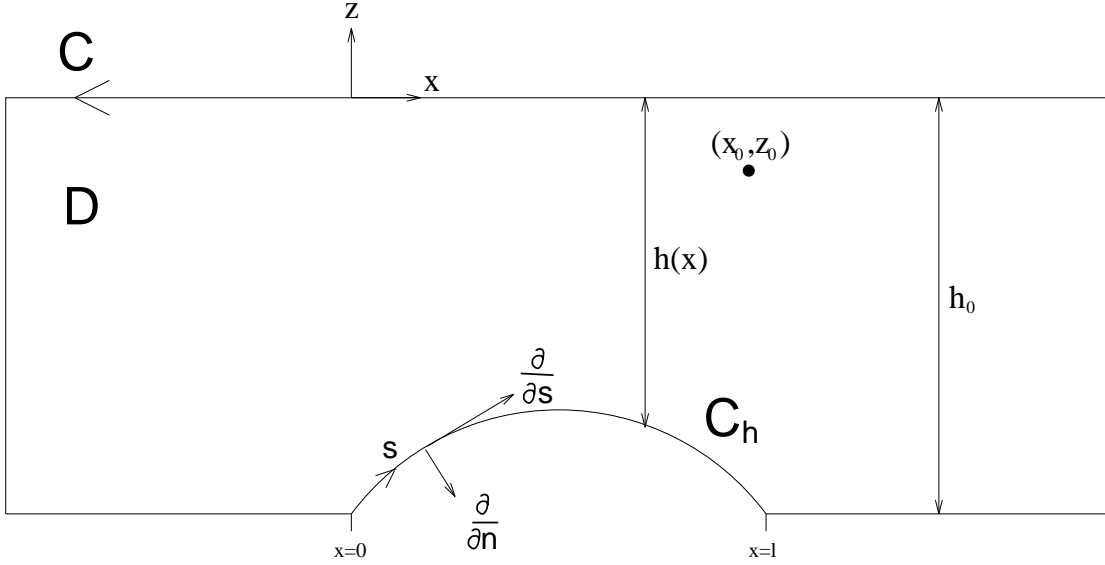


Figure 5.5: The Green's identity domain.

ture, $\frac{\partial}{\partial n}$ denotes the outward normal derivative, $\frac{\partial}{\partial s}$ the tangential derivative and s the arc length along C_h , the curved part of C , measured from $x = 0, z = -h_0$. The outward unit normal was defined in Chapter 2 in terms of two orthogonal horizontal co-ordinates x and y and a vertical co-ordinate z . For the problem domain we are considering, which is independent of y , the outward unit normal \underline{n} at (x, z) on C_h is given by

$$\underline{n} = -\frac{1}{(1 + (h'(x))^2)^{\frac{1}{2}}} (h'(x), 1) ,$$

where the prime denotes differentiation with respect to x . The unit tangent \underline{s} at (x, z) on C_h is given by

$$\underline{s} = \frac{1}{(1 + (h'(x))^2)^{\frac{1}{2}}} (1, -h'(x)) .$$

It follows that the normal and tangential derivatives at (x, z) on C_h are given by

$$\frac{\partial}{\partial n} = \frac{-1}{(1 + (h'(x))^2)^{\frac{1}{2}}} \left[\frac{\partial}{\partial z} + h'(x) \frac{\partial}{\partial x} \right]$$

and

$$\frac{\partial}{\partial s} = \frac{1}{(1 + (h'(x))^2)^{\frac{1}{2}}} \left[\frac{\partial}{\partial x} - h'(x) \frac{\partial}{\partial z} \right] .$$

Taking the normal derivative of equation (5.8), the integral representation of the velocity potential in the fluid, gives

$$\begin{aligned} \frac{\partial \phi}{\partial n_0}(x_0, z_0) &= \frac{\partial}{\partial n_0} \left[\frac{\cosh(k_0(z_0 + h_0))}{\cosh(k_0 h_0)} [A^- e^{ik_0 x_0} + A^+ e^{-ik_0 x_0}] \right] \\ &\quad - \frac{\partial}{\partial n_0} \int_{C_h} \left[\phi \frac{\partial G}{\partial n} \right]_{z=-h(x)} ds \end{aligned} \quad (x_0, z_0) \text{ in } D .$$

The exponential term in the infinite series (5.7) for G guarantees that G is an infinitely differentiable function of (x, z) and (x_0, z_0) for $(x, z) \neq (x_0, z_0)$. As (x_0, z_0) is in D and (x, z) is on C_h , then we can take $\frac{\partial}{\partial n_0}$ under the integral in the above equation to give

$$\begin{aligned} \frac{\partial \phi}{\partial n_0}(x_0, z_0) &= \frac{\partial}{\partial n_0} \left[\frac{\cosh(k_0(z_0 + h_0))}{\cosh(k_0 h_0)} [A^- e^{ik_0 x_0} + A^+ e^{-ik_0 x_0}] \right] \\ &\quad - \int_{C_h} \left[\phi \frac{\partial^2 G}{\partial n_0 \partial n} \right]_{z=-h(x)} ds , \end{aligned} \quad (5.24)$$

where (x_0, z_0) is in D .

Notice that the Green's function G defined by (5.7) can be written as

$$G(x, z|x_0, z_0) = f(x - x_0, z + z_0 + 2h_0) + f(x - x_0, z - z_0) , \quad (5.25)$$

where

$$f(x, z) = \frac{i}{4k_0} c_0^2 \cosh(k_0 z) e^{ik_0 |x|} + \sum_{n=1}^{\infty} \frac{1}{4B_n^0} c_n^2 \cos(B_n^0 z) e^{-B_n^0 |x|} .$$

As G is a Green's function, singular at $(x, z) = (x_0, z_0)$, it follows that the function $f(x - x_0, z - z_0)$ is a Green's function, singular at $(x, z) = (x_0, z_0)$, satisfying

$$\hat{\nabla}^2 f(x, z) = -\delta(x)\delta(z) \quad - h_0)$$

It follows that L is also a Green's function in the sense that

$$\hat{\nabla}^2 L = \delta(x - x_0)\delta(z - z_0) \quad -h_0 < z < 0 .$$

Notice that G behaves like a line source near (x_0, z_0) and L behaves like a line sink near (x_0, z_0) . From the definition of f it is simple to see that L is given by the infinite series

$$\begin{aligned} L(x, z|x_0, z_0) = & \frac{i}{2k_0} c_0^2 \sinh(k_0(z+h_0)) \sinh(k_0(z_0+h_0)) e^{ik_0|x-x_0|} \\ & - \sum_{n=1}^{\infty} \frac{1}{2B_n^0} c_n^2 \sin(B_n^0(z+h_0)) \sin(B_n^0(z_0+h_0)) e^{-B_n^0|x-x_0|}. \end{aligned} \quad (5.26)$$

Lemma 5.1 *suppose $G = G(x, z|x_0, z_0)$ and $L = L(x, z|x_0, z_0)$ are defined by (5.7) and (5.26) respectively. Then $\frac{\partial G}{\partial n}$ and $\frac{\partial L}{\partial s}$ satisfy*

$$\frac{\partial}{\partial n_0} \left(\frac{\partial G}{\partial n} \right) = \frac{\partial}{\partial s_0} \left(\frac{\partial L}{\partial s} \right) \quad \text{and} \quad \frac{\partial}{\partial s_0} \left(\frac{\partial G}{\partial n} \right) = -\frac{\partial}{\partial n_0} \left(\frac{\partial L}{\partial s} \right)$$

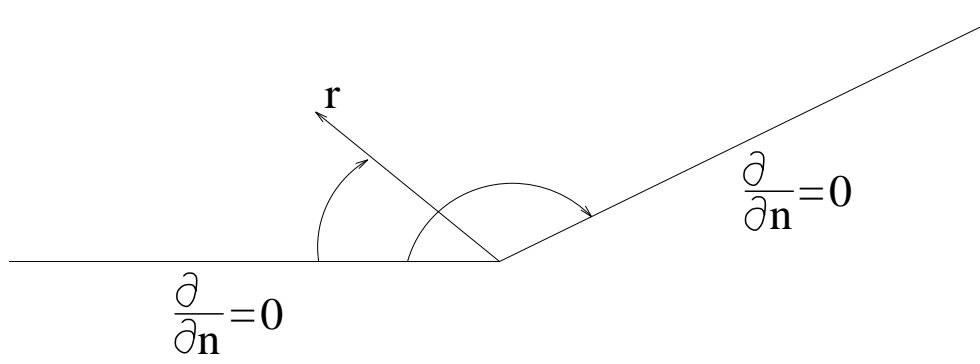


Figure 5.6: Polar co-ordinate system at a corner.

$$\left. \frac{\partial \phi}{\partial s} \right|_{\theta=\alpha} = \left. \frac{\partial \phi}{\partial r} \right|_{\theta=\alpha} = \frac{\pi}{\alpha} \sum_{j=1}^{\infty} (-1)^j a_j j r^{\frac{j\pi}{\alpha}-1} \rightarrow 0 \text{ as } r \rightarrow 0 \text{ since } 0 < \alpha < \pi .$$

The same result clearly holds on the boundary $\theta = 0$. Therefore, as the depth profiles C_h that we are considering are all humps (so that $\alpha < \pi$), it follows that $\frac{\partial \phi}{\partial s}$ evaluated on C_h is zero, and therefore bounded, at the ends of the hump, that is, at $x = 0$ and $x = l$. It follows that as $L(x, z|0, -h_0) = 0$ for (x, z) on C_h , then

$$\left[\int_{C_h} \left[L \frac{\partial \phi}{\partial s} \right] ds \right]_{x_0=0} = 0 .$$

Substituting $x_0 = 0$ in (5.29) then gives $c = 0$ and so it follows that the tangential fluid velocity evaluated on the hump satisfies the first-kind integral equation

$$\int_{C_h} \left[L \frac{\partial \phi}{\partial s} \right] ds + i \sinh(k_0(h_0$$

This first-kind integral equation for $\frac{\partial\psi}{\partial n}$ evaluated on C_h looks like the result of applying Green's identity (5.4) to ψ and L . Indeed, in the next section we show that this is precisely the case and therefore we can give a much more direct derivation of equation (5.31) than we did in this section.

5.4 A direct derivation of the first-kind integral equation

Note that the stream function is arbitrary to within a constant and we have chosen $\psi = 0$ on $z = -h(x)$, that is, we have chosen the streamline $\psi = 0$ to be the bed. We have also expressed the radiation conditions on ψ at $x = \pm\infty$ in terms of the coefficients of the incident and scattered waves. It follows that the coefficients of the reflected and transmitted waves due to an incident wave from either $x = \infty$ or $x = -\infty$ are as given

considering a fourier series expansion for $\frac{\partial L}{\partial z}$, given by

$$\frac{\partial L}{\partial z}(x, z|x_0, z_0) = \sum_{n=0}^{\infty} d_n(x|x_0, z_0)v_n(z) .$$

Here $v_0(z) = c_0 \cosh(k_0(z + h_0))$, $v_n(z) = c_n \cos(B_n^0(z + h_0))$ ($n \in \mathbb{N}$), and the functions d_n ($n + 1 \in \mathbb{N}$) are to be found. All the other functions are defined earlier in this chapter.

Integrating the above expression for $\frac{\partial L}{\partial z}$ with respect to z gives

$$\begin{aligned} L(x, z|x_0, z_0) &= \frac{1}{k_0}d_0(x|x_0, z_0)c_0 \sinh(k_0(z + h_0)) \\ &+ \sum_{n=1}^{\infty} \frac{1}{B_n^0}d_n(x|x_0, z_0)c_n \sin(B_n^0(z + h_0)) , \end{aligned}$$

where there is no constant of integration because we require $L = 0$ on $z = -h_0$. It is clear that L as defined above also satisfies the free surface condition (5.39).

From Chapter 4, we know that the sequence $\{v_n : n + 1 \in \mathbb{N}\}$ is orthonormal for $z \in [-h_0, 0]$. Therefore, the unknown functions d_n are given by

$$d_n(x|x_0, z_0) = \int_{-h_0}^0 \frac{\partial L}{\partial z}(x, z|x_0, z_0)v_n(z)dz \quad (n + 1 \in \mathbb{N}) . \quad (5.42)$$

Integration by parts gives

$$\begin{aligned} d_0(x|x_0, z_0) &= \frac{c_0}{k_0} \sinh(k_0 h_0) \frac{\partial L}{\partial z} \Big|_{z=0} - \frac{1}{k_0} \int_{-h_0}^0 \frac{\partial^2 L}{\partial z^2} w_0(z) dz , \\ d_n(x|x_0, z_0) &= \frac{c_n}{B_n^0} \sin(B_n^0 h_0) \frac{\partial L}{\partial z} \Big|_{z=0} - \frac{1}{B_n^0} \int_{-h_0}^0 \frac{\partial^2 L}{\partial z^2} w_n(z) dz \quad (n \in \mathbb{N}), \end{aligned} \quad (5.43)$$

where $w_0(z) = c_0 \sinh(k_0(z + h_0))$ and $w_n(z) = c_n \sin(B_n^0(z + h_0))$ ($n \in \mathbb{N}$). Differentiating (5.42) twice with respect to x and then integrating the result by parts gives

$$\begin{aligned} d_0''(x|x_0, z_0) &= c_0 \cosh(k_0 h_0) \frac{\partial^2 L}{\partial x^2} \Big|_{z=0} - k_0 \int_{-h_0}^0 \frac{\partial^2 L}{\partial x^2} w_0(z) dz , \\ d_n''(x|x_0, z_0) &= c_n \cos(B_n^0 h_0) \frac{\partial^2 L}{\partial x^2} \Big|_{z=0} + B_n^0 \int_{-h_0}^0 \frac{\partial^2 L}{\partial x^2} w_n(z) dz \quad (n \in \mathbb{N}), \end{aligned} \quad (5.44)$$

where the prime denotes differentiation with respect to x .

From (5.38), it follows that

$$\int_{-h_0}^0 (\hat{\nabla}^2 L) w_n(z) dz = \delta(x - x_0) w_n(z_0) \quad (n + 1 \in \mathbb{N}) . \quad (5.45)$$

Substituting equations (5.43) and (5.44) into (5.45) and employing the equations $\nu = k_0 \tanh(k_0 h_0)$ and $-\nu = B_n^0 \tan(B_n^0 h_0)$ ($n \in$

The method that we have used to construct L here can be used to construct the Green's function G given by (5.7). Notice that L and G are only defined for $-h_0 < z < 0$. Hence, it is clear that these two Green's functions are not suitable to be used with other types of depth profiles that satisfy $h(x) = h_0 \forall x \in (-\infty, 0] \cup [l, \infty)$, such as ripples in the sea bed or a trench, as h_0 is no longer the greatest fluid depth. The issue of finding the Green's functions L and G for depth profiles corresponding to ripples and trenches is a separate problem and is not pursued here. This is the reason why we just consider

h

by

$$\begin{aligned} & \int_{-h_0}^0 \left[\psi \frac{\partial L}{\partial x} - L \frac{\partial \psi}{\partial x} \right] \Big|_{x=\infty} dz + \int_0^{-h_0} \left[-\psi \frac{\partial L}{\partial x} + L \frac{\partial \psi}{\partial x} \right] \Big|_{x=-\infty} (-dz) \\ &= \frac{-2k_0}{\cosh(k_0 h_0)} \int_{-h_0}^0 \left[A^- e^{ik_0 x} L|_{x=-\infty} - A^+ e^{-ik_0 x} L|_{x=\infty} \right] \sinh(k_0(z + h_0) \end{aligned}$$

Evans [16], whilst considering water wave scattering by a shelf, showed that as the point (x, z) approaches (x_0, z_0) ,

$$G \approx \frac{1}{2\pi} \left[\log \left\{ (x - x_0)^2 + (z - z_0)^2 \right\}^{\frac{1}{2}} \right]$$

For an incident wave from $x = -\infty$, the coefficient of the reflected wave was defined as

$$R_1 = \frac{c_0^2 \cosh(k_0 h_0)}{2A^-} \int_0^l \left[-h'(x) \cosh(k_0(h_0 - h(x))) \right. \\ \left. + i \sinh(k_0(h_0 - h(x))) \right] e^{ik_0 x} \phi(x, -h(x)) dx.$$

Integration by parts gives

$$R_1 = \frac{c_0^2 \cosh(k_0 h_0)}{2A^- k_0} \left[\phi \right.$$

5.5 Non-dimension l i s t i o n

We use the same scaling procedure as used in previous chapters, which is briefly summarised as follows. Let

$$\hat{x} = \frac{x}{l},$$

$$\hat{z} = \frac{z}{h_0}$$

The coefficients of the reflected and transmitted waves due to an incident wave from $x = -\infty$ are given by

$$R_1 = -\frac{C_0^2 \cosh(\kappa_0 \tau)}{2A^- \kappa_0} \int_0^1 e^{i\kappa_0 x} \sinh(\kappa_0 \tau(1-H(x))) \chi(x) dx \quad , \quad (5.49)$$

$$T_1 = 1 + \frac{C_0^2 \cosh(\kappa_0 \tau)}{2A^- \kappa_0} \int_0^1 e^{-i\kappa_0 x} \sinh(\kappa_0 \tau(1-H(x))) \chi(x) dx \quad , \quad (5.50)$$

and for an incident wave from $x = \infty$ are given by

$$R_2 = \frac{C_0^2 \cosh(\kappa_0 \tau)}{2A^+ \kappa_0} \int_0^1 e^{-i\kappa_0 x} \sinh(\kappa_0 \tau(1-H(x))) \chi(x) dx \quad , \quad (5.51)$$

$$T_2 = 1 - \frac{C_0^2 \cosh(\kappa_0 \tau)}{2A^+ \kappa_0} \int_0^1 e^{i\kappa_0 x} \sinh(\kappa_0 \tau(1-H(x))) \chi(x) dx \quad . \quad (5.52)$$

5.6 A v r i t i o n 1 p r i n c i p l e

We start this section by recasting the first-kind integral equation (5.48) on the Hilbert space $L_2(0, 1)$, which is the set of all equivalence classes of complex-valued Lebesgue measurable functions ζ satisfying the condition $\int_0^1 |\zeta|^2 < \infty$. This space has pointwise operations with inner product defined by $(f, g) = \int_0^1 f \bar{g}$

then

$$\begin{aligned}\|f_n\| &= \sqrt{\int_0^1 \int_0^1 |f_n(x_0, x)|^2 dx dx_0} \\ &\leq \frac{1}{(2\beta_n^0)^{\frac{3}{2}}} C_n^2 \left(2 + \frac{1}{\beta_n^0} (e^{-2\beta_n^0} - 1)\right)^{\frac{1}{2}} < \infty \quad (n \in \mathbb{N}).\end{aligned}$$

Hence $f_n \in L_2(0, 1) \times L_2(0, 1) \forall n \in \mathbb{N}$.

Now $\forall n \in \mathbb{N}$, C_n^2 is bounded and for a fixed τ , $\beta_n^0 \sim \frac{n\pi}{\tau} + O(\frac{1}{n})$ as $n \rightarrow \infty$ (see Wehausen and Laitone [59], for example). Therefore, it follows that $\sum_{n=1}^{\infty} \|f_n\|$ converges and hence $\sum_{n=1}^{\infty} f_n$ converges in $L_2(0, 1) \times L_2(0, 1)$. Hence

$$k(x_0, x) = \sum_{n=0}^{\infty} f_n(x_0, x)$$

converges in $L_2(0, 1) \times L_2(0, 1)$, where

$$f_0(x_0, x) = \frac{i}{2\kappa_0} C_0^2 \sinh(\kappa_0 \tau (1 - H(x))) \sinh(\kappa_0 \tau (1 - H(x_0))) e^{i\kappa_0 |x - x_0|}.$$

We also have that for all $n \in \mathbb{N}$, the functions f_n are continuous and are therefore measurable and

$$\begin{aligned}\|k(x_0, x)\| &= \sqrt{\int_0^1 \int_0^1 |k(x_0, x)|^2 dx dx_0} \\ &\leq \sum_{n=0}^{\infty} \sqrt{\int_0^1 \int_0^1 |f_n(x_0, x)|^2 dx dx_0} < \infty,\end{aligned}$$

and so k

The first-kind integral equation (5.48) can now be written as an operator equation in $L_2(0, 1)$ by defining g as

$$g(x_0) = -\frac{i \sinh(\kappa_0 \tau (1 - H(x_0)))}{\cosh(\kappa_0 \tau)} [A^- e^{i\kappa}$$

Lemma 5.2 *The functional $J(p)$ defined by (5.58) is stationary at $p = \chi$, the solution of (5.55), with stationary value (χ, \bar{y}) .*

Proof

Suppose that $p = \chi + \delta\chi$ where $\delta\chi$ represents the error in this approximation to χ

The constants $a_j \in \mathbf{C}$ ($j = 1, \dots, N$) are determined by using the fact that the variational principle $\delta J = 0$ is stationary at $p = \chi$. Therefore, we choose p so that

$$\frac{\partial J}{\partial a_j} = 0 \quad (j = 1, \dots, N) .$$

Hence the unknown constants $a_j \in \mathbf{C}$ ($j = 1, \dots, N$) satisfy the N simultaneous, linear equations

$$\sum_{j=1}^N a_j (K\psi_j, \psi_n) = (\psi_n, \bar{g}) \quad (n = 1, \dots, N) . \quad (5.61)$$

We can actually evaluate the functional J without needing to find explicitly the approximation to χ . This procedure is given in Porter and Stirling ([51] p.268-269), where the stationary value is expressed as the quotient of the determinants of two $N \times N$ matrices. The entries in the j^{th} column of each matrix correspond to an inner product involving ψ_j . If we did not require to know the values of the constants

shown, by a simple application of Green's identity to ϕ and its complex conjugate for an incident wave from $x = -\infty$, that

$$|R_1|^2 + |T_1|^2 = 1 .$$

5.7 Numeric 1 solution method

In order to determine the approximation to the reflection coefficients and to χ , we see from equation (5.61) that we need to calculate the inner products

$$(\psi_j, \bar{g}) \quad (j = 1, \dots, N)$$

and

$$(K\psi_j, \psi_n) \quad (j, n = 1, \dots, N) .$$

In the previous section, we pro

where

$$(K_r \psi)(x_0) = - \left\{ \frac{C_0^2}{2\kappa_0} w_0(x_0) \int_0^1 w_0(x) \sin(\kappa_0|x-x_0|) \psi(x) dx \right. \\ \left. + \sum_{n=1}^{\infty} \frac{C_n^2}{2\beta_n^0} w_n(x_0) \int_0^1 w_n(x) e^{-\beta_n^0|x-x_0|} \psi(x) dx \right.$$

and

$$(K_i \psi)(x_0) = \frac{C_0^2}{2\kappa_0} w_0(x_0) \left\{ \cos(\kappa_0 x_0) \int_0^1 w_0(x) \cos(\kappa_0 x) \psi(x) dx \right. \\ \left. + \sin(\kappa_0 x_0) \int_0^1 w_0(x) \sin(\kappa_0 x) \psi(x) dx \right\} .$$

Similarly, we write $(K \psi_j, \psi_n)$ ($j, n = 1, \dots, N$) in terms of real and imaginary parts as

$$(K \psi_j, \psi_n) = (K_r \psi_j, \psi_n) + i (K_i \psi_j, \psi_n) \quad (j, n = 1, \dots, N) .$$

Finally we express (ψ_j, \bar{g}) ($j, n = 1, \dots, N$) in terms of real and imaginary parts.

For a wave of unit amplitude incident from $x = -\infty$ ($A^+ = 0$), we write

$$(\psi_j, \bar{g}) = (\psi_j, \bar{g}_-) = [(\psi_j, f_1) - i(\psi_j, f_2)] \quad (j = 1, \dots, N) \quad (5.68)$$

and for a wave of unit amplitude incident from $x = \infty$ ($A^- = 0$), we write

$$(\psi_j, \bar{g}) = (\psi_j, \bar{g}_+) = [(\psi_j, f_1) + i(\psi_j, f_2)] \quad (j = 1, \dots, N) , \quad (5.69)$$

where the functions f_1 and f_2 are given by

$$f_1(x) = \frac{\sinh(\kappa_0 \tau (1 - H(x)))}{\cosh(\kappa_0 \tau)} \sin(\kappa_0 x) \quad \text{and} \quad f_2(x) = \frac{\sinh(\kappa_0 \tau (1 - H(x)))}{\cosh(\kappa_0 \tau)} \cos(\kappa_0 x) .$$

It is clear that once the real-valued inner products on the right-hand side of (5.68) have been calculated to give (ψ_j, \bar{g}_-) ($j = 1, \dots, N$), then as these are the same inner products that appear in the right-hand side of (5.69), we can find (ψ_j, \bar{g}_+) ($j = 1, \dots, N$) without calculating any more inner products. In other words, w

are only known at a finite number of points. We use 10 point composite Gauss-Legendre quadrature to calculate the integrals because it delivers highly accurate answers very economically for well-behaved integrands. Details of this quadrature rule can be found in Johnson and Riess [24], for example.

Chamberlain [7] used Gauss-Legendre quadrature to calculate

$$I(x_0) = \int_0^1 f(x) \sin(\kappa_0|x$$

$(j = 1, \dots, N)$ are calculated for an incident wav

as M is increased.

Instead of showing the convergence of $(K_r\psi_j)(x_0)$ for chosen values of x_0 in $[0, 1]$, we show the convergence of $\|K_r\psi_j\|$ as M increases, to give an overall

M	$\ \sum_{n=0}^{M-1} K_n^r \psi_1\ $	$\ \sum_{n=0}^M K_n^r \psi_1\ $	$\ \sum_{n=0}^{M-1} K_n^r \psi_3\ $	$\ \sum_{n=0}^M K_n^r \psi_3\ $
10	0.023965	0.024160	0.015655	0.015851
20	0.024793	0.024819	0.016441	0.016463
30	0.025027	0.025046	0.016667	0.016687
40	0.025154	0.025161	0.016791	0.016797
50	0.025224	0.025230	0.016859	0.016865
60	0.025274	0.025277	0.016907	0.016910
70	0.025307	0.025310	0.016940	0.016943
80	0.025333	0.025335	0.016966	0.016967
90	0.025353	0.025355	0.016985	0.016986
100	0.025369	0.025371	0.017001	0.017002

Table 5.1: Illustrating the convergence of $\|\sum_{n=0}^M K_n^r \psi_j\|$ ($j = 1, 3$).

impression of the convergence of $(K_r\psi_j)(x_0)$ in $[0, 1]$ as M increases. Table 5.1 gives $\|\sum_{n=0}^{M-1} K_n^r \psi_j\|$ and $\|\sum_{n=0}^M K_n^r \psi_j\|$ for $j = 1$ and $j = 3$ as M takes values from 10 to 100. We can see from Table 5.1 that for this depth profile and parameter values, $\|K_r\psi_j\|$ ($j = 1, 3$) converges quite slowly, but has converged to 3.d.p. when $M = 40$.

Now let us examine the convergence of the approximation to the reflection coefficient as M increases. Table 5.2 gives the approximation to the reflection coefficient R_1 delivered by a 4-term and an 8-term trial approximation as M takes values from 10 to 100. It is clear from Table 5.2 that when $M = 40$, the appro

M	R_1 (4 - term)	R_1 (8 - term)
10	$0.095878 + 0.078823i$	$0.094665 + 0.078163i$
20	$0.094260 + 0.076531i$	$0.093248 + 0.075982i$
30	$0.093712 + 0.075775i$	$0.092755 + 0.075256i$
40	$0.093435 + 0.075395i$	$0.092503 + 0.074890i$
50	$0.093268 + 0.075168i$	$0.092352 + 0.074671i$
60	$0.093156 + 0.075016i$	$0.092250 + 0.074525i$
70	$0.093076 + 0.074908i$	$0.092177 + 0.074421i$
80	$0.093016 + 0.074827i$	$0.092122 + 0.074342i$
90	$0.092970 + 0.074764i$	$0.092080 + 0.074282i$
100	$0.092932 + 0.074713i$	$0.092046 + 0.074233i$

Table 5.2: Illustrating the convergence of the approximation to R_1 as M increases.

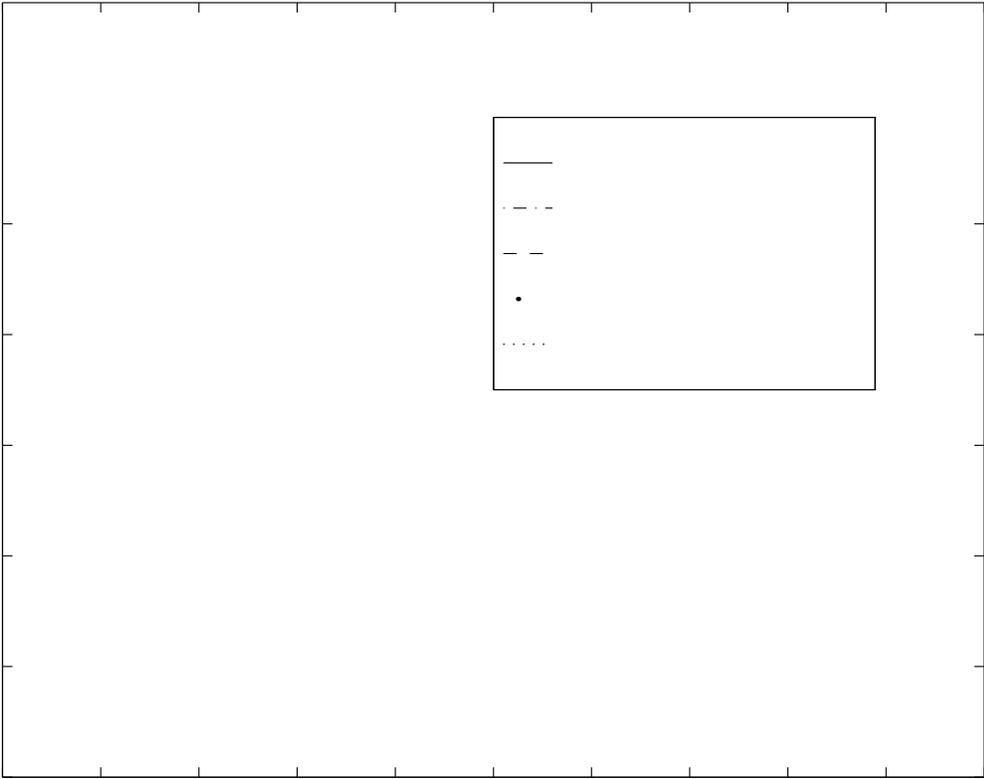
3.d.p. for any num

delivers an approximation to the reflection coefficient that has converged to 3.d.p.

We also note from T

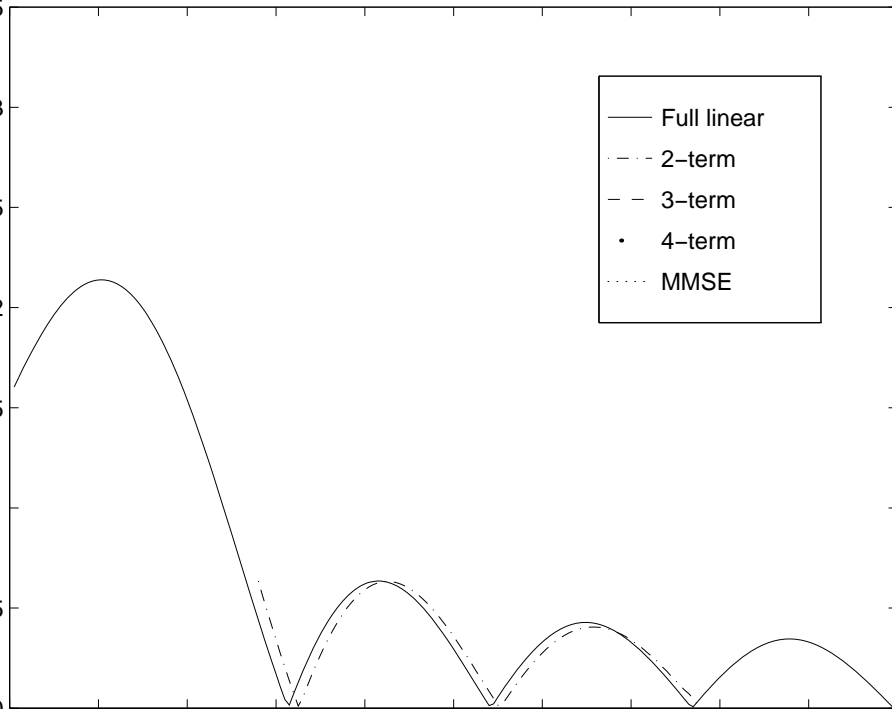
Approximation	R_1	T_1
Full linear	$0.092 + 0.075i$	$0.974 + 0.194i$
3-term	$0.0927 + 0.0727i$	$0.9757 + 0.1916i$
2-term	$0.0917 + 0.0736i$	$0.9747 + 0.1899i$
MMSE (new)	$0.0920 + 0.0735i$	$0.9751 + 0.1878i$
MSE (new)	$0.0883 + 0.0727i$	$0.9727 + 0.2021i$
MMSE (old)	$0.0867 + 0.0673i$	$0.9786 + 0.1741i$
MSE (old)	$0.0829 + 0.0663i$	$0.9763 + 0.1885i$

Table 5.4: A comparison of estimates of R_1 and



are in good agreement with full linear theory.

In Fig.5.8 we present the graphs of $|R_1|$ against ω given using full linear theory and the MMSE, 2-term, 3-term and 4-term approximations. It is clear from the



which corresponds to a hump whose height is half the still-water depth. We seek solutions given by the mild-slope, modified mild-slope and n -term ($n = 2, 3, 4$) approximations and estimates of the solutions of full linear problem at values of a parameter ω starting at 0.05, finishing at 10, with intervals of 0.05. The parameters α_0 and τ are defined in terms of ω by

$$\alpha_0 = \omega, \quad \tau = \frac{1}{\omega}.$$

Again, with these definitions for α_0 and τ , varying ω corresponds to varying the steepness of the depth profile.

Using a 10-term trial function to give estimates of the reflection and transmission coefficients for the full linear problem, we find that the maximum value of $\|Kp - g\|$ over the whole ω range is 3.4×10^{-3} .

In Fig.5.9 we present the graphs of $|R_1|$ against ω estimated using full linear theory and the MSE, MMSE, 2-term, 3-term and 4-term approximations. Again,

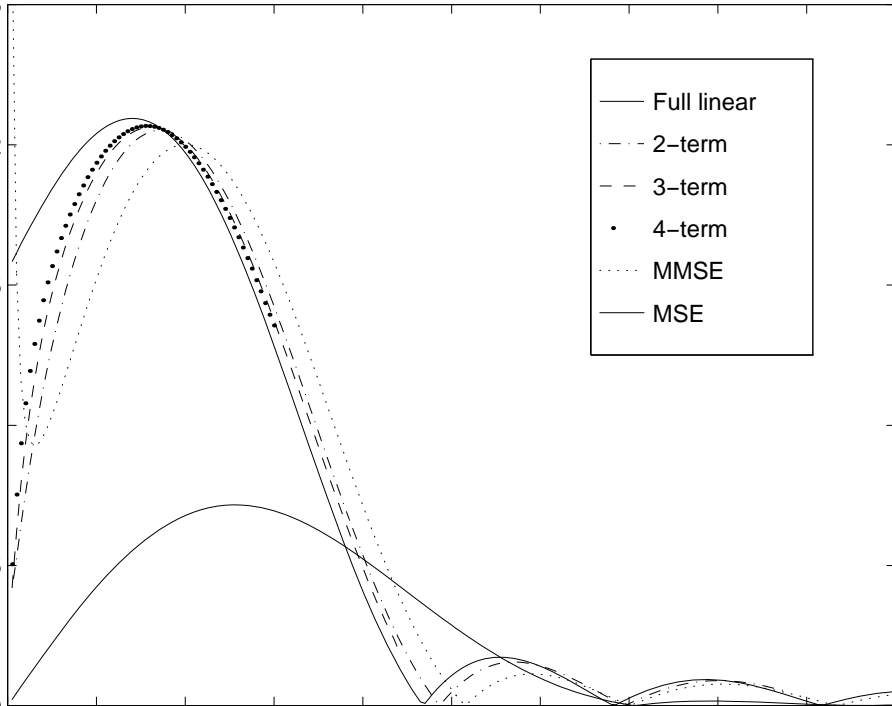


Figure 5.9: Reflected amplitude for depth profile $H(x) = \frac{3}{4} + \frac{1}{4} \cos(2\pi x)$ ($0 \leq x \leq 1$).

it is clear from the graph that, as the number of terms in the n -term approxima-

tion is increased, the closer the results become to the full linear ones. The results given by the MSE over the whole ω range are quite poor. The results given by the MMSE are much closer to the full linear results than those given by the MSE and give good agreement with the full linear results for $\omega > 6.5$. However, for $\omega < 6.5$, it is clear that the slope of the hump is large enough to warrant the inclusion of decaying modes in the approximation to the velocity potential. As usual, we see that the greater the slope of the hump becomes, the more decaying modes we need to use in the approximation to the velocity potential. As there is little difference in the results given by the 3-term and 4-term approximations, we do not calculate results for the 5-term approximation. Again, we notice that the results given by the n -term approximation converge to those given by the $(n - 1)$ -term approximation as ω decreases, that is, as the slope of the hump becomes milder.

In this chapter, we have shown how to obtain estimates of the coefficients of the scattered waves due to waves incident from $x = \pm\infty$ on hump depth profiles for full linear theory. A new first-kind integral equation for the tangential fluid velocity $\frac{\partial\phi}{\partial s}$ on the hump has been derived and a variational approach has been used to generate approximations to the coefficients of the scattered waves which are second-order accurate compared to the approximation of the solution of the first-kind equation. We have shown that estimates of the reflection coefficient can be determined to 3.d.p. using 40 terms in the infinite series of the kernel in the first-kind equation and a 10-term trial function. Results have been presented of how the estimate of the modulus of the reflection coefficient for the full linear model varies as the slope of the hump is varied. These results were compared with the corresponding results given by earlier approximations to the full linear model, namely the mild-slope, modified mild-slope and the n -term approximations, which were derived in Chapter 4. Further evidence was found to support the evidence given in Chapter 4, that the new boundary conditions derived in Chapter 4, were the appropriate ones to use with the MSE and MMSE. We also showed that the

mild-slope and modified mild-slope approximations give good agreement with the full linear results for humps with mild slopes, and that as the slope of the hump becomes large, decaying wave mode terms are required in the approximation to give results that are in good agreement with the full linear results.

These estimates of the solutions of the full linear wave scattering problem over humps will provide an invaluable new test to the accuracy of any new approximation to wave scattering by an arbitrary sea bed.

Summary and Further Work

In this thesis the scattering of a train of small amplitude harmonic surface waves on water by undulating one- and quasi-one-dimensional bed topography has been investigated.

After re-establishing the full linear boundary-value problem satisfied by the velocity potential for the scattering of waves by varying topography in Chapter 2, three approximations to this problem were given, namely the mild-slope, Eckart and linearised shallow water appro

cant, the results given by the new approximation agreed much more closely with the results Booij [5] obtained using full linear theory. The maximum number of decaying modes used in the new approximation was three. This was because the difference in the results obtained using two and three decaying modes in the new approximation was only very small for even the steepest depth profiles. In other words, the results given by the new approximation had essentially converged for the steepest depth profiles when the number of decaying modes included had reached three. The less steep the depth profile, the fewer the number of decaying modes required for convergence until eventually the gradient of the depth profile becomes mild enough to make all the decaying modes negligible. The solution method, in which the governing system of second-order differential equations was converted into a first-order system and then solved using a Runge-Kutta procedure, could not be used for some values of the parameters of the problem, which not

of boundary conditions was derived for the mild-slope and modified mild-slope equations. Previously, the boundary conditions for these equations had been obtained by enforcing the continuity of the approximation to the free surface and its slope at the ends of the varying depth region. The new boundary conditions arise from enforcing the continuity of the approximation to the velocity potential and its horizontal velocity throughout the fluid at the ends of the varying depth region. The results given by the mild-slope and modified mild-slope equations with these new boundary conditions are in much better agreement with results that have been computed using full linear theory and results that have been found by using a type of approximation in the full linear wave scattering problem different to the ones that have been used in this thesis. The modified mild-slope equation together with these new boundary conditions can be derived from a variational principle. The details of this process are the subject of a paper by Porter and Staziker (in preparation).

Finally, we showed how to obtain estimates of the coefficients of the scattered waves due to plane wave incidence on hump depth profiles for full linear theory. A new first-kind integral equation for the tangential fluid velocity on the hump was derived and a variational approach used to generate approximations to the reflection coefficients which are second-order accurate compared to the approximation of the solution of the first-kind equation. The symmetry relations satisfied by the reflection and transmission coefficients were then used to calculate the transmission coefficients. An alternative variational principle can be found which gives approximations to both the reflection and transmission coefficients. However, this alternative process is computationally more expensive than the method used because a larger trial space is required. The reflection coefficient was determined to three decimal places using the first 40 terms of the infinite series which defines the kernel in the first-kind equation and a 10-term trial function. Further work to remove the logarithmic singularity in the infinite series will improve the convergence of this series and thus improve computational efficiency. These estimates of the solutions of the full linear wave scattering problem over humps provide an invaluable new test of the accuracy of any new approximation to wave scattering by an arbitrary sea bed.

The modified mild-slope approximation to the velocity potential is derived by using a 1-term plane wave trial function in a variational principle. The results obtained give good agreement with full linear theory for all but the steepest of depth profiles. An apparently similar approximation in the variational principle which was used for the first-kind integral equation is to omit all the decaying wave mode terms in the series for the kernel, so that only the first term in the series is used. However the results obtained by this approximation are poor and we find that the amplitude of the reflected wave increases as the water depth increases which is exactly opposite to the behaviour of the exact solution. So the following question arises: what approximation in the variational principle for the first-kind integral equation corresponds to the modified mild-slope approximation? Further work is clearly required here to fully understand this approximation process. Once it is understood, it could be used in other more complicated integral equations arising from wave scattering, such as that derived by Evans [16] for scattering by a shelf of arbitrary profile. So far this second-kind integral equation has not been solved due to the extremely complicated form of the kernel. If an approximation equivalent to the modified mild-slope approximation could be made in a variational principle, which is equivalent to solving this equation, then not only could powerful solution techniques such as reiteration be used to solve the approximate equation, but it could also be possible to find explicit bounds on the error incurred by making the approximation.

Bibliography

Bibliography

- [1] E. F. Bartholomeusz. The reflexion of long waves at a step. *Proc. Camb. Phil. Soc.*, 54:106–118, 1958.
- [2] J. C. W. Berkhoff. Computation of combined refraction-diffraction. In *Proc. 13th Int. Conf. on Coastal Eng.*, pages 471–490. Vancouver, Canada, ASCE, New York, N. Y., July 1973.
- [3] J. C. W. Berkhoff. Mathematical models for simple harmonic linear water waves. Rep. W 154-iv, Delft Hydr., 1976.
- [4] J. L. Black and C. C. Mei. Scattering of surface waves by rectangular obstacles in waters of finite depth. *J. Fluid Mech.*, 38:499–511, 1969.
- [5] N. Booij. A note on the accuracy of the mild-slope equation. *Coastal Engineering*, 7:191–203, 1983.
- [6] P. G. Chamberlain. *Wave Propagation on Water of Uneven Depth*. PhD thesis, University of Reading, 1991.
- [7] P. G. Chamberlain. Wave scattering over uneven depth using the mild-slope equation. *Wave Motion*, 17:267–285, 1993.
- [8] P. G. Chamberlain. Symmetry relations and decomposition for the mild-slope equation. *J. Eng. Math.*, 29:121–140, 1995.
- [9] P. G. Chamberlain and D. Porter. The modified mild-slope equation. *J. Fluid Mech.*, 1995a. (to appear).

- [10] P. G. Chamberlain and D. Porter. Decomposition methods for wave scattering by topography with application to ripple beds. *Wave Motion*, 1995b. (to appear).
- [11] K. W. E. Chu and D. Porter. The solution of two wave-diffraction problems. *J. Eng. Math.*, 20:63–72, 1986.
- [12] A. G. Davies and A. D. Heathershaw. Surface-wave propagation over sinusoidally varying topography. *J. Fluid Mech.*, 144:419–443, 1984.
- [13] W. R. Dean. On the reflection of surface waves by a submerged plane barrier. *Proc. Camb. Phil. Soc.*, 41:231–238, 1945.
- [14] B. A. Ebersole. Refraction-diffraction model for linear water waves. *Journal of Waterway, Port, Coastal and Ocean Engineering*, 111(6):939–953, 1985.
- [15] C. Eckart. The propagation of gravity waves from deep to shallow water. In *Gravity Waves: (Proc. NB Centennial Symp. on Gravity Waves, NB, June 15-18, 1951)*, pages 165–175, Washington: National Bureau of Standards, 1952.
- [16] D. V. Evans. The application of a new source potential to the problem of the transmission of water waves over a shelf of arbitrary profile. *Proc. Camb. Phil. Soc.*, 71:391–410, 1972.
- [17] D. V. Evans. A note on the total reflexion or transmission of surface waves in the presence of parallel obstacles. *J. Fluid Mech.*, 67:465–472, 1975.
- [18] D. V. Evans and C. A. N. Morris. Complementary approximations to the solution of a problem in water waves. *J. Inst. Math. Applics.*, 10:1–9, 1972.
- [19] E. Fehlberg. Klassische runge-kutta formeln vierter und niedrigerer ordnung mit schrittweiten-kontrolle und ihre anwendung auf warmeleitungs-probleme. *Computing*, 6:61–71, 1970.
- [20] G. F. Fitz-Gerald. The reflexion of plane gravity waves travelling in water of variable depth. *Phil. Trans. Roy. Soc.*, A286:49–89, 1976.

- [21] G. E. Forsythe, M. A. Malcolm, and C. B. Moler. *Computer Methods for Mathematical Computations*. Prentice-Hall, 1977.
- [22] J. Harband. Propagation of long waves over water of slowly varying depth. *J. Eng. Math.*, 11:97–119, 1977.
- [23] R. J. Jarvis. The scattering of surface waves by two vertical plane barriers. *J. Inst. Math. Applics.*, 7:207–215, 1971.
- [24] R. J. Johnson and R. D. Riess. *Numerical Analysis*. Addison-Wesley, 2nd edition, 1982.
- [25] I. G. Jonsson, O. Skovgaard, and O. Brink-Kjaer. Diffraction and refraction calculations for waves incident on an island. *Journal of Marine Research*, 34:469–496, 1976.
- [26] J. T. Kirby. A general wave equation for waves over rippled beds. *J. Fluid Mech.*, 162:171–186, 1986.
- [27] G. Kreisel. Surface waves. *Quart. Appl. Math.*, VII(1):21–44, 1949.
- [28] H. Lamb. *Hydrodynamics 6th Ed.* Cambridge University Press, 1932.
- [29] J. D. Lambert. *Numerical Methods in Ordinary Differential Equations*. Wiley, 1992.
- [30] C. C. Lautenbacher. Gravity wave refraction by islands. *J. Fluid Mech.*, 41:655–672, 1970.
- [31] B. Li and K. Anastasiou. Efficient elliptic solvers for the mild-slope equation using the multigrid technique. *Coastal Engineering*, 16:245–266, 1992.
- [32] C. Lozano and R. E. Meyer. Leakage and response of waves trapped by round islands. *The physics of fluids*, 19:1075–1088, 1976.
- [35] 1r1088,1088,e r-rhe Tf4TTf4eTAe for incidensincideTfpTDTheTD4vaTeffJ4TwiCamof

- [35] S. R. Massel. Hydrodynamics of coastal zones. *Elsevier Oceanography series*, 48, 1989.
- [36] S. R. Massel. Extended refraction-diffraction equation for surface waves. *Coastal Engineering*, 19:97–126, 1993.
- [37] C. C. Mei. *The applied dynamics of ocean surface waves*. Wiley Interscience publishers, 1983.
- [38] R. E. Meyer. Surface wave reflection by underwater ridges. *Journal of Physical Oceanography*, 9(1):150–157, 1979.
- [39] J. W. Miles. Surface wave scattering matrix for a shelf. *J. Fluid Mech.*, 28(4):755–767, 1967.
- [40] J. W. Miles. Variational approximations for gravity waves in water of variable depth. *J. Fluid Mech.*, 232:681–688, 1991.
- [41] J. N. Newman. Propagation of water waves past long two-dimensional obstacles. *J. Fluid Mech.*, 23:23–29, 1965a.
- [42] J. N. Newman. Propagation of water waves over an infinite step. *J. Fluid Mech.*, 23(2):399–415, 1965b.
- [43] J. N. Newman. Interaction of water waves with two closely spaced vertical obstacles. *J. Fluid Mech.*, 66:97–106, 1974.
- [44] J. N. Newman. Numerical solutions of the water-wave dispersion relation. *Applied Ocean Research*, 12(1):14–18, 1990.
- [45] T. J. O’Hare and A. G. Davies. A new model for surface wave propagation over undulating topography. *Coastal Engineering*, 18:251–266, 1992.
- [46] T. J. O’Hare and A. G. Davies. A comparison of two models for surface-wave propagation over rapidly varying topography. *Applied Ocean Research*, 15:1–11, 1993.
- [47] D. Porter. The transmission of surface waves through a gap in a vertical barrier. *Proc. Camb. Phil. Soc.*, 71:411–421, 1972.

- [48] D. Porter. The radiation and scattering of surface waves by vertical barriers.
J. Fluid Mech., 63(4):625–634, 1974.
- [49] D. Porter. Approximate solutions to a multiple barrier diffraction problem.